PLASTIC DEFORMATION OF OXIDE FILMS DURING GROWTH

Submitted for the Degree of Ph.D.

in the University of London

by

Peter Neufeld

1967

ABSTRACT

The plasticity of the oxide film on a metal has an important influence on its resistance to damage, and hence its effectiveness in impeding corrosion. It has been reported that the anodic film on aluminium can show enhanced plasticity while an anodic current is flowing. The strengthening effect of a surface film on a metal specimen was made use of in this work, and the apparent enhanced oxide plasticity was explained in terms of a diffusional mechanism.

There were several possible interpretations of this original work and the purpose of the present investigation was to obtain sufficient information to enable these interpretations to be more fully considered. The surface strengthening effect, electron microscopy and spectrophotometry were all employed to study the properties of anodic films grown on aluminium and on an aluminium-magnesium alloy under a wide variety of conditions.

It is concluded that enhanced oxide plasticity during the passage of an anodic current provides the most likely explanation of the observed effects on fine wire specimens. A diffusional mechanism for oxide deformation is the one that best fits the experimental data.

Information has also been obtained on the changes that occur during the initial stages of growth of a porous type anodic film. It is suggested that the best criterion for distinguishing between the

two classes of anodic films is the presence or absence of continued steady film growth at a constant applied voltage.

CONTENTS

Page.

ABSTRACT 2

A. INTRODUCTION

1. Importance of the Mechanical Properties of Oxide Films 8

B. REVIEW OF PREVIOUS WORK

1. Methods of Testing the Mechanical Properties of Oxides 13

a. Bulk Oxides 13

b. Stripped Oxide Films 14

c. Oxide Films on the Metal 15

2. Plastic Deformation of Oxides 19

a. Principles of Deformation Mechanisms 19

b. Single Crystals 20

c. Polycrystals and 'Amorphous' Oxides 21

3. Diffusion Related to Deformation 25

a. General Connection 25

b. Grain Boundary and Disorder Effects 25

c. Defect Structure and Alloying 28

d. Effect of External Conditions on Oxide Plasticity 32

4. Conclusions 36

a. Oxide Plasticity 36

b. Materials and Techniques for Further Work .. 37

Page.

C. EXPERIMENTAL TECHNIQUES

1. Materials 41

a. Aluminium 41

b. Aluminium-Magnesium Alloy 41

c. Specimen Preparation 42

d. Electrolytes 44

2. Apparatus and Techniques 46

a. Anodic Film Growth 46

b. Electrical Measurements 47

c. Spectrophotometry 47

d. Electron Microscopy 50

e. Tensile Tests on Wires 50

f. Constant Load Tests on Wires 50

g. Constant Strain Tests on Wires 52

h. Bending Tests on Foil 53

i. Temperatures During Anodising 54

D. RESULTS

1. Modes of Growth of Anodic Films 56

a. Barrier Films 56

b. Porous Films 59

c. Temperatures During Anodising 62

2. Mechanical Properties of Anodic Films 64

a. Strengthening of Wires by Oxide Films .. 64

b. Constant Load Tests 64

Page.

c. Constant Strain Tests 69

d. Bending Tests 71

E. DISCUSSION

1. Nature of the Anodic Films 74

a. Barrier Films 74

b. Porous Type 77

2. Analysis of Stress Conditions During Tests .. 81

a. Stress on the Oxide 81

b. Constant Load Conditions 82

c. Constant Strain Conditions 84

3. Interpretation of Results in Terms of Oxide Plasticity 85

a. Previous Interpretation 85

b. Surface Removal (Dislocation 'Pop Out') .. 86

c. Temperature Effects 87

d. Electrostatic Effects 92

e. Coherence at Metal-Oxide Interface 94

f. Present Interpretation 95

4. Features of Oxide Plasticity 96

a. Field Dependence 96

b. Current Dependence 98

c. Load Dependence 100

d. Effect of Alloying 101

Page.

5. Diffusional Theory of Oxide Plasticity 101

6. General Application of Plasticity Theory 107

a. Anodic Films 107

b. Other Oxide Films 108

F. CONCLUSIONS

1. Oxide Plasticity 111

2. Other Properties of Anodic Films 113

ACKNOWLEDGEMENTS 115

REFERENCES 116

INDEX TO DIAGRAMS 123

DIAGRAMS 128

SECTION A

INTRODUCTION

A. INTRODUCTION

A.1. Importance of the Mechanical Properties of Oxide Films

The rate of reaction between a metal and a potentially aggressive environment is often reduced by a high concentration of reaction products at the metal surface. Often a substantially continuous solid oxide film (which may be hydrated in aqueous surroundings) is formed and the transport of reactants through this film is the rate-determining step in corrosion.

In the case of oxide films grown at elevated temperatures in gaseous environments theories of the mechanism of oxidation have been extensively developed. Understanding of the processes involved has grown to the point where successful attempts have been made to predict reaction rates from theoretical considerations (1, 2, 115). Wagner(3, 4) first pointed out that ions and electrons are the migrating species in thermal films. Later workers such as Hauffe(5, 6, 7) showed that movement of these charged particles would be strongly influenced by the defect structure of the oxide and hence a small degree of alloying might produce large changes in oxidation rates.

Oxide films formed in aqueous environments are liable to be hydrated and are likely to be more complex in nature than thermally-produced films. Amongst aqueous films a group particularly suitable for investigation is that comprising the anodically

formed films on the valve metals. This name arises from the fact that oxide-coated electrodes of these metals have a rectifying action, but their useful properties from the point of view of the investigation of film growth are the appreciable thickness to which films can be grown and the ease with which growth can be controlled by varying the potential applied to the electrodes. There is considerable published information on the growth of anodic films on valve metals[8], which includes data on defect structure[9], electrical properties[10, 11], ionic diffusion[12], pore structure and formation[13, 14, 15, 16, 17, 18, 19], and the crystal structure of the film[20, 21].

When the oxide film forms a continuous barrier on the metal surface, Pourbaix diagrams[22, 23] can be used to predict the thermodynamic conditions for slow corrosion due to the presence of a film (passivity) or rapid corrosion due to film instability. If, however, mechanical damage to the film occurs, unexpectedly high corrosion rates may result. Such damage could arise from several causes, for example:

1. Abrasion
2. Deformation of the metal under load
3. Differential thermal expansion
4.. Internal stresses in the film.

Internal stresses require some further discussion. In 1923 Pilling and Bedworth[24] suggested that stresses could arise when

an oxide occupied a different volume from that of the metal from which it was formed. Other workers have since questioned whether this volume ratio is in fact of significant importance in most practical cases[1, 25]. It is certainly true that internal stresses in oxides are complex in nature, both tensile and compressive stresses have been observed at different stages of a single oxidation reaction[26, 27, 28]. Measurement of stresses may be confused by stresses induced in the metal by cation removal[27]. Stresses in anodically formed oxides bear many resemblances to the stresses in electrodeposited metals[29], and similar theories involving hydration processes have been proposed to account for both[28, 30].

Whatever the origins of stresses, it is clear that the ability of an oxide to deform will be important in determining its resistance to mechanical rupture. The plasticity of oxide films has been discussed with reference to the corrosion of a variety of metals, including iron[31] and zirconium[32]. It has not been found possible to predict the properties of surface oxides by extrapolating data on bulk material of similar composition[33, 34] even after allowing for size effects[36]. This makes it necessary to measure the mechanical properties of oxide films under conditions of growth on the metal surface.

Bradhurst[33] reported that the anodic film formed on aluminium appeared to have enhanced plasticity during the application of

anodic current, compared with its plasticity in the absence of anodic current. This implies that during oxide growth the properties of the oxide may be different from its properties after growth is completed. In view of the importance of oxide plasticity and the suitability of anodic oxide films for experimental investigation, the present work was undertaken in an attempt to obtain more complete information about the apparently plastic behaviour of the anodic film on aluminium and to develop a satisfactory understanding of the processes involved. This would be a first step in determining the factors affecting plasticity in a wider range of oxides and perhaps in developing alloys producing protective films of improved properties.

SECTION B

REVIEW OF PREVIOUS WORK

B.1. Methods of Testing the Mechanical Properties of Oxides

a. Bulk Oxides

When oxides are available in bulk form the techniques normally employed for testing other materials may be used.

Beam specimens may be subjected to three or four-point bending[37, 38]. The specimen is under maximum tensile stress at the convex surface and under maximum compressive stress at the concave surface. The stresses on a specimen may become even more complex if yielding occurs in the more highly stressed regions, this will produce a non-uniform stress gradient through the thickness of the specimen. Thus, while it may be easy to prepare simple-shaped bending specimens, a quantitative interpretation of results may be difficult.

Suitably shaped specimens may be stressed in tension[39]. With this method a fairly uniform stress may be applied over the cross-section of the specimen. It is, however, necessary to devise a suitable means of gripping the ends of a specimen so that stress concentrations do not lead to premature failure at the points of application of the load.

Compression tests on cylindrical specimens offer an alternative method of applying uniform stress, with the advantage over tensile tests of allowing the use of more simple specimens and means of applying stress. The ultimate failure of specimens under

compression is caused by resolved shear components of the applied stress in the same way as the failure of tensile specimens, but the results of compression tests are less likely to be affected by the presence of Griffith cracks or stress-raisers[36]. This is because the extensive regions of tensile strain necessary for the propagation of such cracks are not present. Compression tests are therefore suitable for the testing of oxide materials, and have been so used[40].

b. Stripped Oxide Films

When an oxide film can grow to thicknesses of the order of a millimetre or more it might be possible to prepare specimens that permit the use of the conventional testing techniques discussed above. Usually, however, oxide films on metals grow to thicknesses very much less than this. While a film may be stripped off its metal substrate by dissolution of the metal in a suitable reagent, it would be difficult to apply bending or compression tests to very thin specimens. An extremely small force would suffice to bend a thin film specimen and a very large force would be needed to compress it so as to obtain a measurable deflection. In either case measurements would be difficult. This leaves tensile testing as the most suitable method to apply to stripped oxide films.

Bradhurst[33, 34] measured the tensile strength of stripped anodic oxide films. Ribbon-like specimens were loaded by means of weights suspended from their ends. He found that the film material was much stronger than would have been predicted from information on the strength of bulk oxide. A 1500 Å thick alumina film was found to extend by about 2.5% before fracture occurred at a stress of about 10,000 Kg. cm^{-2}. This compared with an extension of about 0.07% at a fracture stress of about 2,000 Kg. cm^{-2} for bulk alumina. The lower Young's modulus of the film material confirmed that there was a real difference in mechanical properties which was due to a difference in oxide structure and not simply to size effects. No plastic deformation was detected in these experiments.

c. Oxide Films on the Metal

Usually the strength of a thin oxide film is negligible compared with that of the metal specimen it is on. The total strain an oxide film on the metal can undergo before fracturing may be measured by using electrical tests for continuity. Bradhurst[33, 34] used resistance and capacitance measurements to detect film rupture. Bubar and Vermilyea[114] made use of the fact that a thick anodic oxide film has low electronic conductivity

while a very thin film has relatively high conductivity. They grew a thin anodic film on the base metal surfaces exposed by cracking of a strained film; this enabled estimates of the area exposed by cracking to be made from conductivity measurements.

Bradhurst found that oxide films on aluminium could undergo between 0.5% and 2.0% extension before cracking. Bubar and Vermilyea confirmed these results and found that thin (< 100 Å) films on zirconium could sustain about 15% deformation and on tantalum the anodic film could deform by up to 50%. Both groups of workers found that films grown on annealed metal specimens could undergo a greater amount of deformation before fracture than films grown on unannealed specimens.

The response of oxide films to stresses less than the ultimate fracture load is more difficult to measure, required data must be extracted from measurements of the behaviour of the composite metal-oxide specimen. The strength of metal single crystals, or specimens whose dimensions are comparable with the crystal size, is considerably influenced by surface effects. Some of the properties of surface films may thus be indirectly deduced from their effects on the properties of such specimens.

Even an unfilmed metal surface may be able to impede dislocation movement. Kramer and co-workers[41-49] reported that during electropolishing the plasticity of aluminium single

crystals was enhanced. Similar results were obtained with gold, copper, zinc and iron[44, 47] and led to the theory of a high dislocation density "debris layer" at the surface which impeded dislocation movement. Continued removal of the surface by dissolution prevented the re-formation of this layer and allowed dislocations to move out of the surface more easily to produce surface steps as a result of slip. This phenomenon was given the name "dislocation pop-out". For aluminium the debris layer was estimated to be about 0.05 mm. deep[48], but the conclusions were complicated by the presence of a surface oxide film. Kramer found that aluminium specimens showed greater plasticity in a high vacuum than in air[45, 46] and suggested that even a 10 Å thick oxide film can affect the strength of single crystals. He also noted that during the electropolishing experiments there seemed to be a "decrease in the effectiveness of the oxide coating"[45].

It was in 1934 that Roscoe[50] first reported that oxide films could strengthen single crystal specimens of cadmium. Andrade[51] confirmed this effect for a variety of other metals. Annealed fine aluminium wires have grain dimensions of the same order of magnitude as the wire diameter, and the strengthening effect of oxide films on such specimens strained in torsion was measured by Barrett et al.[52] and Holt[53]. There are two ways in which surface oxides can strengthen a crystal. Firstly, the movement of dislocations at the surface can be impeded, and secondly

the movement of dislocations out of the surface to form slip steps can be prevented. The first effect would be independent of the thickness of the film, but the second one would be shown most markedly by films which were thick compared with the size of surface steps. It is this second mode of strengthening which would be dominant when the metal is stressed in the plastic range. Other workers have pointed out that surface films can influence the movement of point defects also[54].

The surface strengthening effect of oxide films suggests a means of investigating oxide plasticity. Only rigid oxide films would provide permanent barriers to the movement of dislocations out of a surface. A film exhibiting plasticity would tend to conform to the changes in surface topography caused by step formation. If this plastic behaviour was such that appreciable time-dependence was shown, i.e. creep was occurring, the rate of deformation of the metal specimen would be controlled by the rate of creep of the oxide film.

In his work referred to above, Bradhurst[33] anodised fine aluminium wires and subjected them to tensile testing. He found that the presence of an oxide film had a small effect on the stress strain curve in the elastic range of stresses but when the wires were stressed in the plastic range the anodised wires showed considerably less extension than unanodised ones under the same load. He also found that these specimens could be induced to behave

as if the oxide film was showing appreciably plastic behaviour. This is discussed in detail in Section B.3d.

B.2. Plastic Deformation of Oxides

a. Principles of Deformation Mechanisms

A theoretically 'perfect' crystal could not remain 'perfect' while undergoing plastic deformation. This is because during deformation some atoms or ions must be in non-equilibrium conditions, i.e. some disorder or defect structure is present. Three types of defect can take part in deformation processes.

1. Point Defects. The movement of vacancies in a lattice can lead to an effective transfer of mass through the crystal (see Section B.2c). The presence of point defects can also affect the movement of line defects.
2. Line Defects. Movement of dislocations enables the initially localised lattice distortion that they represent to extend across a two-dimensional surface in a crystal and produce relative movement between the portions of a crystal on either side of this surface.
3. Plane (Surface) Defects. The formation in a lattice of surfaces across which there is an angular difference between corresponding crystallographic planes can occur by a shear

process. This produces relative movement between the parts of the crystal on either side of the surface.

It is difficult formally to assign a specific deformation mechanism to the deformation of fluids or 'amorphous' materials since these lack long range ordering. Such materials may be regarded as containing very high concentrations of defects of the types mentioned above, or perhaps as comprising a fourth class of three-dimensionally defective lattices. An alternative approach would be to regard them as being essentially amorphous and deforming by viscous flow, the regions of ordering that are present forming the 'defective' part of the structure that modifies the mechanical properties.

b. Single Crystals

Plastic deformation of single crystals of oxides is most commonly ascribed to dislocation movement[55, 56]. Sapphire shows appreciable plasticity only at elevated temperatures. Slow creep tests give measurable results at about 900°C[57, 58] while more rapid tensile tests indicate the onset of plastic behaviour in the higher range of 1270°-1520°C[59]. Chang[60] considered that the creep of sapphire at 1550°C could best be accounted for by a dislocation climb mechanism, which involves lattice diffusion. Slip along crystallographic planes is not

an easy mode of deformation for alumina, which is why elevated temperatures must be reached before it becomes significant.

c. Polycrystals and 'Amorphous' Oxides

Passmore et al.[38] detected plasticity at high deformation rates of alumina of 2μ grain size. This was in the temperature range 1300°-1400°C which corresponds to results for single crystal material quoted above. This plasticity was attributed to basal slip, but in general deformation by dislocation movement tends to be inhibited by small grain sizes. The Petch equation indicates how the yield stress, σy, varies with the grain size d. σi is a constant stress value, and Ky is a constant of appropriate dimensions.

$$\sigma y = \sigma i + Ky\, d^{-\frac{1}{2}} \qquad (1)$$

Since at small grain sizes grain boundaries can offer substantial resistance to plastic deformation by means of dislocation movement, other mechanisms which enable polycrystalline materials to deform in a plastic manner may become important.

1. Grain Boundary Sliding. The grain boundary is a highly disordered region. At temperatures of the order of half

the melting point (absolute scale) the grain boundary regions may weaken to the extent that deformation may occur by the relative movement of grains. He viewed the grain boundary as a sort of viscous fluid. This view was later modified by Mott and others who showed that the plasticity of the grain boundary material was reduced by the presence of relatively ordered regions[62-65, 116].

Wachtman and Lam[61] report a drop in the Young's modulus of polycrystalline alumina at 1000°C which they attribute to the onset of grain boundary sliding.

2. Herring-Nabarro Creep. Herring and Nabarro independently proposed a mechanism for deformation involving the diffusion of vacancies in the lattice. A grain boundary under tension will tend to have an excess of vacancies compared with the bulk of the crystal. A grain boundary under compression will tend to have a deficiency of vacancies. If diffusion rates in the lattice are sufficiently high these vacancies may migrate under the influence of the concentration gradient. This produces an effective mass flow in the opposite direction and hence the grain changes shape in conformity to the applied load[66, 67]. The equation for the creep rate of a polycrystalline material by this mechanism is as follows:

$$\frac{ds}{dt} = \frac{10\sigma D a^3}{A^2 kT} \qquad (2)$$

where $\frac{ds}{dt}$ is the rate of deformation, σ is the applied stress, D is the lattice diffusion coefficient, a^3 is the vacancy volume, A is the grain size, k is Boltzmann's constant and T is the temperature.

Where this form of deformation is likely it often becomes the dominant mode under conditions of relatively low stress. It is not limited to crystals of elements, but may occur in ionic crystals containing more than one species in the lattice[68]. This mechanism in a modified form has been invoked to account for the deformation of polycrystalline alumina at elevated temperatures (see Section B.3b).

Anodic films grown on aluminium and tantalum are often described as having an 'amorphous' or 'glassy' structure[8] since only diffuse X-ray or electron diffraction rings can be obtained; if any ordered regions are present their size must be of the order of 50 Å or less. The structure of such films may therefore be regarded as analogous to that of grain boundary material. It is difficult to postulate a specific model for the deformation of such material but in view of the high apparently plastic deformability of tantalum oxide and the low deformability of aluminium oxide reported by Bubar and Vermilyea[114] it seems logical to take different views for the two cases. Tantalum oxide may be regarded as an essentially fluid material that deforms by means of viscous type flow. The deformation of aluminium oxide,

on the other hand, may be considered to be controlled by the regions of short-range order that must be present in any non-gaseous material. In discussing the plastic deformation of anodic alumina films it should thus be possible to apply the mechanisms that describe the deformation of crystalline materials.

Evidence is slight that anodic alumina films can undergo plastic deformation under normal conditions. Holt[53] observed apparent deformation of anodic films, but, if present, this was only by very low amounts. While Bradhurst[33, 34] did not attempt to measure creep of stripped oxide films during his tensile tests he did observe that films grown on alloys containing 2-4% magnesium showed less extension before fracture than films grown on commercially pure aluminium. It could be argued that ribbon-like specimens of a relatively brittle material would be susceptible to failure by tearing initiated at stress concentrations. A further decrease in plasticity due to alloying would accentuate these stress concentrations and lead to failure at lower total applied loads. Such an argument would imply that the plasticity of anodic alumina is sufficiently high to affect the mechanical properties at normal temperatures.

B.3. Diffusion Related to Deformation

a. General Connection

Most of the deformation processes discussed above may be influenced by diffusion. Dislocations whose movement is impeded by the presence of point defects can be released when diffusion permits the defects to move. Movement of dislocations by climb also requires diffusion.

In the case of a deformation process involving the movement of vacancies only, there must be diffusion in both the anionic and cationic lattices. Electrical charge imbalance would prevent vacancies in one lattice from migrating at a rate appreciably different from those in the other lattice. For this reason the rate of diffusional creep would be controlled by diffusion in the lattice with the lower diffusion coefficient.

b. Grain Boundary and Disorder Effects

At grain boundaries and other disordered regions such as dislocations, diffusion rates may be enhanced[69, 70, 71]. A common feature of many oxides seems to be that anion diffusion is enhanced in these regions but cation movement is unaffected. Nickel oxide[72], magnesia[73, 74] and zirconia[75] have been reported as showing effects of this kind. This behaviour could

be interpreted as indicating that the movement of metal ions is interstitial and hence not greatly affected by lattice defects, while oxygen movement is normally by means of jumps from one lattice site to an adjacent vacant one.

Fig. 1 shows data obtained by a variety of techniques for diffusion coefficients in alumina. The diffusion coefficient of oxygen in polycrystalline alumina is some two orders of magnitude greater in polycrystalline alumina than in single crystal material. The results of Foweiler[79], shown in this diagram appear to show that the cationic diffusion coefficient may also be enhanced in polycrystalline material but Paladino and Coble[82] consider that these are misleading results attributable to an unsatisfactory measuring technique.

Even for polycrystalline alumina the diffusion coefficient of oxygen ions appears to be less than that of metal ions. In spite of this many workers believe that the cations are the slower-moving rate-controlling species in diffusional creep[82, 83, 84]. The model for the deformation mechanism differs from the simple Herring-Nabarro theory modified for ionic materials by Ruoff[68] in that while it is assumed that cation diffusion is through the crystal lattice without following preferred paths, anion diffusion is assumed to occur almost entirely at grain boundaries. By following grain boundary paths vacancies in the anionic lattice could move from vacancy-rich to vacancy-deficient regions

(perhaps on the surfaces of other grains) over a shorter route than would otherwise be followed. Such a mechanism would facilitate the movement of anions even more than might be expected from simple diffusion data. Creep of alumina has been reported as being controlled by lattice diffusion of cations for materials of grain size ranging from 2μ [84] to 108μ [81].

There is evidence from radioactive tracer measurements that thermally formed oxide films on aluminium grow by anionic diffusion only[85] while in the case of anodic films it appears that appreciable cationic diffusion may also occur, particularly at high applied fields[12, 86, 87]. Young[9] reports that Frenkel defects occur in anodic films on tantalum during the application of a high field. These disappear when the field is removed, suggesting that metal ion movement in alumina films also may be interstitial but can only take place when a high applied field provides the energy required to remove the ions from stable lattice positions[8]. The data available for anodic alumina therefore suggests that diffusion conditions suitable for supporting deformation may well be present during film growth under high applied fields, while such may not be the case for thermal films where high fields are not applied.

c. Defect Structure and Alloying

Hauffe considered the effect that the valency of an alloying element would have on the defect structure of an oxide[6, 7] and the predictions of Wagner-Hauffe oxidation theory in cases of alloying have been recently summarised by Stringer[115]. The predictions that are of particular interest to a consideration of diffusional deformation by vacancy migration are those which concern vacancy concentrations in the oxide lattice. Additions of a cation of lower valency than the major cationic species will tend to reduce the cationic vacancy concentration and increase the anionic vacancy.concentration. Additions of a cation of higher valency will have the reverse effect. It would be expected that an increase in the vacancy concentration in the slower-moving lattice would facilitate diffusional deformation by increasing the diffusion coefficient.

If the ionic radius of an alloying cation differs markedly from that of the dominant ionic species size effects may become important. A very small ion might be considered as being associated with a 'partial vacancy', while a very large ion

could be thought of as carrying with it a 'partial negative vacancy'. In either case, even if alloying did not result in the formation of a separate phase in the oxide, size effects on defect structure might counteract or hide any valency effects that might be expected. This factor should be borne in mind when suitable elements for experiments on alloying in oxides are being considered.

Considerable data are available on the effects of alloying and non-stoichiometry on diffusion rates and plasticity in uranium dioxide. In general it confirms that changes which increase diffusion rates also tend to increase oxide plasticity.

Belle and co-workers[88-91] report that in oxygen deficient yttria-doped uranium dioxide ($U_{0.9}\ Y_{0.1}\ O_{1.98}$), oxygen diffusion is enhanced compared with stoichiometric oxide, but metal ion diffusion is relatively unaffected. In this case the oxygen diffusion coefficient is an order of magnitude higher than the metal coefficient even in the stoichiometric oxide.

Scott et al.[93] studied the plastic deformation of sintered uranium dioxide. They found that stoichiometric oxide began to show plastic behaviour at about 1600°C while oxygen-rich oxides ($U_{1.0}\ O_{2.06}$ and $U_{1.0}\ O_{2.16}$) showed plasticity at about 800°C. It would be expected that oxygen-rich material would tend to have a larger concentration of cationic vacancies and hence a higher cationic diffusion rate than stoichiometric oxide.

If the deformation measured was diffusion-controlled the observed results would be in agreement with the principles outlined above. Christie and Williams[92] found that the enhanced plasticity of oxygen-rich uranium dioxide ($U_{1.0}O_{2.2}$) was reduced by additions of yttria. Additions of this trivalent ion to the four-valent uranium lattice would be expected to reduce metal diffusion and increase oxygen diffusion. Since metal diffusion would be the slower rate-controlling step in diffusion-controlled deformation the observed results again agree with expectations.

Stobbs and Whittle[94] found that the presence of carbide inclusions in a uranium dioxide film could lead to cracking and accelerated corrosion. This emphasised the importance of oxide plasticity in the oxidation of uranium, particularly in view of earlier work by Antill[101] who found that accelerated attack due to the presence of carbides was more marked in carbon dioxide at 1 atmosphere pressure than at 20 atmospheres. Presumably the oxide formed in the 20 atmospheres pressure gas was in a more plastic condition and hence was able to relieve stresses set up by the presence of inclusions.

Douglass[32, 95] has pointed out that oxide plasticity can be an important factor in the high-temperature corrosion of zirconium. He found that alloying additions of iron, nickel and chromium produced a softer oxide. In this case predictions of

diffusion rates from the Hauffe rules do not appear to correlate well with the observed changes in oxide plasticity and it may well be that deformation is not controlled by diffusion in the cationic lattice. It is interesting to note that Douglass found that chromium additions improved corrosion resistance in steam at 400°C as well as increasing oxide plasticity.

If it is desired to examine the effect of substitutional alloying on the plasticity of aluminium oxide, the following conditions should be observed:

1. The ionic radius of the alloying metal should be close to that of aluminium, so as to reduce size effects.
2. The metal should not show multiple valency states in the oxide, thus introducing uncertainty as to its valency.
3. Both the metals and the oxides should form solid solutions without the formation of separate phases.

The metal that best meets these conditions is magnesium. It is soluble in aluminium and its oxide is soluble in alumina when the metal is present at about the 1% level. If deformation of alumina is controlled by cationic diffusion, the presence of lower-valency magnesium ions would be expected to reduce oxide plasticity in the same way as yttrium additions reduce plasticity in oxygen-rich uranium dioxide. Ionic radii are 0.5Å for Al^{+++} and 0.65Å for Mg^{++}, so magnesium additions might tend to reduce the concentration of cationic vacancies.

d. Effect of External Conditions on Oxide Plasticity

Any external influence that increases the energy content of a solid might tend to encourage diffusion and diffusion-controlled deformation. Other modes of deformation might not be enhanced; for instance a high concentration of dislocations in a cold-worked metal would tend to impede further dislocation movement along slip planes, though diffusional climb of dislocations might be increased. Some of the ways in which diffusion coefficients or creep rates may be increased are described below.

1. Temperature. The diffusion coefficient usually increases with temperature according to the normal activation energy formula:

$$D = D_o \exp -(\frac{\Delta H}{RT}) \qquad (3)$$

where ΔH is the heat of activation and D_o is a constant. Thus, as shown in Fig. 1, there is a logarithmic increase of the diffusion coefficient with temperature. For this reason equation (2) predicts that diffusional creep increases with increasing temperature, a fact which might not be obvious at a first glance since the only temperature term directly shown indicates a reverse trend.

2. Irradiation. High energy neutron irradiation can mechanically damage silica specimens[97]. Presumably enough ions are removed from their stable positions to induce internal stresses in the

lattice that lead to fracture. Under favourable conditions, however, irradiation can induce stress relaxation and creep. Such effects have been reported for silica[97] and for nickel alloys[98]. In these cases it may be supposed that the energy imparted to ions by irradiation is insufficient to remove them from stable positions in the lattice but is sufficient to produce increased diffusion rates in much the same way as would be caused by increases in the energy of ions due to a temperature rise.

3. Light. During the growth of anodic films on tantalum unusual effects were observed by Bray et al.[99] due to the action of ultra-violet light. Continued film growth appeared to be possible under conditions where film growth would normally stop, and the film grown in the presence of ultra-violet light had unusual electrical and chemical properties.

While these effects may not be directly related to diffusion or deformation, they do serve to illustrate that relatively small external influences can affect the physical properties of oxides.

4. Gas Pressure. Variations in the partial pressure of oxygen can affect the composition of the oxide film, altering the oxide plasticity. An example is the oxidation of iron where Wuestite has greater plasticity than Magnetite or Hematite[31]. The composition of the oxidising gas determines which oxide

of uranium will form during high temperature corrosion[100], but the case discussed above of changed susceptibility of uranium dioxide to carbide damage[101] would appear to be one of altered defect structure and plasticity rather than of an altered oxide composition.

5. Mechanical Strain. Diffusion rates may be enhanced by the presence of a high strain field[102, 103]. Under such conditions the higher energy content of the material may enable ions to overcome energy barriers to diffusion more easily. Brown[104], has pointed out that diffusion-controlled processes may be accelerated during deformation. A process such as dislocation climb may therefore be accelerated because of the higher diffusion rate it itself induces[103].

6. Electric Field. Materials such as ionic crystals and semiconductors may contain charged lattice defects. In the presence of an electric field movement of these defects may be encouraged and plastic deformation may become easier. A variety of materials have been found to show enhanced plasticity in the presence of an electric field, these include rock salt[105], germanium, silicon, indium antimonide, silicon carbide[106, 107], and magnesia at elevated temperatures[108, 109]. This mechanical effect is usually attributed to the effect of the field in moving charged dislocations (first proposed by Eshelby et al.[110]) or moving charged defects which would

otherwise impede dislocation movement.

When Bradhurst[33] found that the anodic film on aluminium appeared to show enhanced plasticity during the passage of an anodic current, he ascribed this to increased ionic diffusion under the influence of a high field. The movement of ions in such a field is described by the high-field approximation for ionic conduction[8]:

$$I = a\, n\, \nu \exp -\left(\frac{W}{kT}\right) \exp \left(\frac{qaE}{kT}\right) \qquad (4)$$

where a is the lattice spacing, ν is a vibrational frequency, n is the number of diffusing ions, q is the ionic charge, W is the activation energy for ionic diffusion, k is Boltzmann's constant, T is the temperature and E is the applied field.

According to equation (4) the ionic flux increases logarithmically with the applied field in much the same way as the diffusion coefficient increases with the temperature (equation 3). Although, strictly speaking, equation (4) should be modified to allow for the high degree of disorder in the anodic oxide lattice[111], a simple application of it led to the conclusion that the ionic flux in an anodic film that was passing an anodic current of 7 m A cm.$^{-2}$ was equivalent to that produced by a temperature of 1700^{o}C. Bradhurst therefore concluded that the rate of diffusion-controlled deformation could

be raised sufficiently by the passage of an ionic current to account for the plasticity effects he had observed.

B.4. Conclusions

a. Oxide Plasticity

From theoretical considerations, the ability of oxide films to relieve stresses by plastic deformation would be expected to have an important influence on their protective qualities. Specific examples of cases where oxide plasticity has been shown to be important are the oxidation reactions of uranium, zirconium and iron.

Studies of plasticity in bulk oxides have been useful in investigating the mechanisms that can produce plasticity. In many instances diffusion processes have been found to be the rate-controlling steps in deformation. The results of work on bulk oxides cannot, however, be applied directly to predict the mechanical properties of oxide films on metals. It has been shown that the oxide films formed during corrosion can often show very much greater strength and plasticity than would be expected from a consideration of data for the bulk material. The condition of the metal surface on which a film is grown can also influence the mechanical properties of the film.

Results that indicate that the mechanical properties of oxide

films are different during growth from the properties after growth further support the view that, in order to obtain meaningful results, it is necessary to measure the plasticity of oxide films under conditions as similar as possible to those obtained during the oxidation process.

b. Materials and Techniques for Further Work

Oxide films can have a strengthening effect on specimens whose external surface is of the same order of magnitude as the total grain boundary area. This effect offers a means of measuring in a quantitative manner the response of films to forces that produce deformation since, under suitable circumstances, the deformation of a metal specimen may be controlled by the deformation of its surface oxide film. The strengthening effect is most marked in a metal that has a low yield stress.

By using this surface strengthening effect previous workers have investigated the plasticity of anodic films on aluminium. It has been found that the film normally demonstrates only elastic behaviour, but during the passage of an anodic current similar to that passing during film growth effects occur which imply that the film exhibits appreciable plasticity. For a variety of reasons aluminium is a suitable material for studies of this sort.

1. The metal has a low yield point, hence the surface strengthening effect is easy to measure.
2. There is a large amount of information on diffusion and deformation in bulk alumina. This provides some basis on which discussions of the behaviour of oxide films may be carried out, though caution must be used in applying such data.
3. Measurements of the mechanical properties of anodic alumina films imply that even though the oxide may have an ill-defined 'amorphous' structure, there is enough ordering present for plastic deformation to be controlled by processes characteristic of regular crystalline lattices. This simplifies the consideration of possible mechanisms for deformation.
4. A suitable metal, magnesium, is available for measuring the effect of alloying on oxide plasticity and for comparing any effect with predictions based on the Hauffe rules.

For these reasons it was decided that an investigation of oxide plasticity would be best directed towards a further study of the effect reported by Bradhurst and interpreted by him as diffusion-enhanced plasticity of anodic alumina. The objects of such an investigation would be as follows:

1. To confirm that the effects found in anodised fine wire specimens are attributable to true plasticity of the oxide film.

2. If possible, to develop alternative techniques for the investigation of oxide plasticity.
3. To determine how oxide plasticity may change with such variables as: electrical conditions, electrolyte composition and temperature, oxide morphology and alloying additions.
4. On the basis of such measurements, to consider whether a diffusional or some other mechanism offers the best explanation of oxide plasticity. This might enable predictions to be made about the plastic behaviour of oxide films on other metals and alloys and might indicate which materials and techniques would be suitable for further investigation.

SECTION C

EXPERIMENTAL TECHNIQUES

C.1. Materials

a. Aluminium

Annealed aluminium foil of 99.99% specified purity was obtained in a thickness of 0.1 mm. This material is referred to in the results section as aluminium sample 'A'.

Johnson-Matthey 'Grade I' aluminium was obtained in the form of 0.1 mm. diameter wire and 6.5 mm. diameter annealed rod. This material is specified to contain less than 50 ppm of metallic impurities and was designated sample 'B'.

All materials not specifically described as being supplied in the annealed condition were annealed for one hour at 350^{o}-400^{o}C. Fig. 5 shows the grain structure of an annealed fine wire specimen. The grain size is seen to be such that at most points along the wire the cross section consists of one grain only.

b. Aluminium-Magnesium Alloy

A low-magnesium alloy was obtained from Messrs. E. & E. Kaye Ltd. The trade name for this alloy is 'Aluflex' and its specified composition is as follows:

Element		%
Mg		0.8
Cu	Less than	0.1
Mn	" "	0.1
Si	" "	0.5
Fe	" "	0.5
Pb	" "	0.05
Sn	" "	0.05

The alloy was supplied as 0.25 mm. diameter wire and 1.1 cm. diameter rod.

The wire was drawn down to 0.1 mm. diameter and annealed. This material did not respond well to etching, so the grain structure of wires can not be illustrated to correspond with Fig. 5 for the aluminium wires of similar diameter.

The rod was rolled into strip approximately 0.5 mm. thick and was annealed.

c. Specimen Preparation

1. Wires. The 0.1 mm. diameter wire specimens were degreased in acetone before annealing and were subsequently mounted so as to leave a 5 cm. length between two glass hooks. This is

illustrated in Fig. 2.A., which shows that the wire was threaded through one of the hooks so that electrical contact could be made with the free end.

These specimens were not etched prior to testing. It was recognised that an anodic film grown on the wires might differ in structure from films grown on freshly etched surfaces but it was felt that such fine wires might have their diameter significantly reduced by etching, this reduction might also be excessively localised. Also, the air-formed film on an annealed specimen would not change with prolonged storage, hence the metal surface would be in a reproducible condition. Re-formation of an oxide film on an etched surface would start after removal from the etch solution and might make it difficult to ensure that the surface condition remained constant over a prolonged series of tests.

The choice of mounting resin was found to be limited, since a very hard resin caused stress concentrations at the ends of the 5 cm. length, leading to premature failure of the specimen under a tensile load. Too soft a mounting resin, on the other hand, tended to show excessive creep under load. A suitable material was found to be:

Araldite MY 752 - 100 cc.

" HY 219 - 50 cc.

" DY 219 - 10 cc.

The resin was introduced into the glass hooks by means of a hypodermic syringe and needle.

2. Rods. The 6.5 mm. aluminium rod was made up into test electrodes to be used for electrical measurements only. Rods were mounted in epoxy resin so that only the cross section was exposed when the specimen was immersed in an electrolyte. After a test had been completed the specimen could be renovated by cutting a thin layer off the exposed metal surface using a sharp knife.
3. Foils. The 0.1 mm. and 0.5 mm. thick foils were cut into suitable shapes for use in the tests described in detail in sections C.2c, d and h.

In contrast to the procedure followed for the wire specimens, all foil specimens were prepared by etching of the surface. This was because the surfaces of these relatively large specimens tended to become dirty and damaged much more easily than the fine wires, which were handled only with forceps. Etching was carried out immediately before anodising a specimen.

d. Electrolytes

1. Etching. For surface preparation of foil specimens before anodising a 10% solution of potassium hydroxide was used,

followed by a prolonged rinse in running water.

Etching of wires to reveal the grain structure was done using an etch of the following composition:

HF	10 cc.
HNO_3	1 cc.
H_2O	200 cc.

2. Anodising. The electrolyte used for most of the anodising experiments was a 3% solution of hydrated ammonium hydrogen tetraborate adjusted to a pH of 9.7 ± 0.1 by additions of 0.880 s.g. ammonium hydroxide solution. In the results and discussion sections this electrolyte is usually referred to simply as 'Borate'. The anodic films grown on aluminium in this electrolyte are usually considered to be of the non-porous barrier type.

A 15% solution of sulphuric acid was used for the growth of porous type anodic films. For the growth of anodic films in a virtually unhydrated condition a 5% solution of hydrated ammonium hydrogen tetraborate in ethanediol (ethylene glycol) was used.

In one experiment fine wires were anodically polarised in an electropolishing electrolyte. This was a solution of 100 cc. nitric acid in 200 cc. methanol at less than $5^{\circ}C$.

C.2. Apparatus and Techniques

a. Anodic Film Growth

A simple two-electrode cell was used for all anodising experiments and electrical measurements of film properties. The aluminium or alloy specimen formed the anode, and a platinum foil cathode of about 5 $cm.^2$ surface area was placed in any convenient position in the cell to serve as a cathode. No specific relative positioning of the electrodes was made and no separate reference electrode was used. These refinements were considered unnecessary in view of the very high anodic polarisation during anodising compared with cathodic polarisation and IR drop. Measurements of voltage, resistance and capacitance made between the anode and cathode were taken as indicating the properties or condition of the anodic film to a sufficiently close approximation.

A two-stage technique was used for the growth of anodic films.

1. A constant anodic current was passed until the cell voltage reached the required value. In general this current was 10 mA. cm^{-2} for foil specimens and 0.5 mA cm^{-2} for wire specimens.
2. The required voltage was maintained at a steady value while the current was allowed to decay.

An automatically controlled power source (Wareham Type C091) was used which switched from stage (1) to stage (2) operation when a pre-set voltage was reached.

The temperature of anodising electrolytes could be controlled to within $\pm$ 0.5°C by immersion of the cell in a thermostatic water bath. For reasons discussed in section D.2b most of the mechanical tests on fine wire specimens were carried out at room temperature, which varied in the range 20°-25°C.

b. Electrical Measurements

The automatic power source described above was equipped with meters measuring the cell current and voltage during anodising. After anodising was completed the equivalent parallel resistance and capacitance of the cell could be measured using a Wayne-Kerr universal bridge B221. This bridge operates at 1592 c.p.s. and produces a low potential of the order of a few millivolts across its terminals.

c. Spectrophotometry

The thickness of a flat sample of a transparent film may be measured by the interference of reflected and transmitted light.

Where the film thickness is t, the wavelength of monochromatic light is λ, the refractive index of the film is μ and the

interference is of order n, the following conditions apply:

For reflection at normal incidence:

$$\text{Maximum light intensity} - \quad t = \frac{n\lambda}{2\mu}$$

$$\text{Minimum light intensity} - \quad t = \frac{(2n + 1)\lambda}{4\mu}$$

For transmission at normal incidence the conditions for maximum and minimum light intensity are reversed.

If the refractive index remains constant, the wavelength at which a certain order interference maximum or minimum appears is directly proportional to the film thickness. This method may thus be applied to measurements of the thickness of oxide films[8].

Specimens of stripped anodic oxide films were prepared from the aluminium and alloy foil specimens. After a small (between 1 $cm.^2$ and 5 $cm.^2$ surface area) square metal specimen had been etched, a central spot on one side was coated with 'Lacomit' laquer. The specimen was anodised and the Lacomit then removed with acetone. The exposed disc of unanodised surface was then dissolved away in a 100 g/l solution of iodine in methanol at 55°-$60^{\circ}C$. This left a clear 'window' of oxide which was easily stored and handled because it was supported by the anodised metal specimen all around. The form of specimen obtained is illustrated in Fig. 6; this method of preparing stripped film specimens is due to Khan[117].

Measurements of the wavelengths at which interference produced intensity minima were made in the wavelength range 2000-25000 Å using a Perkin-Elmer 450 spectrophotometer. For transmission experiments the light beam was passed normally through the oxide film; for reflectance measurements a jig was used which reflected the beam from the film surface at an angle of incidence of 10^{o}. The error introduced by the 10^{o} angle was considered to be negligible for the purposes of the present work.

No absolute measurements of film thicknesses were attempted, this would have involved obtaining an accurate measure of the refractive index. It was assumed, however, that the refractive index did not vary with wavelength in the range of measurement. All thickness measurements were comparative, e.g. a doubling of the wavelength at which a certain order minimum appeared was taken to indicate a doubling of the film thickness. Where an estimate of the absolute film thickness was required it was assumed that the barrier layer films grown in the borate electrolyte at room temperature had a constant ratio of thickness to applied voltage of 14 Ångstroms per volt, the thickness of other films could be estimated by comparison with these films.

d. Electron Microscopy

Samples of stripped oxide film were prepared using the same technique as that described for the preparation of spectrophotometric samples. These were examined by transmission electron microscopy using a Hitachi HU-11 instrument at 100 kV.

e. Tensile Tests on Wires

The fine wires mounted in glass hooks were tested in tension on an Instron testing machine fitted with a sensitive load cell (50 g. maximum load). Wires were tested in the annealed and the anodised conditions using a straining rate of 0.5 mm./min. (1% per min.). The sensitivity of the load cell was such that 40 g. load produced a deflection of approximately 0.1 mm.

f. Constant Load Tests on Wires

A chemical balance was modified as shown in Fig. 2 with a stainless steel hook replacing the right hand pan. A second hook was positioned below this on a stainless steel cantilever arm that could be moved up and down by means of a rack and pinion. The wires were strained between these two hooks while immersed in a beaker of electrolyte fitted with a platinum cathode. If desired, this beaker could be surrounded by a water jacket

(not shown in Fig. 2) connected to a thermostatic water bath via a circulating pump.

Weights were added to the left hand balance arm in order to apply a constant load to the wires, any wire extension was indicated by movement of the balance pointer whose deflection was measured with a travelling microscope equipped with a micrometer eyepiece.

Tests similar to those conducted by Bradhurst[33] on fine aluminium wires were carried out in order to obtain more detailed information on the effects he attributed to oxide plasticity during growth. The following sequence of testing was carried out:

1. Oxide film was grown on specimen, and the anodising current switched off.
2. A fixed load was applied to the specimen and time allowed for any relaxation of the mounting plastic under load.
3. The anodising current was re-applied under either constant current or constant voltage conditions. Any extension of the wire was measured.
4. The anodising current was switched off.

In order to measure effects during the initial growth of oxide films and enable these to be distinguished from effects due to the re-application of a field to a previously anodised specimen the following sequence was used.:

1. An unanodised wire was loaded.
2. An anodic film was grown on the wire. Any change in the

wire length was measured.

3. The current was switched off.

g. Constant Strain Tests on Wires

The Instron hard-beam tester described in Section C.2e. was adapted so that mounted fine wires could be strained between two stainless steel hooks while immersed in a glass vessel containing electrolyte and a platinum cathode. This arrangement is shown in Fig. 3.

Tests equivalent to those described in the previous section, except for being carried out under constant strain conditions, were made on the wires. The first sequence of testing was thus:

1. An anodic oxide film was grown on the wire specimen and the current then switched off.
2. The wire was strained until a predetermined load was reached and then the crosshead of the testing machine was locked.
3. An anodising current was re-applied and any change of stress in the wire was measured.
4. The anodising current was switched off.

The second sequence of testing to check for effects during film growth was:

1. An unanodised wire was strained to a predetermined load and the crosshead locked.

2. An anodic film was grown on the wire. Any changes in stress on the wire were recorded during anodising and when the current was switched off.

h. Bending Tests on Foil

A simple four-point bending jig (see Fig. 4) was made of 1/8" diam. glass rod. The two outer loading points were 8 cm. apart, and the two inner ones were 4 cm. apart. The inner loading points were fitted with a pointer the movement of which could be measured using a travelling microscope, and the weight of this assembly was 4 g. As shown in Fig. 4, a strip of 0.1 mm. thick aluminium foil was loaded between the four points while immersed in a dish of electrolyte. Similarly to the tests on fine wires, two testing sequences were used.

First of all:

1. An anodic film was grown on the strip and the current switched off.
2. The 4 g. load was applied to the strip.
3. The anodic current was re-applied and any deflection of the pointer was measured.
4. The current was switched off.

The second series of tests were:

1. The 4 g. load was applied to an unanodised strip specimen.

2. The specimen was anodised and any deflection of the pointer was measured with the current flowing and after it had been switched off.

The strips used in these tests were 1 cm. wide and 12 cm. long.

i. Temperatures During Anodising

A simple arrangement enabling the resistance of a fine wire to be measured during anodising is illustrated in Fig. 7. The ohm-meter used was a battery-operated AVO type, eliminating the possibility of interaction between the meter and the power source via earth loops.

Measurements of changes in the wire resistance enabled estimates of the temperature changes during anodising to be made.

SECTION D

RESULTS

D.1. Modes of Growth of Anodic Films

a. Barrier Films

The borate electrolyte at a pH of 9.7 is usually considered to sustain the growth of barrier type anodic films on aluminium to a thickness of 14 Ångstroms per volt[33]. If the oxide is growing at a constant applied voltage the current decays to a fairly steady low value, the 'leakage current', as the film approaches its limiting thickness. Fig. 8 shows current-time curves for the growth of anodic films on aluminium 'B' and on 'Aluflex' under the two-stage growth conditions described earlier. The curves are of similar form, but the current on the aluminium specimen decays more rapidly and reaches a lower value than the current on the alloy specimen.

Reflectance and transmittance values are shown in the diagrams of results on an arbitrary scale. This is because in transferring the curves from the spectrophotometer chart, only the positions of the minima have been accurately represented. This is the only information of importance in determining thickness. The general form of the rest of the curves is shown, but this is not a precise replica of the original curves. Fig. 9 shows optical transmittance curves for films grown in borate to 200 volts and an anodic current of 0.1 mA $cm.^{-2}$ on aluminium 'A' and on 'Aluflex'. The very small difference in the wavelengths at which minima appear indicate that the film on 'Aluflex' is no more than about

1.3% thicker than the film on aluminium. Even this difference would probably have been eliminated if the films had been grown to their respective 'leakage' currents. Fig. 8 suggests that during current decay from 0.1 mA $cm.^{-2}$ the further increase in thickness would be greater for a film on aluminium than for one on 'Aluflex'. The results in Fig. 9 therefore show that no significant change in the angstrom/volt ratio has been induced by alloying.

The general structure of a barrier anodic film on aluminium is shown in Fig. 26. Crystalline inclusions are shown as dark angular shapes. The bulk of the film material seems to be featureless and 'amorphous', but very close examination reveals what appears to be a 'granular' structure. The micrographs in Figs. 10 and 11 were processed so as to show up this fine structure in more detail. The process of reproduction has accentuated the grain of the photographic emulsion (the fine granular structure visible) but has also shown the 'granular' structure of the anodic film. These micrographs are shown as 'negatives', darker areas represent thinner portions of the film. This 'granularity' of the anodic film, which is shown as a speckled structure in Figs. 10 and 11, is present on the film on 'Aluflex', but is on a coarser scale than in the film on aluminium.

Some films were grown on aluminium in borate to 200 V but at a constant current density. As soon as the pre-set voltage was reached the current was switched off without being allowed to decay at that voltage. Figs. 12, 13 and 14 show electron micrographs of these films. The illustrations have been processed in the same way as Figs. 10 and 11. It is evident that the fine 'granular' structure of the fully-formed anodic films is not present in the films grown at constant current only. This leads to the conclusion that this structure only develops during the current-decay stage of anodic film growth, when the effective field across the film is falling.

Fig. 15 illustrates optical transmission curves for films grown to 200 V on aluminium at 20°C at varying current densities - again no current decay was permitted after the voltage had been attained. Fig. 16 shows a thickness calibration chart based on the assumption that the film grown at the lowest current density had been growing at the thickness/voltage ratio of 14 Å ngstroms per volt. These results are compared in Fig. 17 with thickness values estimated from capacitance measurements. Again no calibration of thickness against reciprocal capacitance was made, it was assumed that the film grown at the lowest current density was growing at approximately

the equilibrium thickness and the other film thicknesses were estimated by taking the thickness to be proportional to 1/C. Fig. 17 therefore, shows that while capacitance measurements indicate that at higher growth current densities the thickness of the anodic film is reduced during growth, optical measurements show only a slight reduction which may be reversed at very high currents.

The effects of variations in applied voltage and electrolyte temperature on the steady state or 'leakage' current in borate electrolyte are shown in Fig. 18. These results confirm the findings of Stirland and Bicknell[20], that a change of properties occurs at about 100 volts due to the appearance of some crystallinity in the film structure (described in the discussion of Fig. 10). The steady state current is seen to increase markedly as the temperature rises.

b. Porous Films

At elevated temperatures the current decay curves during anodising in borate electrolyte showed a change of form. Aluminium sample 'B' (the purest material used) showed a very rapid attainment of a steady 'leakage' current. Sample 'A' (99.99% pure), on the other hand, showed a definite minimum in the current decay curve at constant applied voltage. A minimum also appeared when an anodic film was thickened by the application

of a higher potential, Fig. 19 shows results of this sort at 50°C. This behaviour is reminiscent of the growth of anodic oxide in a pore-forming electrolyte such as sulphuric acid[112]. Fig. 20 shows that the current decay behaviour of the two samples of aluminium during anodising in 15% sulphuric acid was similar to their behaviour in hot borate electrolyte. Sample 'A' showed the typical current minima but sample 'B' did not. The major difference between anodising behaviour in the borate and sulphuric acid electrolytes was the relatively small variation in 'leakage' current with variations in the applied voltage in the borate, compared with a considerable dependence on the voltage applied during sulphuric acid anodising.

Current-time curves showing the current minima during anodising of aluminium 'A' at 50°C in borate are illustrated in Fig. 21 for films grown at 50 V and 200 V. Similar anodic films were grown on other specimens and were removed from the electrolyte after varying times had elapsed after the fixed voltage had been attained. Figs. 22 and 23 show the reflectance curves obtained from these films. Fig. 24 shows the minima positions calibrated assuming that the film grown to 200 V in borate electrolyte at 25°C was 2800 Å thick. The thickness values estimated in Fig. 24 were plotted in Fig. 25 to show the variation in film thickness with time. For films grown at 200 V and 50 V there is an initial period roughly corresponding to the time taken for the

current minimum to appear in the current decay curve, Fig. 21. During this time, film growth above the initial voltage-dependent thickness is slow. When the current rises again and reaches a steady value, the film thickness increases appreciably and soon a fairly constant rate of film growth, which does not vary much with the applied voltage, sets in.

Although sample 'B' did not show the current minima typical of continued porous film growth, the anodic oxide film grown on it in borate at 50°C also showed film thickening. This could be detected by the appearance of a 'milky' semi-opaque film on the surface after about 30 minutes of anodising, indicating that the film had grown to a thickness much higher than usual.

Electron microscopy confirmed that the films grown in borate at 50°C were of the porous type and Figs. 26 to 30 show how the pore structure develops during growth. Fig. 26 shows for comparison purposes a barrier type film grown on aluminium in borate at 20°C to 100 volts. A crystalline inclusion is shown, though it occupies a large part of the field this is due to the high magnification, the spacing of these inclusions was of the order of 25-50 times their mean diameter. The bulk of the film material barely shows the 'granular' structure shown in Fig. 10 by means of a higher magnification and very high contrast. Fig. 27 shows a film grown in borate at 50°C and removed from the electrolyte

very soon after the pre-set voltage of 100 V had been attained. The important feature of the structure that should be noted is the appearance of a very fine pore structure, shown by the lighter shaded 'spots' in the micrograph. The appearance given to the film by the presence of these pores is very similar to the 'granularity' described above in connection with nominally barrier type films, when allowance is made for the fact that Figs. 10 and 11 are shown as 'negatives' while the other micrographs are reproduced as 'positives'. Dark spots in Fig. 10 must be compared with the lighter shaded pores shown in Fig. 27. Figs. 28, 29 and 30 show how as the film is left to anodise for more extended periods, the lighter spots, representing pores, become individually larger but fewer in number. This change in the pore structure does not seem to be proceeding so rapidly after about 15 minutes as in the earlier stages. The increasing thickness of the films deduced from Figs. 22 to 24 was shown in electron microscopy by a decrease in transmission through the films grown for longer periods; this has been compensated for in reproduction so as to give micrographs of comparable density.

c. Temperature During Anodising

A 30 cm. length of 0.1 mm. diameter aluminium wire was immersed for 20 cm. of its length in borate electrolyte at 20°C. The wire was anodised at 155 mA $cm.^{-2}$ to a voltage of 250 V. The following measurements were made.

	Resistance Ω
Resistance before anodising	1.0
Resistance during anodising	2.0 max.
Resistance with 'leakage' current flowing	1.3
Resistance after current switched off	1.3

The resistance of 1.3 Ω probably represents the true resistance of the wire at 20°C, the initially lower value being due to shunting of the unfilmed wire by the electrolyte. The experimental results therefore imply that the resistance of the immersed 20 cm. of wire rose from about 0.8 Ω to about 1.5 Ω during anodising.

The following data are available for the resistivity of aluminium[118].

Temperature °C	ρ Ω cm.$^{-3}$ x 10^6
0	2.5
100	3.6
300	5.9

The rise in resistance of the wire is thus consistent with a rise of temperature from 20°C to about 260°C during anodising at 155 mA cm.$^{-2}$.

D.2. Mechanical Properties of Anodic Films

a. Strengthening of Wires by Oxide Films

The effect of the presence of an anodic oxide film on a fine wire is shown in the stress-strain curves in Figs. 31 and 32. The whole of the stress-strain curve is raised by the presence of a film, the effect being particularly marked in the region of plastic deformation. The significance of the correction lines in the diagrams is discussed in Section E.2c. Fig. 33 shows the comparative effects of anodic films grown to different voltages. Up to 100 V an increased voltage (and hence film thickness) produces an increased strengthening effect, but films grown above 100 V do not appear to give much additional strengthening.

b. Constant Load Tests

An aluminium wire anodised to 200 V in borate electrolyte at room temperature was subjected to a 25 g. load in the modified balance apparatus. Initially no anodic voltage was applied, then a small voltage was applied and this was increased in steps. The further extensions of the loaded wire that occurred when the applied voltage was increased are shown in Fig. 34. An applied voltage of 50 V had no effect on the wire extension, but above this value measurable extensions occurred each time the voltage was increased. Increments above 200 V, the original

growth voltage of the film, produced relatively low further extensions. Fig. 35 shows that during this test the current flowing did not differ significantly from that on a similar specimen not under load.

Another wire was anodised to 200 V and loaded with 25 g. but instead of a controlled voltage being applied, a constant anodic current rather more than the 'leakage' current was passed. Fig. 36 shows that as the cell voltage rose, so did the extension of the wire specimen. The rate of extension of the wire reached a maximum when about 200 V was reached and then reduced until little further extension was occurring.

Further tests were made in which wires not previously anodised were loaded and then anodised under load. These wires too showed further extensions when the anodic current was passing and the extension-time curves for these specimens are compared with the extensions of pre-anodised wires under the re-application of the anodic growth voltage in Fig. 37. Curves 'b' and 'c' represent the extensions of wires during initial anodising under load. It is seen that even during the passage of a relatively high anodic current the extensions shown by the wires loaded during initial anodising were much lower than the extensions shown by pre-anodised wires. There tended to be a reduction in this extension once the pre-set voltage was attained and current decay set in. When initial anodising under load was

carried out at current densities similar to those used in the experiments described above for pre-anodised wires, the extensions that did occur were negligible and are probably attributable to creep of the mounting plastic (this is also the probable cause of the extensions shown in Fig. 34 before the application of a field).

A series of wires were pre-anodised to 200 V, loaded with 25 g., and controlled anodic currents were re-applied. These currents were above the 'leakage' current but below the current which Fig. 37 shows has a negligible mechanical effect on a wire during initial anodising under load. Fig. 38 shows that the wires to which higher currents had been applied tended to extend the most rapidly.

Another series of wires were pre-anodised to 200 V and were subjected to different loads. An anodic voltage slightly above that originally used for anodising was then re-applied to the specimens and the total further extensions that took place were measured. Fig. 39 shows how these extensions increased with the applied load (the significance of the 'expected' curve that is shown is discussed later).

It is implied in the results shown in Fig. 34 that a 'critical applied voltage' must be present before measurable extensions of loaded anodised wires can take place in the presence of an anodic current. A series of tests was therefore made in order to find out whether this voltage varies with the applied load.

Pre-anodised wires were loaded and an anodic voltage was applied which was increased in 10 V steps at 5 minute intervals. The extension increment at the end of each 5 minute period was measured and the results are shown (with arbitrary units of extension increment) in Fig. 40. Although there is a wide scatter of results it is clear that detectable extensions occur at lower voltages when increased loads are applied, and vice versa.

In view of the changes occurring in films grown in the borate electrolyte at elevated temperatures a comparison was made between the extensions under the influence of an applied field of pre-anodised wires at room temperature and at 50^{o}C. Fig. 41 shows that there was no significant difference between results at the two temperatures. This justifies the procedure described in Section C.2a., where the electrolyte temperature was not closely controlled, since variations in electrolyte temperature do not greatly affect the results of these mechanical tests.

No extensive tests were made using the other electrolytes, but simple re-application of anodic fields to pre-anodised loaded specimens showed that extension effects similar to those found with borate electrolyte also occurred with films grown in sulphuric acid and ethanediol, see Figs. 42 and 43. For ethanediol the extension was made under constant voltage conditions, while for the sulphuric acid a constant anodic current was applied.

No extension of aluminium wires under load was found during

electropolishing at current densities of the same order as those used during the experiments with anodising electrolytes. At very high current densities, however, an extension was noted which reduced somewhat when the current was switched off. The curve in Fig. 44 is approximate only, as can be seen only two experimental points were plotted, but there is a similarity with curve 'b' in Fig. 37.

A few tests were made of extension of pre-anodised 'Aluflex' wires under constant load. Fig. 45 shows that the extension of a pre-anodised loaded wire upon re-application of an anodic field was relatively small, and was of the same order as the final extension found during the initial anodising of a loaded wire. The latter experiment showed a reduction in the extension of the wire as the set voltage was reached and current decay set in; there was little change in extension when the current was subsequently switched off. This again was similar to the behaviour shown by curve 'b' of Fig. 37.

Some aluminium wire specimens were pre-anodised, loaded with 25 g., and then a high cathodic current was passed. Due to the rectifying action of the anodic film a current of 100 mA $cm.^{-2}$ could be passed without the applied voltage rising above one or two volts. Under these conditions no further extensions of wires were found.

An attempt was made to anodise aluminium wires, drain away

the electrolyte and replace it with mercury. The wires were then loaded and an anodic voltage was applied. It was not found possible to raise the voltage applied to a 200 V anodic film much above 50 V before electrical breakdown of the film occurred. No extensions of wires were observed in these experiments.

c. Constant Strain Tests

Effects which in experiments conducted at constant load are detected as extensions of wire specimens are shown in constant strain tests as reductions in the tensile load. Fig. 46 complements the results of the constant load tests. It shows the changes in load on pre-anodised wires which were subjected to a fixed strain and then had the original anodic voltage re-applied. The aluminium wires showed an appreciable load reduction on the application of the voltage, the 'Aluflex' wires, in contrast, showed an extremely small effect. The constant strain apparatus seems to be more sensitive than the constant load equipment since it detects a slight increase in the load when the anodising voltage is removed. No corresponding effect was detected using the constant load equipment.

A series of tests was made for aluminium and for 'Aluflex' wires at constant strain. Wires were pre-anodised, strained

by different amounts and an anodic voltage similar to that applied during anodising was re-applied. The total reduction of load accompanying the application of the anodic voltage was measured and the results are summarised in Fig. 47. They show that the aluminium wires gave load reductions that increased with the amount of pre-strain, the 'Aluflex' specimens gave very small load reductions that did not become larger as the pre-strain was increased. The significance of the 'expected' curves marked on these figures is discussed later.

In order to measure effects during the initial growth of anodic films on wire specimens, some wires were first strained and then anodised to 200 V in borate electrolyte. Fig. 48 shows that during the initial growth stage when a constant anodic current is flowing the load on the wires is progressively reduced. The reduction in load is most marked at high current densities. Once the pre-set voltage is reached and the current begins to decay to a low value the load reduction effect becomes less marked until the load on the wire is not far removed from the original load; any difference that remains is attributable to permanent plastic deformation of the specimen. Fig. 49 shows in greater detail the changes in stress that occur when an aluminium specimen is anodised under a fixed strain. During anodising at constant current there is a steady decrease in the indicated load. If the current is switched off there occurs a rapid increase in load, δ,

followed by a more gradual increase. If the current is then switched on again there is a rapid load reduction, δ', approximately equal to δ. The load then steadily reduces until the pre-set voltage is reached and current decay starts. At this stage the indicated load increases and even appears to pass through a maximum value and decrease again slightly. If the same voltage as that the film was grown to is now switched on and off relatively small changes in load occur, these correspond to the small changes in load shown at 'stage 3' in Fig. 46.

d. Bending Tests

Fig. 50 shows the deflection of the pointer in bending experiments on aluminium strips; the deflection axis shows deformation in the sense of decreasing the radius of curvature of the specimen. When a field is re-applied to a stressed pre-anodised specimen there is a measurable deflection indicating a reduction of the radius of curvature. Removal of the field has no detectable effect. If, however, an etched specimen is loaded and then anodised a relatively large deflection is measured. This deflection lessens once the pre-set voltage has been reached and current decay starts. The effects displayed by this bent strip specimen seem different from those shown by wires where, except

at very high current densities, effects during the anodising of loaded specimens were very much smaller than effects during the re-application of an anodic voltage to a pre-anodised specimen.

SECTION E

DISCUSSION

E.1. Nature of the Anodic Films

a. Barrier Type

Anodic films grown on aluminium in the borate electrolyte at normal ambient temperatures are of the barrier type and have the structure usually described as 'amorphous' or 'glassy'. Some crystalline inclusions may be present in these films. No evidence has been found of any deviation from the constant thickness/voltage ratio that is characteristic of barrier films, although films grown to a constant voltage and low 'leakage' current show what has been described as a 'granular' structure. This feature resembles in appearance the fine pore structure that is present during the initial stages of growth of porous type films in this electrolyte at elevated temperatures. This resemblance may be seen by comparing Figs. 11 and 27. The 'granularity' may therefore be interpreted as an incipient ultra-fine pore structure.

During the growth of barrier films at controlled current density this incipient pore structure is not seen; it only develops when the film is allowed to grow at a fixed voltage till the current has decayed to a steady low value (see Figs. 10 to 14). This is in agreement with the observations of Hoar and Yaholom[112] who described how the initiation of pores is inhibited by the presence of a high anodic field.

When a film is being grown at a controlled current density it is found that at a given voltage the thickness varies with the

current density. It would be expected from the high-field conduction equation (equation 4) that the film thickness would reduce as the current increases according to a relationship of the form:

$$t \propto - \text{Log } I$$

where t is the film thickness at a fixed voltage.

Capacitance measurements indicate that the film thickness does indeed reduce as the growth current density increases, this is shown by the results in Fig. 17. The straight line relationship that would be expected from the logarithmic plot is, however, not shown. The results of optical thickness measurements, in contrast, do not even show the continuous reduction in thickness with increasing current that the capacitance measurements do. The optical thickness decreases as the current is raised up to about 20 mA $cm.^{-2}$, but above this current density further increases lead to an increase in the indicated thickness.

These unexpected results of optical measurements may be explained in several ways. It could be that the refractive index of a film growing at very high current densities is higher than that of films grown to a 'leakage' current, there is, however, no independent evidence to support such a view. It has been shown in this work that the temperature of the anodic film may rise by the order of hundreds of degrees Centigrade during

anodising at high current density. It might be suggested that under these conditions the electrolyte temperature in the vicinity of the oxide surface is raised and some porous film growth could proceed due to increased oxide solubility. The electron micrographs shown in Figs. 10 and 12 do not support such a view, since there is a marked absence of any detectable pore structure in the film grown at 100 mA $cm.^{-2}$. A third explanation to which there seems no obvious objection is that during growth at very high applied fields or temperatures an effect occurs similar to that found by Bray et al.[99], during the anodising of tantalum under ultra-violet irradiation. These conditions led to film growth above the usual thickness but not detectable by capacitance measurements. The mechanism by which this type of growth may proceed is still rather obscure.

Anodic oxide films grown on the 0.8% magnesium alloy 'Aluflex' are similar in properties to the films grown on pure aluminium. As shown by Fig. 8, the anodic current that passes when the alloy has been anodised to a steady state current at a given voltage is higher than that passed on an aluminium specimen. This could be attributed to increased imperfection of the film due to impurities in the alloy or to the effect of the lower-valency addition in increasing n-type conduction in the oxide. The ratio of thickness to voltage does not significantly differ for barrier films grown on the alloy and films grown on

aluminium (see Fig. 9). This implies that ionic diffusion rates under similar applied fields do not differ and hence, as shown by the similarity between the micrographs in Figs. 10 and 11, the structure of anodic films is not greatly affected by this alloying addition.

b. Porous Type

In the borate electrolyte at 50°C the anodic films grown on aluminium changed from the usual 'barrier' type growth and showed the continued thickening with time at a fixed voltage that is characteristic of 'porous' films. Electron microscopy confirms that a well-developed pore structure appears during the growth of these films. The important difference between electrolytes which sustain the growth of the two types of anodic film is the low solubility of alumina in barrier electrolytes and its high solubility in pore-forming electrolytes. It is therefore probable that the change of anodising characteristics in the borate electrolyte is caused by increased solubility of the film due to the rise of temperature.

The minimum that often appears in current decay curves during porous film growth has been discussed by other workers[112]. The initial drop in current is associated with thickening of the barrier layer. The rise in current that follows is due to the

pore formation process. A curve of this form implies that the porous layer is not simply growing on top of an unaltered barrier layer, if this were so no current rise could occur. The nature of the structural change that must take place in the barrier film was discussed in terms of proton entry into the film by Hoar and Yaholom[112], and more recently in terms of a change in chemical bonding in the film by Dorsey[117]. An interesting feature revealed by the present work is that the appearance of the minimum can be affected or even suppressed by very slight variations in the level of impurities. The metal that was nominally of the highest purity did not show current minima at all, although the film thickening typical of porous growth was taking place. A possible explanation of these results could be that in the case of the ultra-high purity aluminium the secondary processes leading to the current rise can take place extremely rapidly. Fig. 51 illustrates diagramatically how the total current curve (which equals the sum of the barrier layer decay curve, a, and the secondary pore current curve, b) will not show a current minimum if the secondary process starts very quickly.

The rate of porous film growth in the borate electrolyte does not vary very much with the applied voltage (see Fig. 25). If it is assumed that the current which sustains porous growth is equal to the difference between the steady state currents at

50°C and 25°C (where barrier behaviour is shown) the similarity in growth rates can be accounted for. It can be seen from Fig. 18 that at 50 V this difference amounts to some 0.6 mA $cm.^{-2}$ and at 200 V it is about 0.7 mA $cm.^{-2}$. Thus it would be expected that the difference between growth rates at these two applied voltages would be very small. The properties of porous films grown in hot borate electrolyte seem to differ from those grown in sulphuric acid in this respect. Sulphuric acid films show a considerable variation in the steady-state current with the applied voltage (see Fig. 20). This behaviour implies that alteration of the barrier layer structure is more pronounced in the case of these films.

Especially during the initial stages of porous film growth the pore structure changes markedly with time. Previous workers have investigated the effect of changes in the electrolyte composition and the applied voltage on the size and spacing of pores[19]. It has also been shown that 'barrier' type films can develop a pore structure and that pores do not usually appear in the very earliest stages of film growth[15-18, 112]. Little attention, however, seems to have been paid to studying the changes that occur in the pore structure during anodising. As has been shown from the electron micrographs in Figs. 27-30 these changes could well be large enough to mask effects due to other causes.

The alterations in pore structure that take place during film growth are consistent with effects due to dissolution acting primarily on the inside of the pore walls. It appears that for this borate electrolyte a slight solvent action at 25°C or less is able to produce a very fine pore structure on even a 'barrier' type film. At higher temperatures the solubility of alumina is increased. Dissolution of the pore walls enlarges pores and enables them to pass a higher anodic current. This higher current in turn may raise the local temperature at a pore and enhance the solvent action of the electrolyte. Such an accelerating process would tend to favour the growth of the larger pores in a film. The additional film material grown as a result of the enhanced pore current would tend to fill in those smaller pores which were not passing so much current. The net result of such a process would be to reduce the number of pores but increase the size of remaining ones, just as is observed in the series of micrographs of porous films grown for increasing times. As the film thickened the length of the pores would increase and pore resistance would tend to limit the current flowing. This effect would tend to reduce the rates of pore enlargement and of reduction in numbers as the film thickness increased, as is also shown by the micrographs.

Although the morphology of films grown in borate electrolyte alters at elevated temperatures the results shown in Fig. 41

indicate that there is no corresponding change in the results of mechanical tests. The reasons why the changes in film thickness accompanying the temperature changes did not influence mechanical properties are discussed in Section E.2a.

E.2. Analysis of Stress Conditions During Tests

a. Stress on the Oxide

The dominant stresses on the anodic oxide film on a fine wire loaded in tension are not of a simple tensile nature. This is shown by the results in Fig. 33, where the specimen anodised to 200 V is shown to be not significantly stronger than one anodised to 100 V and hence carrying an oxide film of half the thickness. The presence of an oxide film on a wire loaded within the elastic range prevents dislocations from moving out of the surface to form slip steps. It is the stress field set up in the oxide by these dislocations that gives rise to the strengthening effect on wire specimens; because the dislocation slip planes will not all be on similar crystallographic planes the stresses set up in the oxide film will be complex in nature. The results in Fig. 33 which indicate that the strengthening effect increases with film growth voltage below 100 V, but not above this value, lead to the conclusion that the stress field extends no more than about 1500 Å from the metal-oxide

interface for wire extensions of 1.5% or less.

This would explain why the thicker porous film showed results in a mechanical test (Fig. 41) similar to a thinner barrier film; both films were thicker than 1500 Å.

If the mean stress in the inner 1500 Å of an anodic film on a stressed wire is called Σ, then it is reasonable to assume that:

$$\Sigma \propto \sigma$$

where σ is the difference between the load carried by an anodised wire and that carried by an unanodised wire at the same extension.

b. Constant Load Conditions

Fig. 52 illustrates the stress conditions when an anodised fine wire specimen is loaded in tension. 'A' is the stress-strain curve for an anodised wire, 'B' is the curve for an unanodised wire.

When an anodised wire is subjected to a fixed load, P_4, the stress on the oxide is proportional to σ where

$$\sigma = (P_4 - P_6)$$

The results plotted in Fig. 39 show that if an anodic field is re-applied to this specimen an extension approximately equal to $(X_3 - X_1)$ takes place (the 'expected' curve is a plot of the difference in extension at a fixed load between the two stress-strain curves in Fig. 31). After such an extension it is seen that:

$$\sigma = 0$$

If this extension is attributed to enhanced oxide plasticity the anodic film may be considered to have undergone deformation under the influence of a steadily decreasing load. Since curve 'B' in Fig. 52 approximates to a straight line between X_1 and X_3, at an intermediate stage of the extension, X_2, the stress on the oxide is given by:

$$\sigma = (P_4 - P_5)$$

There should thus be a straight-line relationship between σ and the amount of extension that has taken place.

c. Constant Strain Conditions

An anodised wire subjected to a constant strain, X_4, will carry a load, P_1, and:

$$\sigma = (P_1 - P_3)$$

If the oxide was able to relieve stresses in a plastic manner the load would reduce from P_1 to a final value of P_3, σ reducing to zero during this process. If, however, a load cell with a measurable deflection under stress was being used to measure the load carried by the wire, the relaxation in stress on the wire would be accompanied by an extension of the wire $(X_5 - X_4)$ where the sensitivity of the load cell is equal to:

$$\frac{(X_5 - X_4)}{(P_1 - P_2)}$$

The final relaxation in load on the wire would be smaller than expected, by the amount $(P_2 - P_3)$. For this reason the dotted sloping lines indicating the sensitivity of the load cell used were added to Figs. 31 and 32 and a correction was applied when plotting the 'expected' curves marked in Fig. 47. These 'expected' curves represent the difference in load between anodised and unanodised wires at the same extension and were obtained from Figs. 31 and 32.

This correction was not needed in the case of the 'expected' curve marked in Fig. 39 since at a constant load the load cell error is the same for all specimens.

E.3. Interpretation of Results in Terms of Oxide Plasticity

a. Previous Interpretation

The extension of loaded anodised wires when subjected to an anodic field was considered by Bradhurst[33] to be due to enhanced oxide plasticity. This plasticity was attributed in a general way to the increased ionic diffusion flux in the oxide under the influence of the applied field. Calculations indicated that this diffusion flux was probably of the correct order of magnitude to account for the oxide plasticity.

The fact that the extensions measured (and in the case of the present work, the reductions in load) correspond closely to the difference between the stress-strain curves for anodised and unanodised wires was a strong indication that they are due simply to the removal of the strengthening effect of the surface oxide film. There are, however, several other possible explanations for the observed effects, and it is necessary to consider each one in greater detail.

b. Surface Removal (Dislocation 'Pop Out')

The work of Kramer and associates[41-48] has shown that the intrinsic resistance of a metal surface to the passage of dislocations can strengthen single crystal specimens, and enhanced plasticity can result when this surface layer is removed by continuous dissolution. This surface layer was estimated to extend about 0.05 mm. below the surface. In the case of the fine wire specimens used in the present work this would mean that the surface effect extended right through the specimen, hence surface dissolution might not be expected to influence the plasticity of the wires very much. Nevertheless, since during anodising some removal of surface metal is taking place, it is necessary to consider this effect as a possible source of the wire extensions.

The results shown in Fig. 44 show that at extremely high current densities of electropolishing some wire extension under a constant load can be detected. Dislocation 'pop out' is a likely cause of this deformation. The slight reduction in extension when the current was switched off corresponds to effects noted by Kramer[44] and ascribed by him to variations in the temperature of specimens.

Electropolishing at current densities (hence also rates of metal removal) similar to those used during the extension of anodised wires (under 10 mA $cm.^{-2}$) showed no detectable effect.

The evidence is, therefore, that though dislocation 'pop out' can affect wire strengths at very high rates of dissolution, the phenomenon does not play a significant part in the extensions of wires at the low current densities used in the present work.

c. Temperature Effects

The effect of temperature changes during electropolishing have been mentioned above. It might be thought that the extensions and stress reductions shown by anodised wires in the experiments described above are also due to temperature rises caused by the passage of an electric current.

It is most improbable that the temperature of the oxide film could be raised to about 1000°C so as to produce oxide plasticity due to thermal activation. At such temperatures visible radiation would be emitted. In view of the relative thinness of the oxide film and its intimate contact with the metal substrate it seems likely that the temperatures of the metal and its oxide film will be very close.

Almost all the energy that is consumed during the anodising of a wire is dissipated in the oxide film itself. For example, a film growing at 100 V and 100mA cm^{-2} is absorbing 10 watts $cm.^{-2}$. If only a small proportion of this energy appeared in the form of heat the temperature of a fine wire specimen could be raised

considerably. The equilibrium temperature of a specimen would depend on the rate of heat transfer to the electrolyte. As a film increased in thickness at a constant applied current the temperature of a specimen would tend to rise as the power dissipated in the film increased with the increasing voltage, and film thickness increased, reducing heat transfer.

The thermal coefficient of linear expansion of aluminium is about $25 \times 10^{-6}\ ^{o}C^{-1}$ (118). Thus, the stress relaxation during the growth of an anodic film at 375 mA $cm.^{-2}$, (see Fig. 48), which approximates to an extension of 0.1%, could be accounted for by a temperature rise of some 400 ^{o}C. The extension of about 0.04% indicated for the specimen anodised at 62.5 mA $cm.^{-2}$ would require a rise of about 160^{o}C. These figures seem consistent with the temperature rise of 240^{o}C measured for a wire anodised at 155 mA $cm.^{-2}$ and lead to the conclusion that the changes in length or stress observed during the growth of anodic films may be largely accounted for by temperature changes. In the present results such temperature effects are seen in Fig. 37 (curve b but not curve c); Fig. 45 (curve A); Fig. 48 and Fig. 49. It may be that the small changes in indicated stress shown when the 'leakage' current was switched on and off in Fig. 46 (stage 3) and Fig. 49 (stages 5, 6 and 7) are also due to temperature changes, but it may be possible to ascribe these changes to electrostatic forces, as discussed below.

The effect of temperature on metal specimens is reversible, so when currents decay to low values when a fixed voltage is applied to a film the extensions produced at high current densities are reversed. The permanent extensions that are indicated by the results in Fig. 48 are due to the wires having been stressed beyond the elastic limit, removal of the thermal forces in this case does not permit the wires to return completely to their original state. Effects of this sort are more likely to be noticeable under conditions of constant load stressing than under constant strain conditions. Extension of a wire under constant strain produces a relaxation of stress in the load cell thus the load on the wire is relieved in a way that does not occur when a constant load is applied. This is why, for instance, the recovery of an extended wire during the current decay period is much less marked in Fig. 37 (curve b) than in Fig. 48 (6.3 mA or 18.8 mA curves). It also explains why the very small changes in extension that occur when the steady state current is switched on and off are detectable in constant strain tests, e.g. Fig. 49 (points 5, 6 and 7), but are not shown in constant load tests, e.g. Fig. 45 (current 'off' points on both curves).

When an electric field is re-applied to a pre-anodised wire the currents that flow are much less than those which can flow during the initial anodising. This can be shown by

comparing the results in Fig. 35, which show a maximum current of about 1 mA cm.$^{-2}$ when 200 V is re-applied to a 200 V film, with the current densities of up to 375 mA cm.$^{-2}$ that were passed during the initial anodising of specimens. It would, therefore, be expected that thermal effects are not likely to be so important during the re-application of a field to an anodised specimen as during initial anodising. This is confirmed by the results of constant strain tests on pre-anodised wires shown for aluminium in Fig. 46. The initial stress relaxation at stage 1 is attributable to creep of the mounting plastic. At stage 2 the field was re-applied and a large stress relaxation was shown. When the field was switched off again, at stage 3, only a very small recovery of stress was noted. Judging by the large recovery after the removal of thermal effects shown by the curves in Fig. 48 it may be deduced that the stress relaxation shown by aluminium at stage 2 in Fig. 46 was not due to thermal expansion. The relaxation shown by the 'Aluflex' wire under similar conditions is seen to be relatively small and of the same order as the recovery in stress that accompanies the removal of the field at stage 3. In this case, therefore, it must be assumed that thermal effects (and perhaps electrostatic effects also - see below) can account for most of the observed mechanical effects.

These conclusions on thermal effects are supported by the

results of constant-load tests on wires. Fig. 36 shows that the application of a relatively low current (0.156 mA cm.$^{-2}$) can produce 0.4% extension of a pre-anodised wire loaded at 25 g. In contrast, Fig. 37 (curve 'b') shows that a much higher current (10 mA cm.$^{-2}$) passed during the initial anodising of a similarly loaded wire produces the far smaller (thermal) extension of 0.1%.

It has therefore been shown that while thermal effects can account for the mechanical changes observed in wires during anodic film growth at high current densities, they are not sufficient to explain the deformation and stress relaxation effects observed on pre-anodised aluminium wires.

Measurements of the deflection of a loaded aluminium strip specimen during initial anodising (Fig. 50, curve 'a') bear a superficial resemblance to the thermal effects described above. There is a deflection during anodising that reduces once the pre-set voltage is attained and current decay starts. In view of the results of temperature measurements during anodising of wires it does not seem probable that the relatively low current density used could heat the metal strip sufficiently to affect Young's Modulus. It would appear that a deflection of the sort observed can only be accounted for by asymmetrical growth of the oxide film on either side of the strip. During film growth the thickness and internal

stress of the film might differ on the two sides, leading to a temporary stress on the strip which would disappear when the films on each side had fully grown and were in more similar conditions. Since the 'throwing power' of an electrode-electrolyte combination is high when electrode polarisation is high, it does not seem possible that uneven oxide growth is caused simply by geometrical factors leading to uneven current density. A more likely explanation would be that the rate of oxide growth is affected by the state of compression or tension of the metal surface. In any event it is clear that while it may be possible to carry out experiments on the mechanical properties of oxide films using metal strip specimens, there may be complicating factors which make interpretation difficult. It was for this reason that this method of testing was not used more extensively in the present work.

d. Electrostatic Effects

There is an attractive force, P, between oppositely charged sides of a film or layer of dielectric which, ignoring edge effects, is described by the equation for a unit area of the film[113]:

$$P = \frac{E^2 k}{8\pi} \qquad (5)$$

E is the field in the dielectric and k is the dielectric constant.

In the case of the oxide films on wire specimens this electrostatic force would produce a compressive force in the longitudinal direction arising from the tendency of the oxide to relieve the pressure by expanding laterally, a tendency quantitatively assessed by Poisson's ratio.

Such an electrostatic force during the application of an anodic field would act in the same sense as the thermal effects discussed above. It would be difficult to distinguish between thermal and electrostatic forces unless accurate temperature measurements were made. Since, however, it has already been shown that most of the observed effects during film growth at high current density can be adequately explained in terms of temperature fluctuations, there does not seem to be any reason for postulating the existence of a large electrostatic effect. It is possible that the very small reversible mechanical effects which appear when 'leakage' currents are switched on and off, such as those seen in Fig. 49 (points 5, 6 and 7), are due at least in part to electrostatic forces. Even if this were so, it would show that electrostatic forces are not of the magnitude required to produce the relatively large mechanical effects found on the re-application of an anodic field to pre-anodised specimens.

e. Coherence at Metal-Oxide Interface

A mechanism was suggested by Vermilyea[25] for the relief of constraint between a metal and its oxide film during film growth. If growth of a film at this interface proceeded not by a uniform removal of metal all over the surface, but by the removal of metal at the edges of 'steps' or other surface defects, the incoherency at the step edge would traverse the metal surface and would permit relative movement between the metal and the oxide, thus relieving stresses. Such a mechanism would remove the strengthening effect of a surface film during growth, but without enhancing the plasticity of the film material.

If such a mechanism were in operation it would require that before complete stress relief could be achieved metal must be removed from the oxide-metal interface to a depth approximating to the size of the slip steps that would form as the wire specimen deformed. The only indication of the size of these slip steps is the extent of the stress field in the oxide film, which appears to be about 1500 Å. It is reasonable to assume that slip steps on the metal surface would not be less than say an order of magnitude less than this distance. If then, complete stress relief were to occur on a strained wire bearing a 200 V anodic film, something like a 5% additional film thickness would need to be grown. If, for example, the extension curve shown in Fig. 34 is examined, it will be seen that considerable wire

extension occurs when 150 V is applied to a film originally grown to 200 V. In this case the additional film growth that can occur must be very small indeed, certainly well below the 1%-5% range. On the available evidence, therefore, a stress relief mechanism as suggested by Vermilyea does not seem to provide an acceptable explanation of the observed results.

f. Present Interpretation

Various possible explanations for the deformation and stress relaxation effects on anodised wires have been discussed. While it seems that in the case of 'Aluflex' it is possible to account for all the observed effects in terms of temperature or electrostatic effects, the most satisfactory explanation for the behaviour of pure aluminium wires is that proposed by Bradhurst[33]. This suggested that during the passage of an anodic current the oxide film on aluminium has enhanced plasticity. The rate of extension or of stress relaxation of such a specimen may be expected to be directly related to the rate of deformation of the oxide film. The features of this oxide plasticity may now be discussed in detail and possible mechanisms accounting for it considered.

E.4. Features of Oxide Plasticity

a. Field Dependence

The similarity of the experimental and 'expected' curves shown in Fig. 39 indicates that enhanced oxide plasticity permits virtually complete relief of stresses in an anodic film on aluminium when an anodic field similar to that used during anodising is re-applied. Fig. 34 shows that if a field less than this value is applied some oxide plasticity may be present but measurable creep ceases while there is still appreciable stress on the oxide. In Fig. 53 the results in Fig. 34 are plotted so as to show how the total extension of the anodised wires increases in a linear manner with the applied field above 100 V.

The oxide may be thought of as behaving as if it had a 'yield point' which appears at high stresses when the applied field is low, and which appears at very low stresses when a high field is applied. This behaviour may be represented diagramatically as in Fig. 54. At high applied fields almost all the stress-strain curve consists of a plastic region, while at lower fields there is an appreciable elastic region before plasticity appears. An oxide film bearing a stress, S, would extend by an amount $(X_2 - X_1)$ if a field V' were applied. If a higher field V'' were applied the extension would increase to $(X_3 - X_1)$.

Mechanical properties of the sort represented in Fig. 54 would imply that an oxide film bearing a low stress would require a higher applied field before showing plasticity, for instance at a stress S' no extension would occur if the field V' were applied but the field V'' would produce an extension $(X_5 - X_4)$. That such behaviour is in fact shown is supported qualitatively by the results in Fig. 40 which show that at higher applied loads oxide plasticity appears at lower voltages. There is an apparent discrepancy between these results and those represented in Fig. 53. For a wire pre-anodised to 200 V and subjected to a 25 g. load, for instance, Fig. 40 indicates that oxide plasticity appears at 160 V, while Fig. 53 shows the onset of plasticity at about 75 V. This difference is due to the different methods of applying the field. For the experiments described in Fig. 40 the voltage was increased stepwise in 10 volt increments. This would make it very difficult to detect the small extensions that would occur at low applied voltages, and hence measurable changes in extension only appeared at higher applied voltages. The wide scatter of the results makes it difficult to draw any quantitative conclusions from these experiments but they do confirm the expected qualitative relationship between the applied stress and the 'threshold field' at which plasticity becomes appreciable.

Fig. 34 seems to show that fields in excess of the original growth field can produce additional small extensions of loaded

wires. When such fields are applied, further growth of the anodic film occurs and currents rise to high values. Under these conditions extensions can be caused by thermal effects, as discussed in Section E.3c, and the extensions found at higher applied fields are probably due to this cause.

b. Current Dependence

The electric current flowing through an anodic film may have three components:

1. Ionic current through the film.
2. Electronic (or positive hole) current through the film.
3. Current by-passing the film at defects.

Components 2 and 3 together comprise the major portion of the 'leakage' current that flows through a barrier type film held at a constant voltage. If the total current that flows is significantly larger than this 'leakage' current, ionic conduction will provide a significant proportion of this current. Under these conditions changes in the total current caused by changes in the applied field would be closely related to changes in the ionic current. If, on the other hand, only the steady state or 'leakage' current is varied, for instance by changes in temperature (see Fig. 18), such variations are not likely to be reflected by changes in the ionic flux.

It has previously been pointed out that Fig. 38 shows how the extension rates of loaded anodised wires increase as the anodic current re-applied increases. The currents used in this series of tests range between the 'leakage' current (about 0.06 mA $cm.^{-2}$) and a higher current (0.625 mA $cm.^{-2}$) which has been shown (Fig. 37) not to be high enough to produce thermal effects. The initial rates of deformation of these specimens all represent oxide deformation at a similar maximum applied stress. These initial deformation rates were measured by taking the slopes of the first parts of the extension-time curves. These results were used to plot Fig. 55, which shows that the deformation rate of the specimens (and hence of the oxide also) is proportional to the current flowing.

No such simple relationship is found when the current is altered by other means than by controlling the voltage applied to the cell. The alloy 'Aluflex' passes higher anodic currents than does aluminium at the same voltage, as is shown by the current-time curves in Fig. 8, but it does not show the well-defined oxide plasticity effects that aluminium does. A large rise in the steady state current may be brought about by a rise in temperature (see Fig. 18) but this has no measurable effect on oxide plasticity, as is shown in Fig. 41. In view of the experimental results which show that at 50°C the borate electrolyte may sustain porous film growth, it might be asked

why the increased ionic current that must be passing at this temperature does not produce an increase in oxide plasticity. This increased current is concentrated at pores in the film. Thus a 'skeleton' of non-porous material is always present in the film, and no increased current is passing through this material. This 'skeleton' will thus not have its mechanical properties significantly altered by the presence of increased pore current.

c. Load Dependence

As discussed in Section E.2b the stress in the oxide, Σ, can be directly related to the proportion of deformation that has taken place during an experiment at constant load.

Fig. 56 (derived from Fig. 35 by measuring the slope of the extension curve at various points) shows the deformation rate of an aluminium wire as a function of the total extension. The initially linear form of the graph shows that the creep rate of the oxide is proportional to the applied load. The graph deviates from linearity when the creep rate falls to a low value. Probably under these conditions creep in the mounting resin is of the same order of magnitude as creep of the anodic oxide film and interferes with the results.

d. Effect of Alloying

Tests on anodised wires loaded in tension indicate that the oxide grown on 'Aluflex' has very limited plasticity, if in fact any is present at all. The effects that can be detected are of similar magnitude to effects due to thermal or electrostatic forces.

The only intentional alloying addition in this material is magnesium, but it must be remembered that in this commercial alloy many impurities are also present. Any specific deductions as to the effect of alloying on oxide plasticity must therefore be subject to some uncertainty because of this.

E.5. Diffusional Theory of Oxide Plasticity

It has been shown that the extension effects shown by anodised wires in the present work are most satisfactorily explained in terms of oxide plasticity. It has also been shown that in considering possible mechanisms for the deformation of anodic alumina it is reasonable to consider those mechanisms which apply to crystalline materials. In view of the highly disordered structure of anodic alumina films it seems logical to consider first of all whether a purely diffusional mechanism (as suggested originally by Bradhurst[33]) is able to account for all the observed effects.

In the anodic alumina films considered in this work cationic diffusion is certainly much slower than anionic diffusion. If this were not so it would be difficult for a pore structure to develop at the oxide-electrolyte interface. The movement of cationic vacancies would therefore be the rate-controlling step in diffusional deformation. This would apply even if, as has been suggested earlier, diffusion of cations in the oxide may proceed by an interstitial mechanism. Deformation requires vacancy movement, and movements of vacancies can be assisted by interstitial ionic diffusion so long as an interstitial 'jump' starts and ends at a stable lattice position. In such a case the vacancy may be considered to have migrated by means of a 'long jump' many lattice spacings long, instead of the more usual concept of a 'jump' to an adjacent lattice site.

The high degree of disorder in the structure of anodic alumina films is illustrated by the diffuse diffraction patterns obtained by previous investigators, and the lack of any crystalline structure in the bulk of the film material that the present work has shown using electron microscopy. The presence of this disorder would imply that very many regions are present equivalent to the grain boundaries that take part in Herring-Nabarro creep. Diffusional deformation of ordered regions would therefore be facilitated as in the case of a material of extremely fine grain size. The production of excess

vacancies at sites equivalent to grain boundaries under tension would be controlled by the same factors as in conventional Herring-Nabarro creep. The rate of deformation would thus be directly proportional to the stress, as has been confirmed by the experimental results.

The creep rate would also be directly related to the diffusion flux of ions of the slower-moving species. It would be expected that diffusion of these ions would be related to an applied anodic field in the same way as the diffusion of the faster-moving ions which carry the major proportion of the ionic current. If this were so, the creep rate would be directly proportional to the field-induced ionic current passing through the oxide. Behaviour of this kind is indicated by the experimental results. Changes in anodic current not involving changes in the ionic flux of the slower-moving species would not be expected to affect the oxide creep rate. Again, the results of experiments involving temperature changes are in agreement with this prediction.

Under conditions of high applied field the ionic current would be expected to increase exponentially with the applied field. This means that over a relatively narrow range of field, the 'threshold field', ionic diffusion would increase rapidly from rates insufficient to give measurable creep to a rate where creep becomes marked. At high stress levels the alteration

of vacancy concentrations at grain boundary or equivalent sites is increased, hence the driving force for vacancy migration is also increased and measurable creep would appear at lower applied fields. The observed field-dependence of the oxide creep is therefore largely in agreement with a diffusional mechanism. There is, however, one point that the experimental results leave in doubt. When fields are applied so that the voltage is less than that to which the anodic film was originally grown, the deformation does not appear to proceed to completion but stops while there is still appreciable stress on the oxide. Since the growth voltage represents the field at which movement of the faster-moving ionic species becomes negligible for oxide growth purposes, there is no obvious reason why diffusional creep controlled by the slower-moving species should only proceed to completion at this applied field. It is suggested that creep of the oxide does not cease altogether while there is still appreciable stress applied to it, but at low fields the creep rate rapidly drops to a rate that, though finite, is too small to measure. The ionic flux reduces very sharply as the applied voltage falls and so creep would only proceed at a significant rate at the higher stress levels obtained at the beginning of a deformation experiment. It would be very difficult to make experimental measurements on the creep of wire specimens over long periods of time as creep of the mounting material and the metal might mask oxide creep; also

even slight shocks to the apparatus would interfere with measurements.

The evidence of electron microscopy, spectrophotometry and current-time curves does not suggest that any fundamental difference in the morphology or lattice structure of the anodic film is brought about by the alloying additions or impurities in 'Aluflex'. In particular the unchanged Ångstrom/volt ratio shown by the alloyed film indicates that there is no substantial change in ionic diffusion rates.

Applying Wagner-Hauffe principles, the addition of magnesium divalent ions to the cationic lattice would be expected to decrease the concentration of metal vacancies in the lattice. This would make diffusional deformation more difficult. As has been mentioned previously, however, the presence of metallic impurities in the alloy used for the experimental work makes it difficult to draw unambiguous conclusions from the observed results, which show that alloying reduces or eliminates oxide plasticity.

The question might arise as to whether it is possible for the highly directional ionic flux induced by a high field to support non-directional deformation of the anodic oxide. The actual deformation, however, is accomplished by the migration of vacancies under the influence of a concentration gradient, not an electric field. This migration is facilitated by the enhanced

ionic flux in the presence of a field, since more ions are entering or leaving stable lattice positions, but although the ionic current is directional the movement of vacancies need not be.

This proposed diffusional mechanism for oxide deformation is supported in a semi-quantitative manner in that the stress and current dependence of oxide creep appear to be consistent with diffusional processes similar to those producing Herring-Nabarro creep. It would be more satisfactory if the actual rates of deformation could be calculated. Such a calculation would require data on the activation energy for diffusional deformation, the effective grain size of the oxide and absolute values for the stress acting on the oxide. As has already been mentioned, the mechanical properties of alumina films cannot be predicted from information on bulk oxides. In view of the lack of the necessary data, therefore, calculation of expected deformation rates cannot be at present attempted.

E.6. General Application of Plasticity Theory

a. Anodic Films

The experimental work described and discussed above relates only to aluminium and an aluminium alloy. This is because the practical difficulties in testing specimens of the other valve metals did not permit the apparatus used in the present work to be used for testing these other materials. All the other valve metals are far stronger than aluminium and hence the surface strengthening effect is difficult to detect. It is also difficult to obtain very fine wires of these metals. It would be expected, however, that enhanced oxide plasticity in the presence of an applied field might well show itself in anodic oxides other than alumina.

It is interesting to note that in the work reported by Bubar and Vermilyea[114], the high plasticity of tantalum and zirconium anodic films was shown while the films were extended in the presence of a low anodic field. While no importance was ascribed to this field in connection with the mechanical properties of the oxides it would be instructive to know whether this plasticity is present to the same degree in the absence of any applied field.

The diffusional mechanism discussed for the case of plasticity of anodic alumina films would only apply to films in which both ionic species showed some mobility. It has been reported that

during the growth of an anodic film on zirconium only the anions are mobile[12]. If this is so it should not be possible for field-activated diffusional creep to take place. However, where oxide films have a well-developed crystalline structure it is conceivable that the electromechanical effect[105-109], could produce oxide plasticity in the presence of a high electric field. Such a plasticity effect might be difficult to distinguish from diffusional deformation of the type proposed for anodic alumina.

Enhanced oxide plasticity during anodic film growth can account for the fact that internal stresses in anodic films often seem to be very much less than the ultimate strength of the film material[28]. During film growth there would be a relatively low effective yield stress; internal stresses from any source would be unable to exceed this value unless they developed after the removal of the anodic current.

b. Other Oxide Films

The electric fields associated with the growth of thermal oxide films and non-anodic aqueous corrosion films are relatively low. During the growth of any oxide film, however, diffusion rates much higher than normal are present due to the high activity gradients across the film. Conditions favourable to

enhanced oxide plasticity during growth might therefore be expected to occur in some instances. The predictions of the Wagner-Hauffe theory of oxidation kinetics only consider the effect of the defect structure of the oxide on the rate of movement of reacting species. The theory does not take into account the effect of changes in the mechanical properties of oxide films on corrosion rates. The principles on which it is based, however, might well be of value in predicting changes in diffusional plasticity which are influenced by changes in the defect structure of the oxide.

SECTION F

CONCLUSIONS

1. Oxide Plasticity

The results of previous work on the deformation of oxide-covered aluminium wires have been confirmed. More detailed study has shown that the mechanism postulated by Bradhurst, that the oxide can show enhanced plasticity, seems the most probable one. Various other explanations of the observed phenomena, including dislocation 'pop out', coherence effects at the metal-oxide interface, temperature and electrostatic effects have been considered and eliminated as serious possibilities. It has been shown that experiments in which anodised wires are subjected to a constant strain may be more sensitive in detecting small mechanical effects than experiments conducted at constant load. There appear to be complicating factors which might make the interpretation of tests on oxydised metal foil specimens difficult.

The enhanced oxide plasticity effect is not limited to films grown in a specific electrolyte or to films of a specific morphology; barrier and porous type films show the effect.

A mechanism involving purely diffusional deformation was originally suggested to account for this enhanced plasticity. The present work has confirmed that a diffusional mechanism is consistent with the experimental data. Such a mechanism has been considered and developed in detail with reference to available data on deformation and diffusion in oxides. Some evidence

of a quantitative nature that supports a diffusional mechanism has been obtained from measurements of the dependence of deformation rates on the applied field, the current passing and the applied load. Calculations of expected deformation rates have not been possible owing to a lack of the necessary data.

The presence of small quantities of alloying elements, insufficient to alter significantly the structure of the film as revealed by optical and electron microscopical techniques, is able to alter the plasticity of an anodic alumina film by a considerable amount. As far as can be seen, the effect of magnesium alloying is consistent with the effects on vacancy concentrations predicted by the Wagner-Hauffe theory, though this conclusion is subject to some uncertainty.

Enhanced oxide plasticity during film growth is potentially a common phenomenon and need not be limited to anodic films; any process leading to enhanced diffusion could also produce enhanced diffusional plasticity. In the case of crystalline anodic films an additional mechanism producing enhanced plasticity in the presence of an applied field might possibly arise; this is the electromechanical effect found with many semiconductors.

2. Other Properties of Anodic Films

Interesting information has been obtained on several features of anodic film growth on aluminium. Optical thickness measurements made on barrier films grown at very high current densities give results indicating that the films are much thicker than expected. Electrical measurements do not indicate this behaviour. These results imply that the properties of the oxide film change in some way when growth occurs at very high applied fields. This effect cannot be explained at present, but is reminiscent of similar effects found during the growth of anodic films grown under ultra-violet irradiation.

Previous investigations of the pore structure of anodic films do not appear to have given much attention to changes during the growth process. The present work indicates that even barrier films grown in borate electrolyte can develop a fine 'granular' structure which may be regarded as incipient porosity. At higher electrolyte temperatures the pores may enlarge by dissolution of their inner walls and the continued film growth typical of porous films sets in. This suggests that the controlling factor determining whether a film will be of the barrier or porous type may not be the initial appearance of pores but rather the ability of the electrolyte to enlarge fine pores already present to a point where increased passage

of film-growing current results. The distinction between the two classes of anodic films is thus one of degree rather than kind, but if it is desired to make such a distinction a better criterion would be the presence or absence of continued film growth rather than the presence or absence of porosity.

The typical current minima found during the initial stages of porous film growth are affected by relatively small changes in metal composition. Ultra-pure aluminium does not appear to show these minima even though porous film growth is proceeding. This could be because the changes in the initially-formed barrier film that produce the minima are extremely rapid in the case of high-purity aluminium.

Simple resistance measurements on wire specimens have shown that especially at high current densities temperature rises of the order of several hundred degrees centigrade may occur during anodic oxidation. It is possible that these high temperatures may affect the mode of growth of anodic films. In particular they may influence the changes in pore structure that take place with some films.

ACKNOWLEDGEMENTS

The author wishes to thank Dr. J. S. Ll. Leach for continued encouragement and many valuable discussions. He is grateful to Professor J. G. Ball for the provision of laboratory facilities. Instruction and assistance in making spectrophotometric measurements was kindly provided by Mr. N. J. M. Wilkins, A.E.R.E. Harwell, and by Mr. W. Bishop in the use of the electron microscope.

Financial support for this work was provided by the U.K.A.E.A. and a stipend by the Science Research Council; both of these are gratefully acknowledged.

REFERENCES

1. A. U. Seybolt; Adv. in Phys. 12 1 1963.

2. O. Kubaschewski, B. E. Hopkins; Oxidation of Metals and Alloys, Butterworths, London 1953.

3. C. Wagner; Z. Phys. Chem. B21 25 1933.

4. C. Wagner; Trans. Faraday Soc. 34 851 1938.

5. T. P. Hoar, L. E. Price; Trans. Faraday Soc. 34 867 1938.

6. K. Hauffe; Z. Metallk. 42 34 1951.

7. K. Hauffe; Prog. in Met. Phys. 4 71 1953.

8. L. Young; Anodic Oxide Films, Academic Press, London 1961.

9. L. Young; J. Electrochem. Soc. 111 1289 1964.

10. D. A. Vermilyea; J. App. Phys. 36 3663 1965.

11. G. C. Wood, C. Pearson; Nature 208 547 1965.

12. J. A. Davies, B. Domeij, J. P. S. Pringle, F. Brown; J. Electrochem. Soc. 112 1675 1965.

13. T. A. Renshaw; J. Electrochem. Soc. 108 2 1962.

14. T. P. Hoar, N. F. Mott; J. Phys. Chem. Sol. 9 97 1959.

15. G. A. Dorsey Jnr.; J. Electrochem. Soc. 113 169 1966.

16. G. A. Dorsey Jnr.; J. Electrochem. Soc. 113 172 1966.

17. G. A. Dorsey Jnr.; J. Electrochem. Soc. 113 284 1966.

18. Maria Gy Holló; Proc. 1st Int. Cong. Met. Corrosion p. 45, London 1961.

19. F. Keller, M. S. Hunter, D. L. Robinson; J. Electrochem. Soc. 100 411 1953.

20. D. J. Stirland, R. W. Bicknell; J. Electrochem. Soc. 106 481 1959.

21. R. W. Franklin, D. J. Stirland; J. Electrochem. Soc. 110 262 1963.

22. M. Pourbaix; Thermodynamics of Dil. Aq. Solutions, Arnold, London 1949.

23. M. Pourbaix; Corr. Science 5 677 1965.

24. N. B. Pilling, R. E. Bedworth; J. Inst. Met. 29 529 1923.

25. D. A. Vermilyea; Acta Met. 5 492 1957.

26. D. H. Bradhurst, J. S. L. Leach; J. Electrochem. Soc. 110 1289 1963.

27. W. Jaenicke, S. Leistikow, A. Stadler; J. Electrochem. Soc. 111 1031 1964.

28. D. A. Vermilyea; J. Electrochem. Soc. 110 346 1963.

29. M. Clarke; Trans. Inst. Met. Finishing 38 186 1961.

30. J. B. Kushner; Proc. Amer. Electroplaters Soc. 45 28 1958.

31. J. D. Mackenzie, C. E. Birchenall; Corrosion 13 783 1957.

32. D. L. Douglass; Corr. Science 5 255 1965.

33. D. H. Bradhurst; Ph.D. Thesis, Univ. of London 1963.

34. D. H. Bradhurst, J. S. L. Leach; Trans. Brit. Ceram. Soc. 62 793 1963.

36. A. A. Griffith; Phil. Trans. Roy. Soc. A221 163 1920.

37. R. L. Cummerow; J. App. Phys. 34 1724 1963.

38. E. Passmore, A. Moschetti, T. Vasilos; Phil. Mag. 13 1157 1966.

39. J. E. May, M. L. Kronberg; J. Amer. Ceram. Soc. 43 525 1960.

40. C. O. Hulse, J. A. Pask; J. Amer. Ceram. Soc. 43 373 1960.

41. I. R. Kramer, L. J. Demer; Trans. Met. Soc. A.I.M.E. 221 70 1961.

42. I. R. Kramer, L. J. Demer; Prog. Met. Phys. 9 No. 3 1961.

43. I. R. Kramer; Trans. Met. Soc. A.I.M.E. 221 989 1961.

44. I. R. Kramer; Trans. Met. Soc. A.I.M.E. 227 1003 1963.

45. I. R. Kramer, S. Podlaseck; Acta Met. 11 70 1963.

46. H. Shen, S. Podlaseck, I. R. Kramer; Trans. Met. Soc. A.I.M.E. 233 1937 1965.

47. I. R. Kramer; Trans. Met. Soc. A.I.M.E. 230 191 1964.

48. I. R. Kramer; Trans. Met. Soc. A.I.M.E. 233 1462 1965.

49. C. Feng, I. R. Kramer; Trans. Met. Soc. A.I.M.E. 233 1467 1965.

50. R. Roscoe; Nature 133 912 1934.

51. E. N. da C. Andrade; Props. of Met. Surfaces, Inst. of Met. Monograph 13.

52. C. S. Barrett, P. M. Aziz, I. Markson; J. of Met. 5 1655 1953.

53. D. B. Holt; Acta Met. 10 1021 1962.

54. J. E. Harris, B. C. Masters; Phil. Mag. 13 963 1966.

55. P. P. Gillis, J. J. Gilman; J. Appl. Phys. 36 3370 1965.

56. P. P. Gillis, J. J. Gilman; J. Appl. Phys. 36 3380 1965.

57. J. B. Wachtmann Jnr., L. H. Maxwell; J. Amer. Ceram. Soc. 37 291 1954.

58. J. B. Wachtmann Jnr., L. H. Maxwell; J. Amer. Ceram. Soc. 40 377 1957.

59. M. L. Kronberg; J. Amer. Ceram. Soc. 45 274 1962.

60. R. Chang; J. Appl. Phys. 31 484 1960.

61. J. B. Wachtmann Jnr. D. G. Lam Jnr.; J. Amer. Ceram. Soc. 42 254 1959.

62. W. Rosenhain, J. C. W. Humphrey; J. Iron Steel Inst. 87 219 1913.

63. W. Rosenhain, D. Ewen; J. Inst. Met. 10 119 1913.

64. Ting-Sui Ke; Phys. Rev. 71 533 1947.

65. N. F. Mott; Proc. Phys. Soc. 60 391 1948.

66. F. R. N. Nabarro; Report of a Conference on the Strength of Solids, p. 75 The Physical Soc. London 1948.

67. C. Herring; J. Appl. Phys. 21 437 1950.

68. A. L. Ruoff; J. Appl. Phys. 36 2903 1965.

69. J. C. Fisher; J. Appl. Phys. 22 74 1951.

70. R. Smoluchowski; Phys. Rev. 87 482 1952.

71. L. C. Luther; J. Chem. Phys. 43 2213 1965.

72. M. T. Shim, W. J. Moore; J. Chem. Phys. 26 802 1957.

73. I. Zaplatynsky; J. Appl. Phys. 35 1358 1964.

74. R. Shelley, E. B. Rigby, I. B. Cutler; J. Amer. Ceram. Soc. 45 302 1962.

75. T. Y. Tien; J. Appl. Phys. 35 122 1964.

76. A. E. Paladino, W. D. Kingery; J. Chem. Phys. 37 957 1962.

77. E. K. Beauchamp, G. S. Baker, P. Gibbs; WADD (Westinghouse) Report Contract AF 33(610)-6832 Proj. O(7-7350) 1961.

78. S. I. Warshaw, F. H. Norton; J. Amer. Ceram. Soc. 45 4 1962.

79. R. C. Foweiler; J. Appl. Phys. 32 773 1961.

80. Y. Oishi, W. D. Kingery; J. Chem. Phys. 33 480 1960.

81. R. L. Coble, Y. H. Guerard; J. Amer. Ceram. Soc. 46 353 1963.

82. A. E. Paladino, R. L. Coble; J. Amer. Ceram. Soc. 46 133 1963.

83. R. L. Coble; J. Appl. Phys. 34 1679 1963.

84. E. M. Passmore, T. Vasilos; J. Amer. Ceram. Soc. 49 166 1966.

85. G. Amsel; Reported to Symposium on Nuclear Techniques in Corrosion and Oxidation. Wantage Res. Lab. U.K.A.E.A. April 1966.

86. J. A. Davies, J. P. S. Pringle, R. C. Graham, F. Brown; J. Electrochem. Soc. 109 999 1962.

87. J. A. Davies, B. Domeij; J. Electrochem. Soc. 110 849 1963.

88. J. Belle; Westinghouse Atomic Power Div. Report WAPD/MRP-85.

89. J. Belle; Westinghouse Atomic Power Div. Report WAPD/MRP-86.

90. A. B. Auskern, J. Belle; J. Nuc. Mat. 3 277 1961.

91. A. B. Auskern, J. Belle; J. Nuc. Mat. 3 311 1961.

92. G. Christie, J. Williams; J. Nuc. Mat. 5 1 1962.

93. R. Scott, A. R. Hall, J. Williams; J. Nuc. Mat. 1 39 1959.

94. J. J. Stobbs, I. Whittle; J. Nuc. Mat. 19 160 1966.

95. D. L. Douglass; Corr. Science 5 347 1965.

96. O. Kubaschewski, E. L. I. Evans; Met. Thermochemistry, Pergamon, London 1958.

97. W. Primak; J. Appl. Phys. 35 1342 1964.

98. R. Taylor, A. T. Jeffes; J. Nuc. Mat. 19 142 1966.

99. A. R. Bray, P. W. M. Jacobs, L. Young; J. Nuc. Mat. 4 356 1959.

100. J. E. Antill, K. A. Peakall, J. Less Comm. Met. 3 239 1961.

101. J. E. Antill; Props of Reactor Materials and Effects of Rad. Damage p. 379 Butterworths, London 1962.

102. A. F. Forester, L. A. Girifalco; J. Phys. Chem. Sol. 10 99 1959.

103. R. W. Baluffi, D. N. Seidman; J. Appl. Phys. 36 2708 1965.

104. A. F. Brown; Appl. Mat. Res. 5 67 1966.

105. E. S. Machlin; J. Appl. Phys. 30 1109 1959.

106. J. H. Westbrook, I. J. Gilman; J. Appl. Phys. 33 2360 1962.

107. T. A. Kontorova; Sov. Phys. Sol. State 6 1760 1965.

108. A. S. Neiman, W. S. Rothwell; Appl. Phys. Lett. 3 160 1963.

109. W. S. Rothwell, A. S. Neiman; J. Appl. Phys. 36 2309 1965.

110. J. D. Eshelby, C. W. A. Newey, P. L. Pratt, A. B. Lidiard; Phil. Mag. 3 75 1958.

111. P. Winkel, C. A. Pistorius, W. Ch. van Geel; Philips Res. Rep. 13 277 1958.

112. T. P. Hoar, J. Yaholom; J. Electrochem. Soc. 110 614 1963.

113. S. G. Starling, A. J. Woodall; Physics, p. 955 Longmans London 1957.

114. S. F. Bubar, D. A. Vermilyea; J. -Electrochem. Soc. 113 892 1966.

115. J. Stringer; J. Inst. Met. 94 113 1966.

116. R. N. Stevens; J. Inst. Met. 94 129 1966.

117. I. H. Khan, J. S. L. Leach, N. J. M. Wilkins. To be published in Corrosion Science.

118. G. W. Kaye, T. H. Laby; Physical and Chemical Constants, Longmans London 1957.

INDEX TO DIAGRAMS

1. Available data on diffusion in alumina.

2. Balance adapted for constant load tests on wires.

2a. Method of mounting wires in glass hooks.

3. Modification of Instron tester for tensile and constant strain tests on wires.

4. Apparatus for four-point bending tests on foil strips.

5. Grain structure of annealed 0.1 mm. diameter aluminium wire.

6. Form of specimen for examination of stripped oxide films.

7. Apparatus for measuring resistance changes in fine wires.

8. Current decay during growth of 200 V anodic film in borate at 20°C.

9. Optical transmittance of anodic films grown to 100 V in borate on aluminium and 'Aluflex'.

10. Anodic film grown to 100 V in borate at 20°C on aluminium.

11. Anodic film grown to 100 V in borate at 20°C on 'Aluflex'.

12. Anodic film grown on aluminium at 20°C at 100 mA $cm.^{-2}$ to 200 V with no current decay permitted.

13. Anodic film grown on aluminium at 20°C at 10 mA $cm.^{-2}$ to 200 V with no current decay permitted.

14. Anodic film grown on aluminium at 20°C at 1 mA $cm.^{-2}$ to 200 V with no current decay permitted.

15. Optical transmittance curves for 200 V anodic films grown on aluminium in borate at various current densities.

16. Transmittance minima from Fig. 15 calibrated assuming film 'a' is 2800 Å.

17. Estimated thickness of 200 V films grown at varying current densities on aluminium in borate.
18. Equilibrium anodic currents for aluminium in borate at different temperatures.
19. Current-time curves during growth of anodic films on two samples of aluminium at 50 V in borate at 50°C.
20. Current-time curves during growth of anodic films on two samples of aluminium at 5V in 15% H_2SO_4 at 25°C.
21. Current-time curves for anodic film grown on aluminium in borate at 50°C.
22. Reflectance-wavelength curves for stripped anodic films grown on aluminium in borate to 200 V at 25°C and at 50°C for varying times.
23. Reflectance-wavelength curves for stripped anodic films grown on aluminium in borate at 50°C and 50V.
24. Reflectance minima from Figs. 22 and 23 calibrated assuming film 'α' to be 2800 Å.
25. Growth of oxide film on aluminium anodised in borate at 50°C.
26. Anodic oxide film grown on aluminium to 100 V in borate at 20°C.
27. Anodic film grown on aluminium at 100 V for 1 minute after reaching voltage. Borate electrolyte at 50°C.
28. Anodic oxide film grown on aluminium at 100 V for 5 minutes after reaching voltage. Borate electrolyte at 50°C.

29. Anodic oxide film grown on aluminium at 100 V for 15 minutes after reaching voltage. Borate electrolyte at 50°C.
30. Anodic oxide film grown on aluminium at 100 V for 25 minutes after reaching voltage. Borate electrolyte at 50°C.
31. Stress-strain curves for 0.1 mm. diameter aluminium wires.
32. Stress-strain curves for 0.1 mm. diameter 'Aluflex' wires.
33. Strengthening of 0.1 mm. diameter aluminium wires by anodic films grown to varying voltages in borate.
34. Extension under 25 g. load of aluminium wire anodised to 200 V in borate.
35. Current transients shown by aluminium wires previously anodised to 200 V in borate.
36. Voltage and extension at 0.156 mA $cm.^{-2}$ and under 25 g. load of aluminium wires anodised to 200 V in borate.
37. Extension of aluminium wires in borate with 25 g. load, anodised to 200 V.
38. Extension-time curves for aluminium wires anodised to 200 V in borate and extended at constant current under 25 g. load.
39. Total extension of aluminium wires anodised to 200 V in borate and extended under load at 210 V.
40. Extension increments with increasing applied voltage of aluminium wires anodised to 200 V in borate.
41. Effect of temperature on extension of anodised aluminium wires at 50 V and 20 g. load in borate.

42. Extension under 20 g. load of aluminium wire anodised to 50 V in solution of borate in ethanediol.

43. Extension under 20 g. load of aluminium wire anodised for 5 minutes at 10 mA $cm.^{-2}$ in 15% H_2SO_4.

44. Extension of 0.1 mm. diameter aluminium wire under 30 g. load during electropolishing at 625 mA $cm.^{-2}$.

45. Extension of 0.1 mm. diameter 'Aluflex' wires under 40 g. load in borate.

46. Stress changes in 0.1 mm. diameter wires anodised to 200 V and subjected to a fixed strain.

47. Reduction in load on 0.1 mm. diameter wires anodised to 200 V in borate and under a fixed strain when 200 V is re-applied.

48. Stress changes during anodising of 0.1 mm. diameter aluminium wires to 200 V at varying current densities in borate, with a fixed pre-strain.

49. Stress changes, during anodising in borate, of a pre-strained 0.1 mm. diameter aluminium wire.

50. Deflection of aluminium strip anodised to 200 V in borate under 4-point bending.

51. Current-decay curves during formation of porous anodic films.

52. Stress conditions during tests on anodised wires.

53. Total extension (as function of applied voltage) of aluminium wire under 25 g. load anodised to 200 V in borate.

54. Apparent mechanical properties of anodic film on aluminium when subjected to applied fields.

55. Initial creep rate of aluminium wires anodised to 200 V in borate and extended at 25 g. load at varying current densities.

56. Creep rate vs. extension, plotted from Fig. 36.

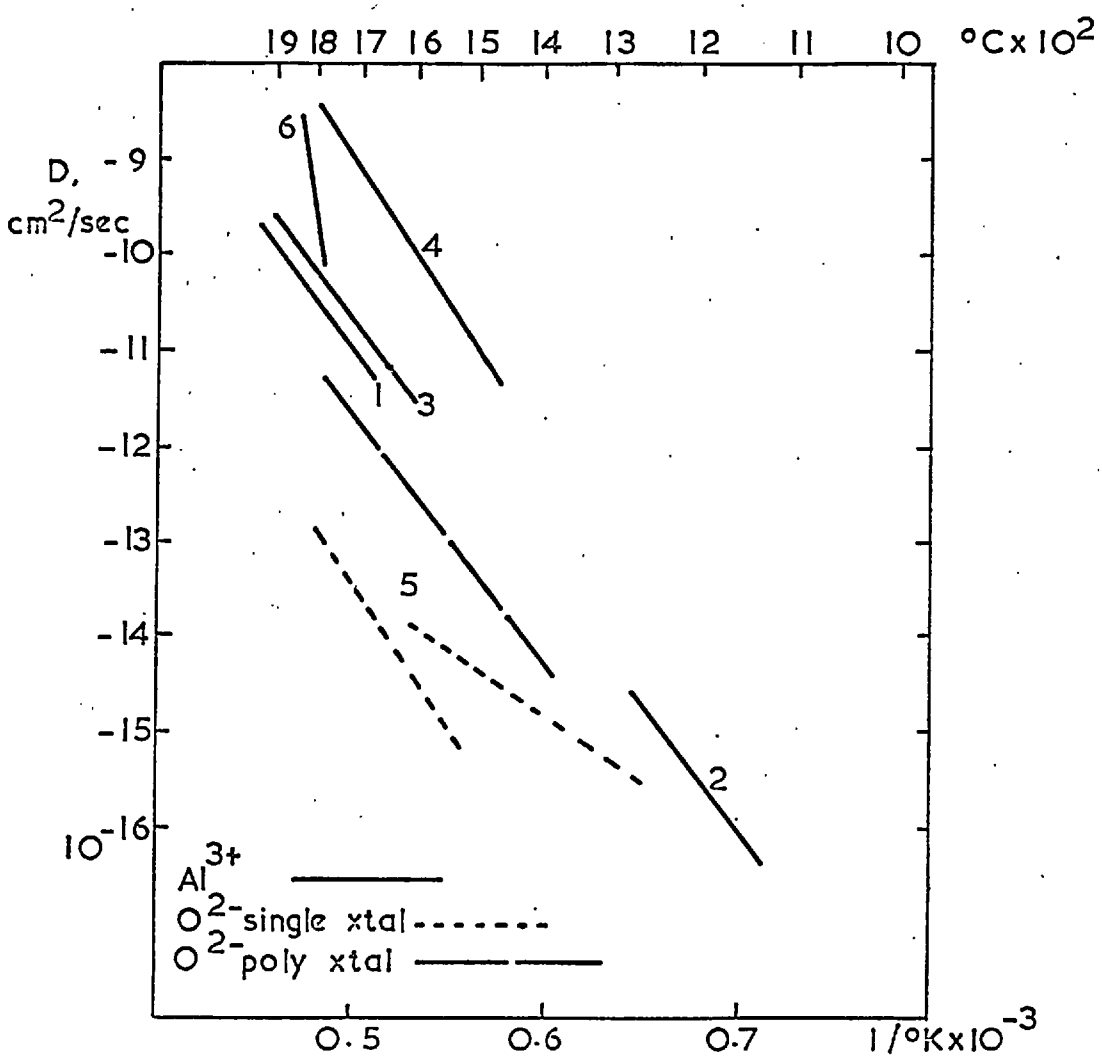


Fig.1 Available data on diffusion in alumina
Nos. 1–6 correspond to references 76–81

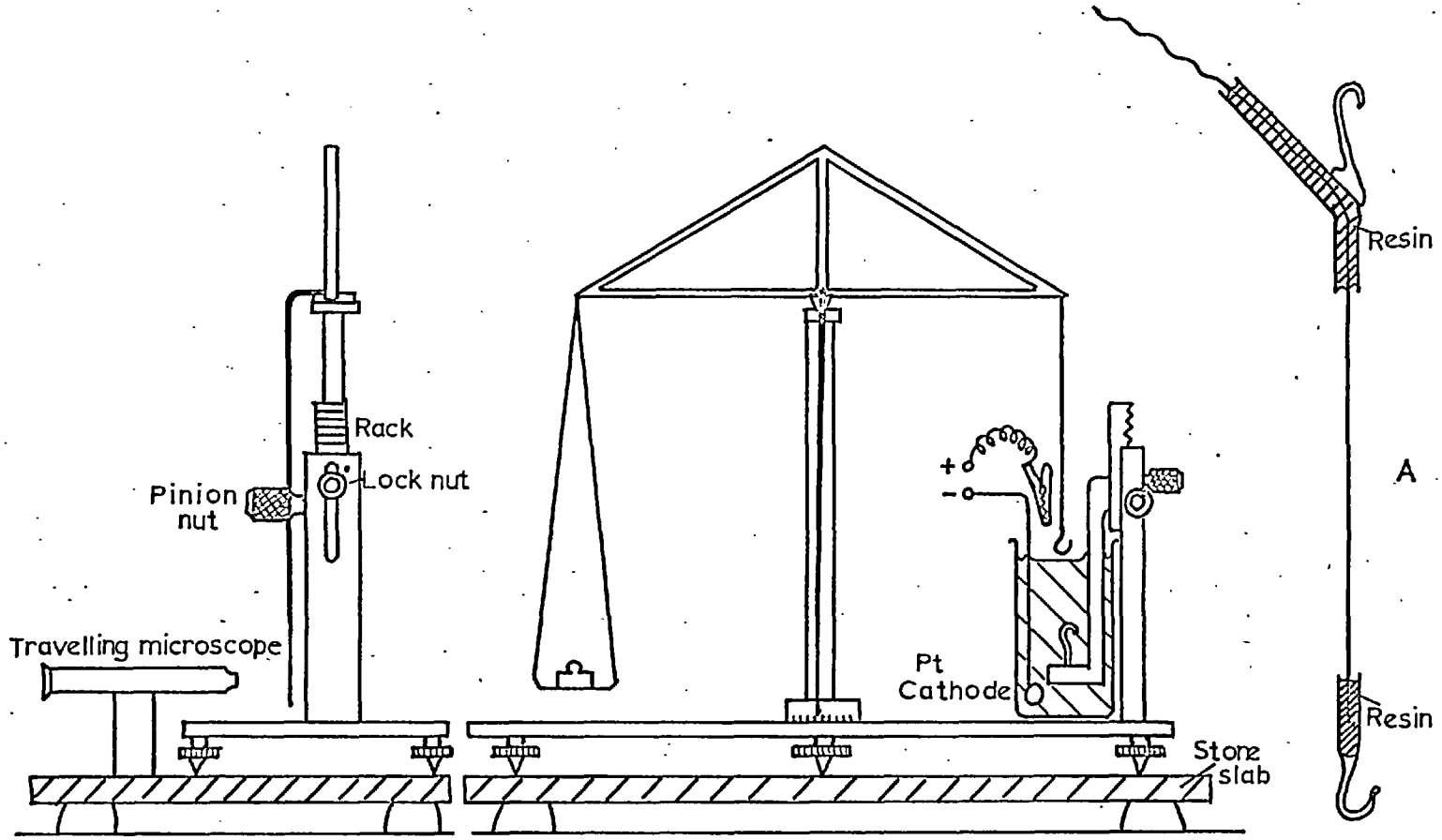


Fig.2 Balance adapted for constant load tests on wires

A) Method of mounting wires in glass hooks

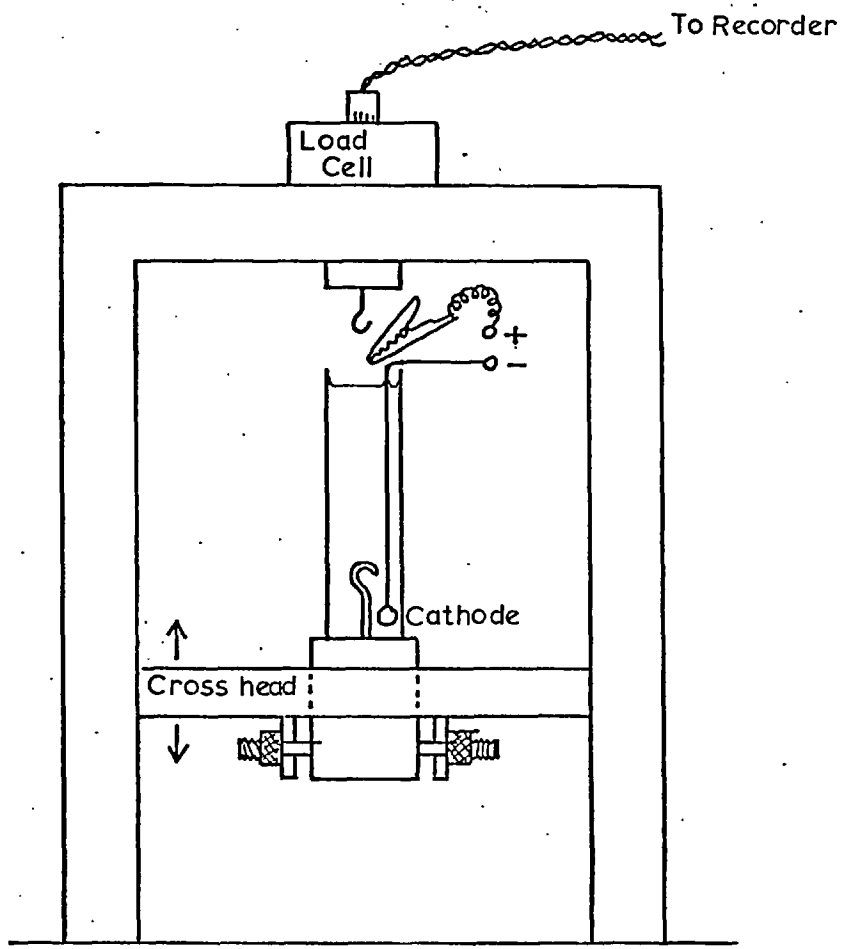


Fig.3 Modification of Instron tester for tensile and constant strain tests on wires

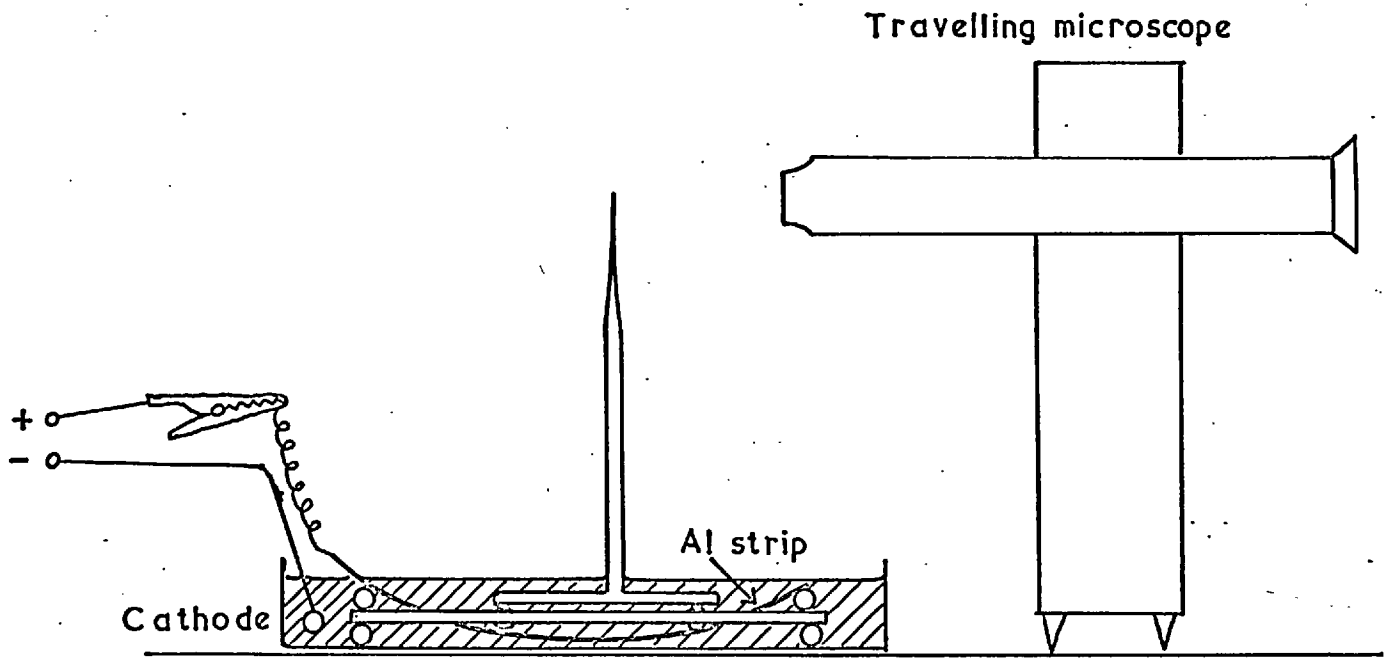


Fig. 4 Apparatus for four-point bending tests on foil strips.

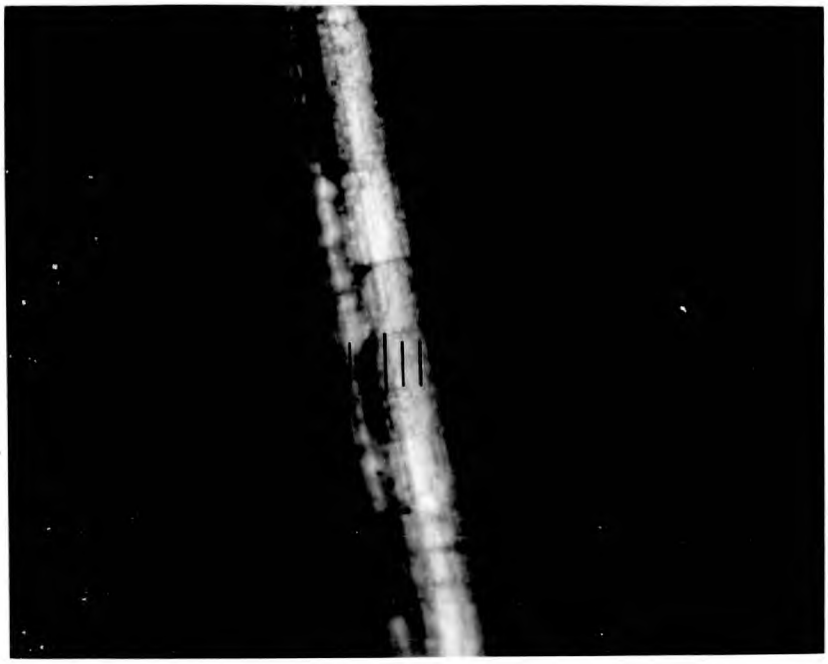


Fig. 5. Grain Structure of Annealed 0.1 mm. Diameter Aluminium Wire.

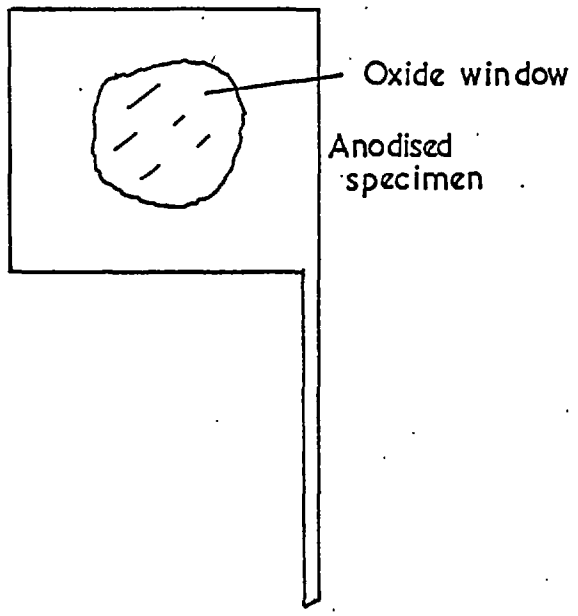


Fig. 6 Form of specimen for examination of stripped films

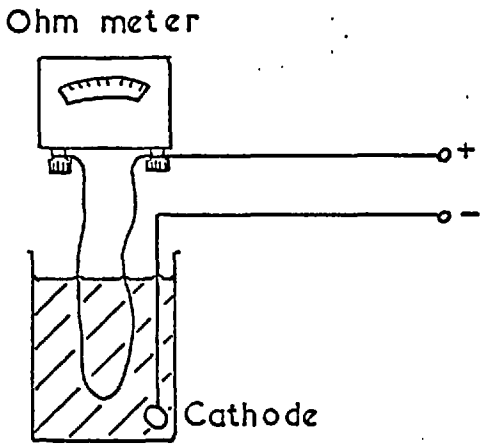


Fig.7 Apparatus for measuring resistance changes in fine wires during anodising

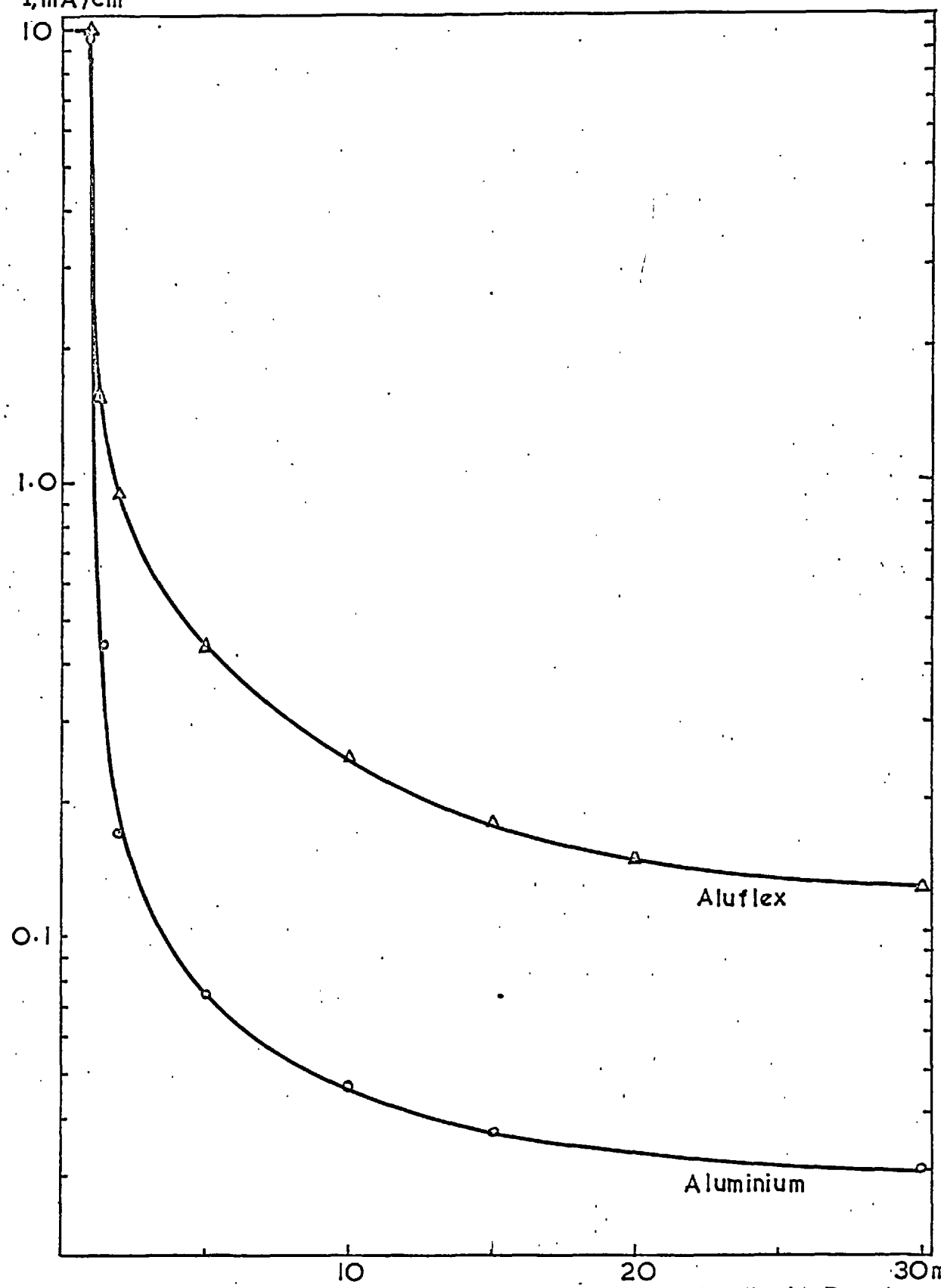


Fig. 8 Current decay during growth of 200 V anodic film in Borate at 20° C

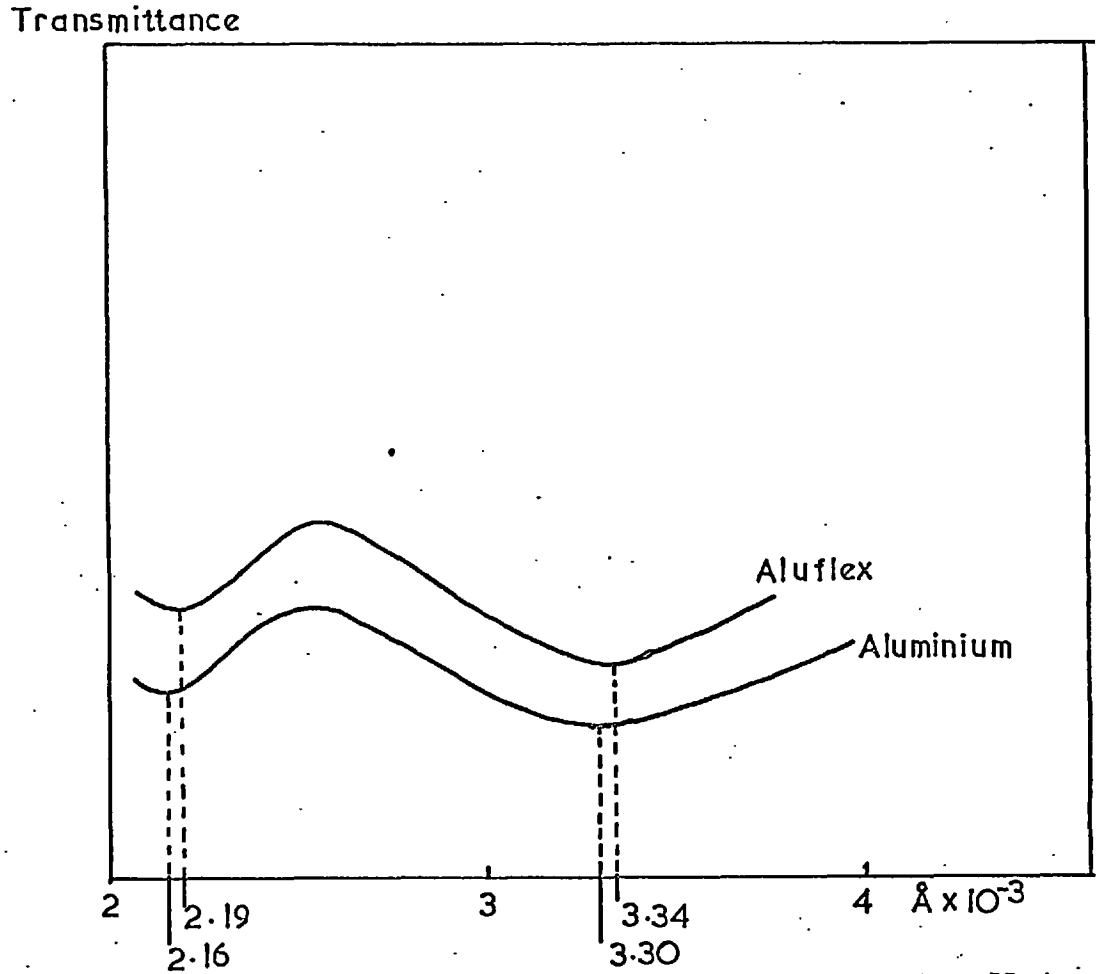


Fig.9 Optical transmittance of anodic films grown to 100V in Borate on Aluminium and Aluflex

Fig. 10. Anodic film grown to 100 V in borate at 20°C on Aluminium.

Fig. 11. Anodic film grown to 100 V in borate at 20°C on 'Aluflex".

Fig. 12. Anodic film grown on aluminium at 20°C at 100 mA $cm.^{-2}$ to 200 V with no current decay permitted.

Fig. 13. Anodic film grown on aluminium at 20°C at 10 mA $cm.^{-2}$ to 200 V with no current decay permitted.

Fig. 14. Anodic film grown on aluminium at 20°C at 1 mA $cm.^{-2}$ to 200 V with no current decay permitted.

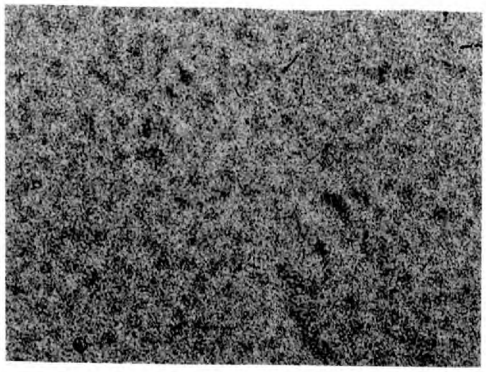


Fig 10 0.1 μ

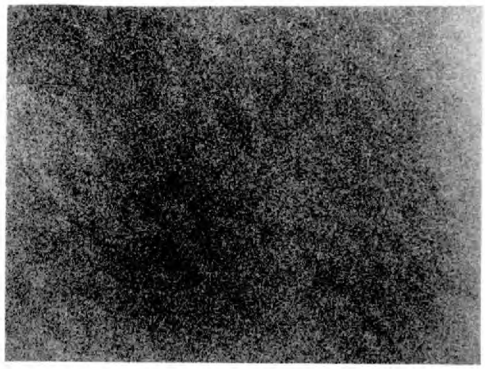


Fig 11 0.1 μ

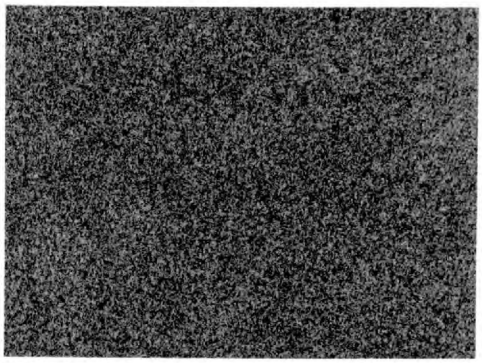


Fig 12 0.1 μ

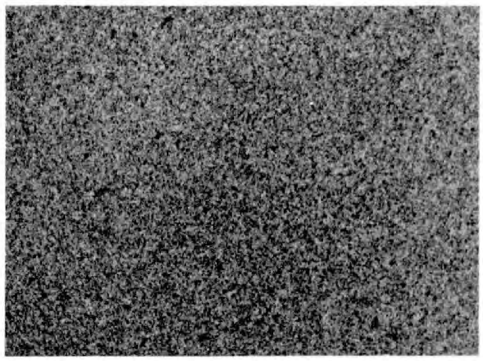


Fig 13 0.1 μ

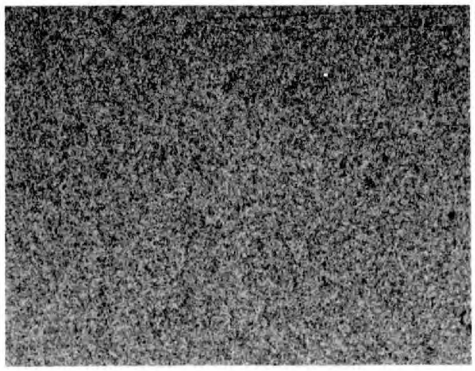


Fig 14 0.1 μ

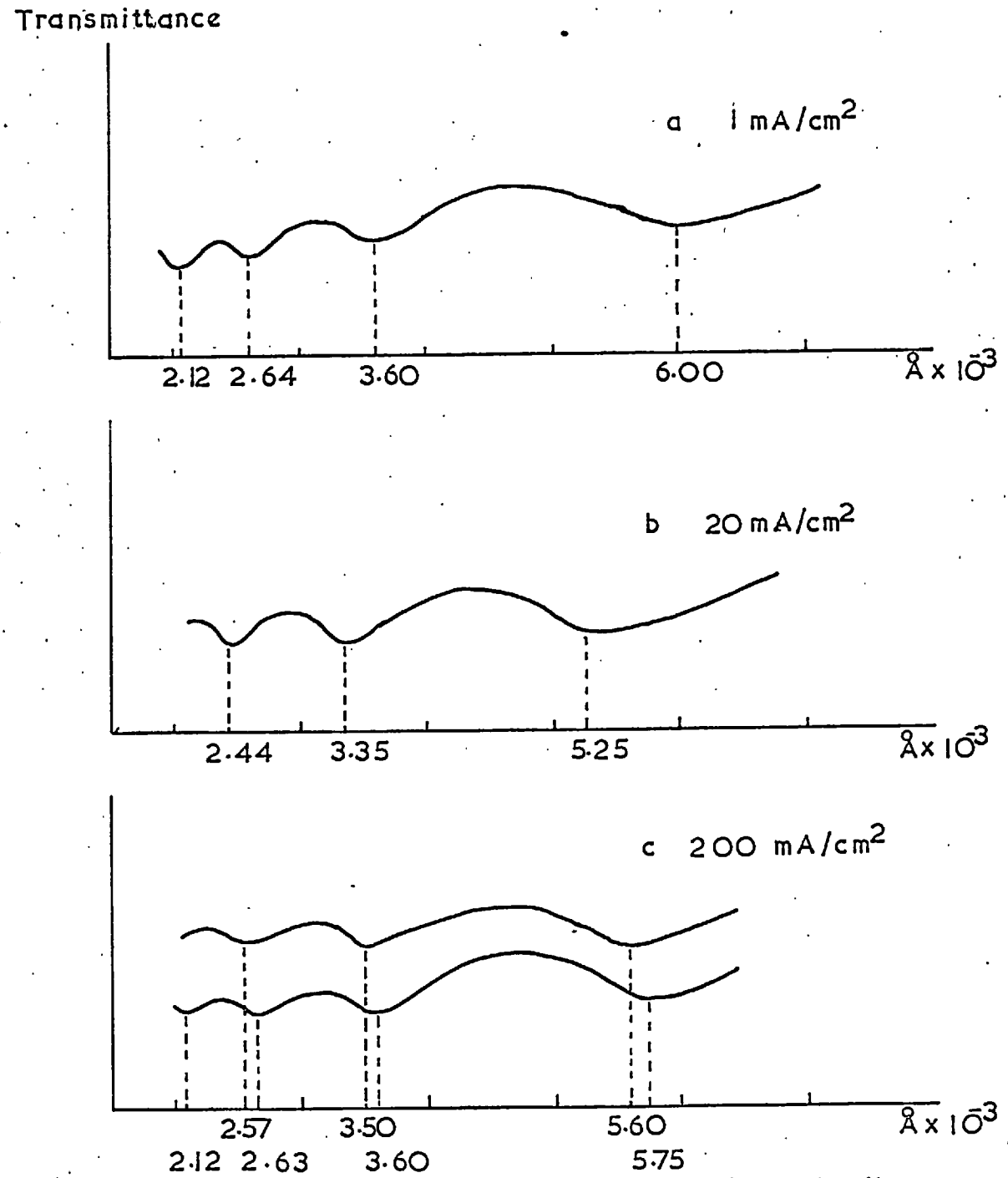


Fig.15 Optical transmittance curves for 200V anodic films grown on Aluminium in Borate at various current densities

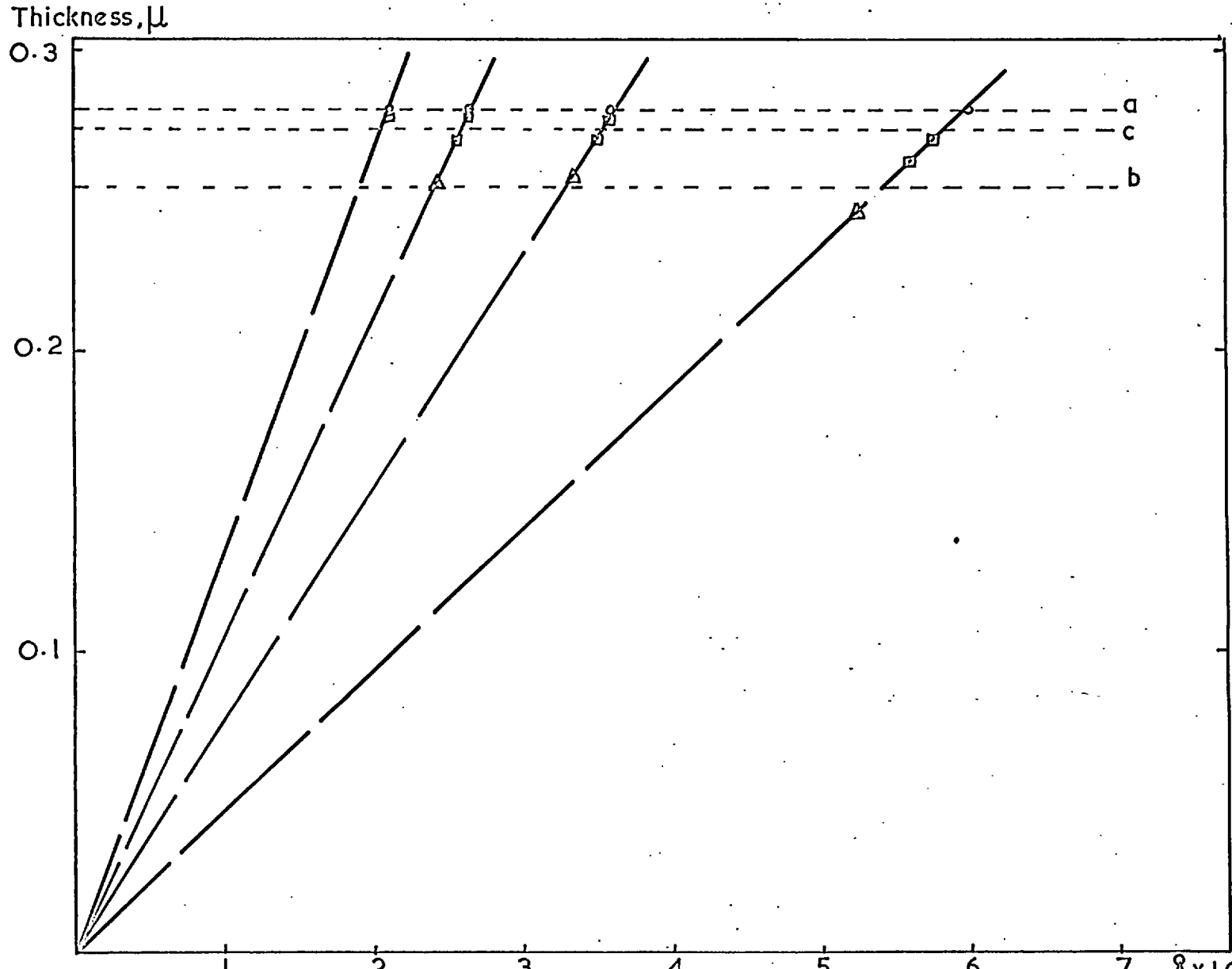


Fig.16 Transmittance minima from Fig.15 calibrated assuming film a is 2800 Å

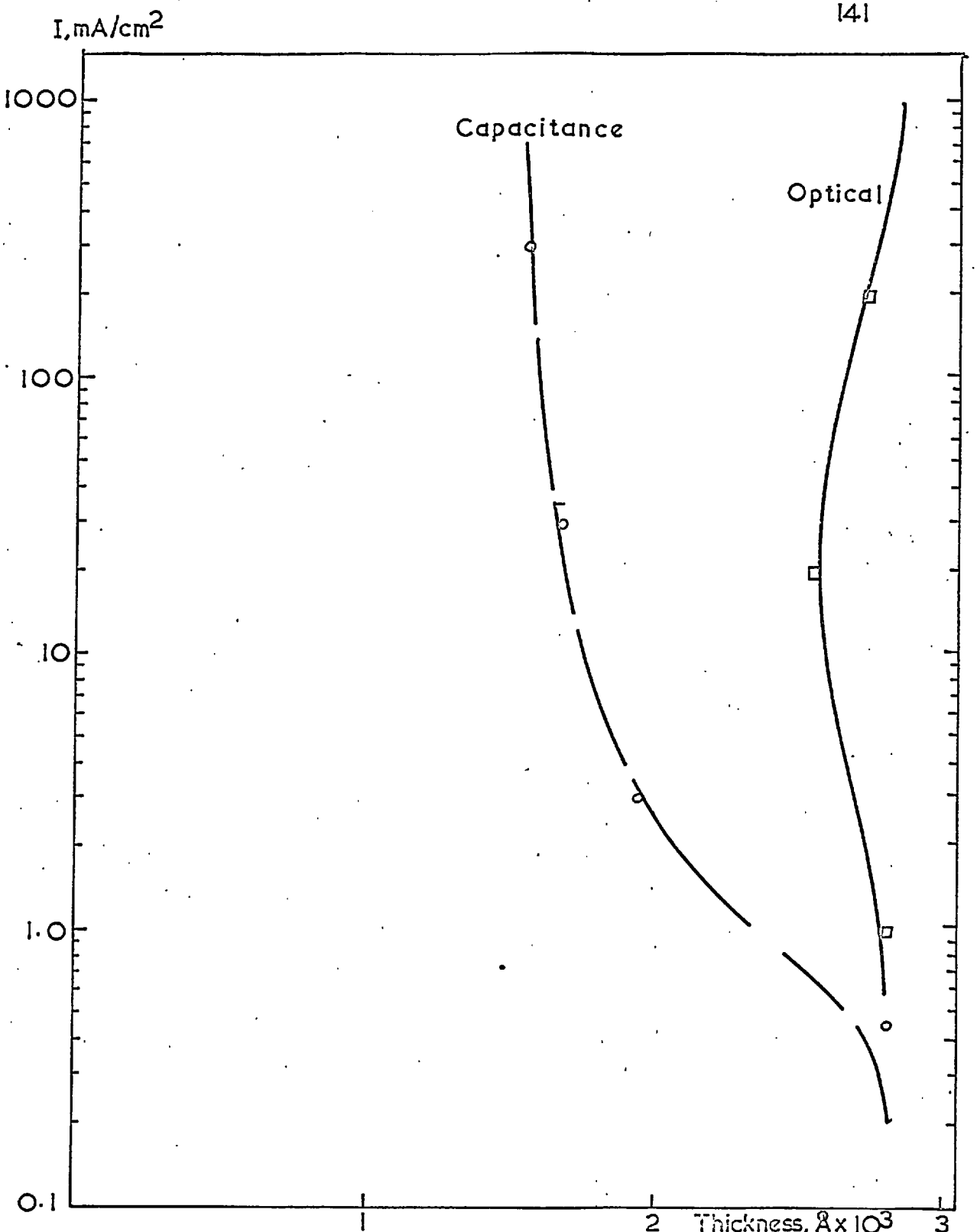


Fig. 17 Estimated thickness of 200V films grown at varying current densities on Aluminium in Borate.

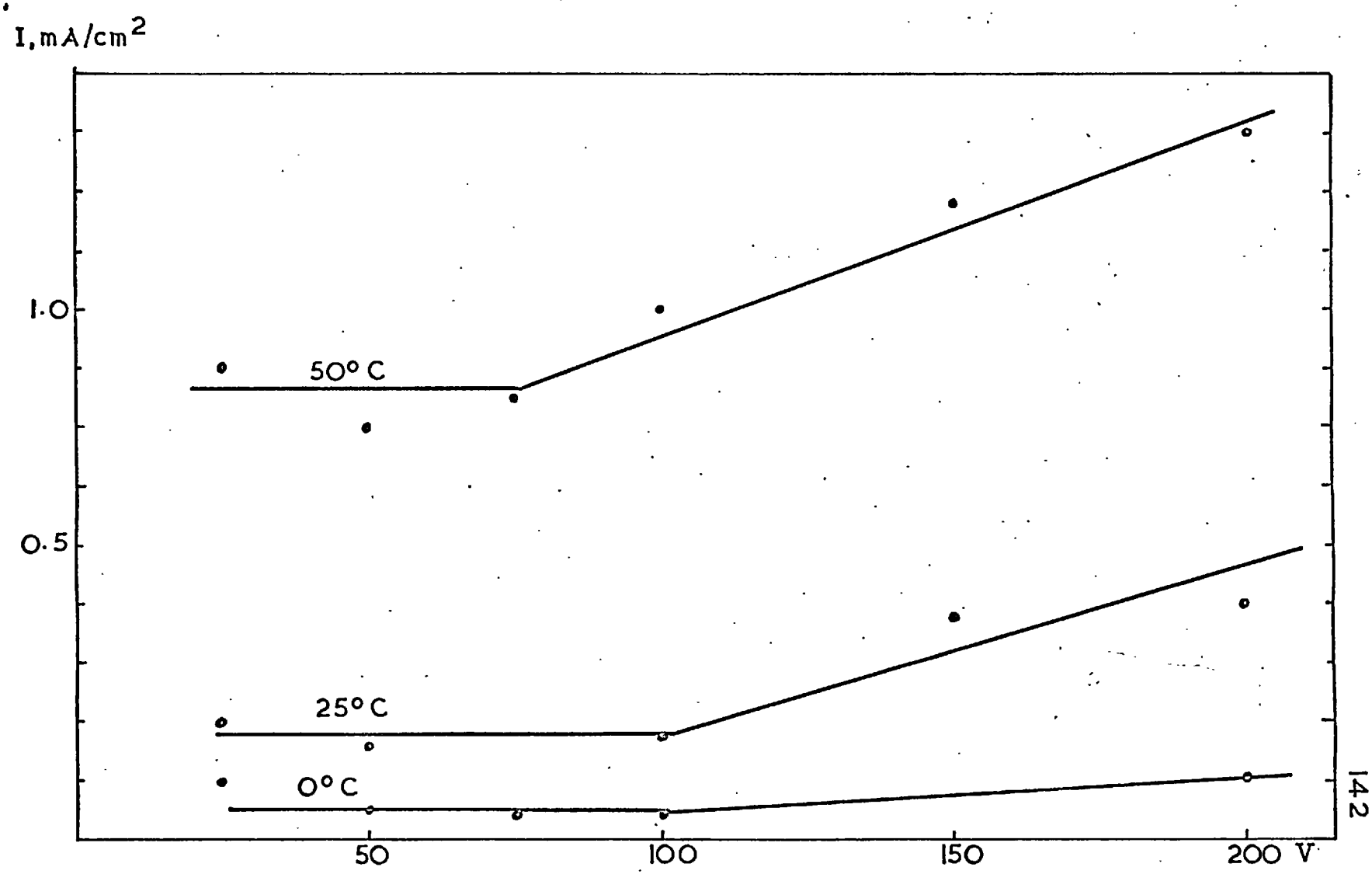


Fig. 18 Equilibrium anodic currents for Aluminium in Borate at different temperatures.

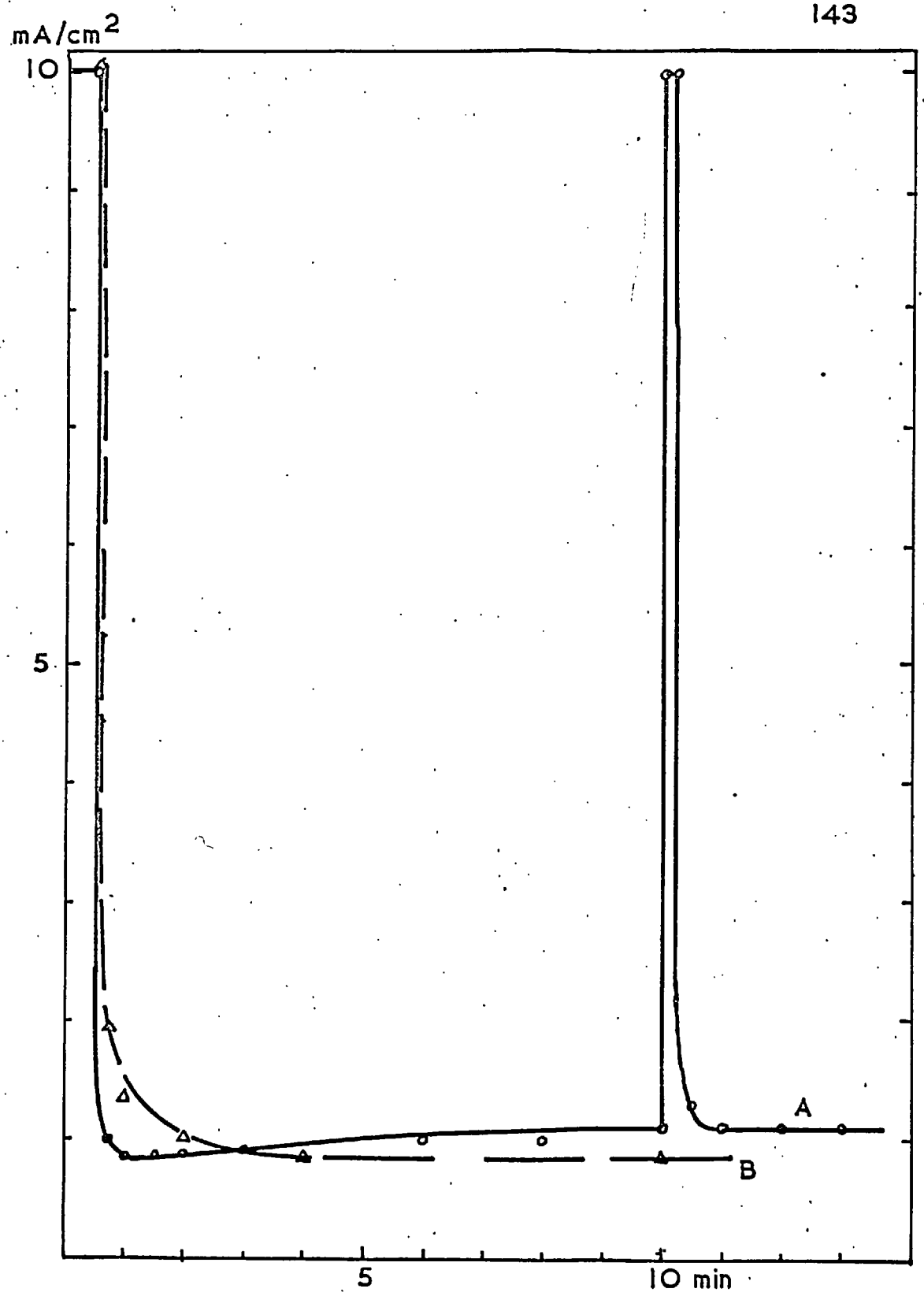


Fig.19 Current–Time curves during growth of anodic films on two samples of Aluminium at 50V in Borate at 50°C. After 10 min. the potential applied to A was raised to 100 V.

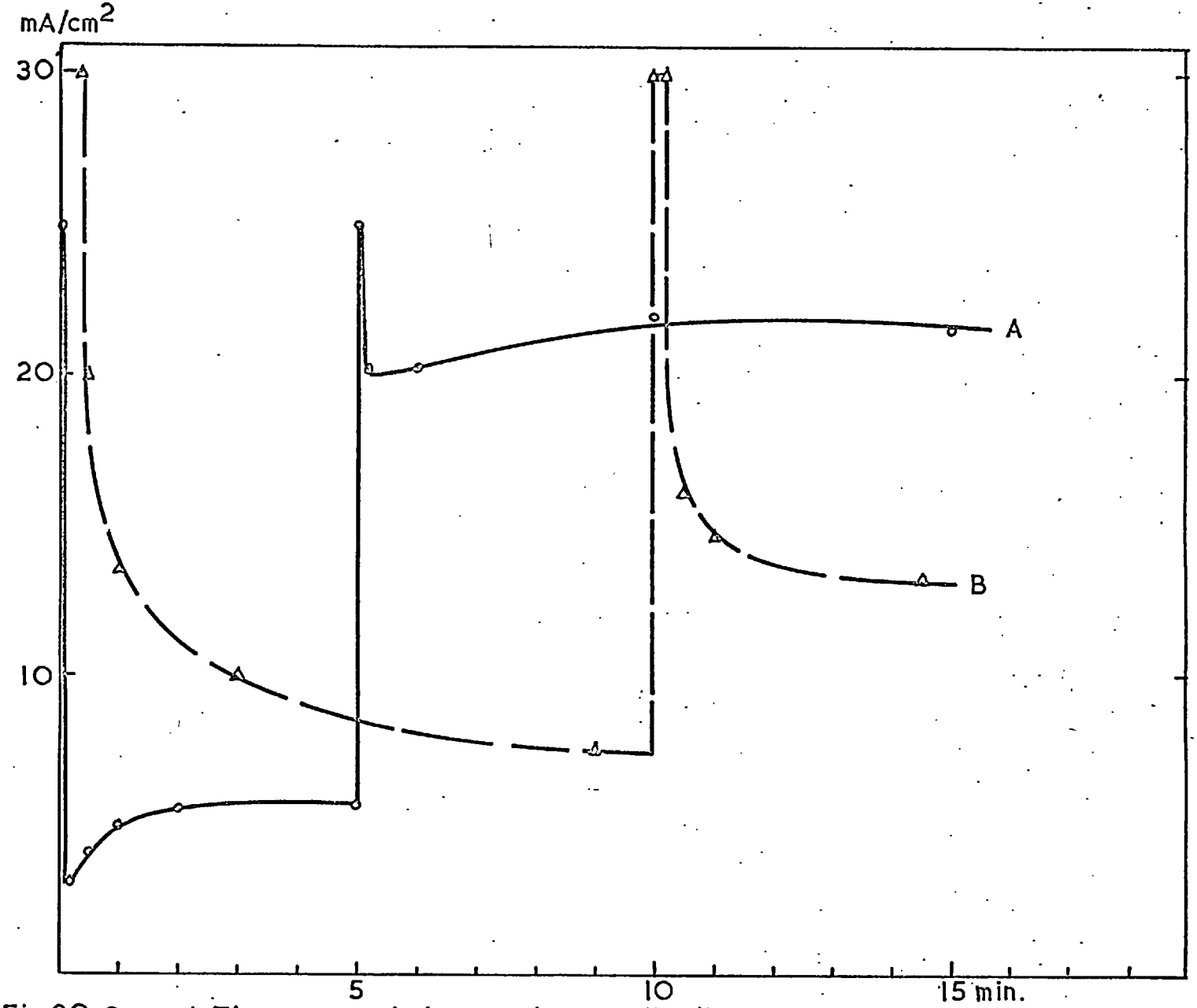


Fig.20 Current-Time curves during growth of anodic films on two samples of Aluminium at 5 V in 15% H_2SO_4 at 25°C. After 5min. for A and 10min. for B applied potential was raised to 10V.

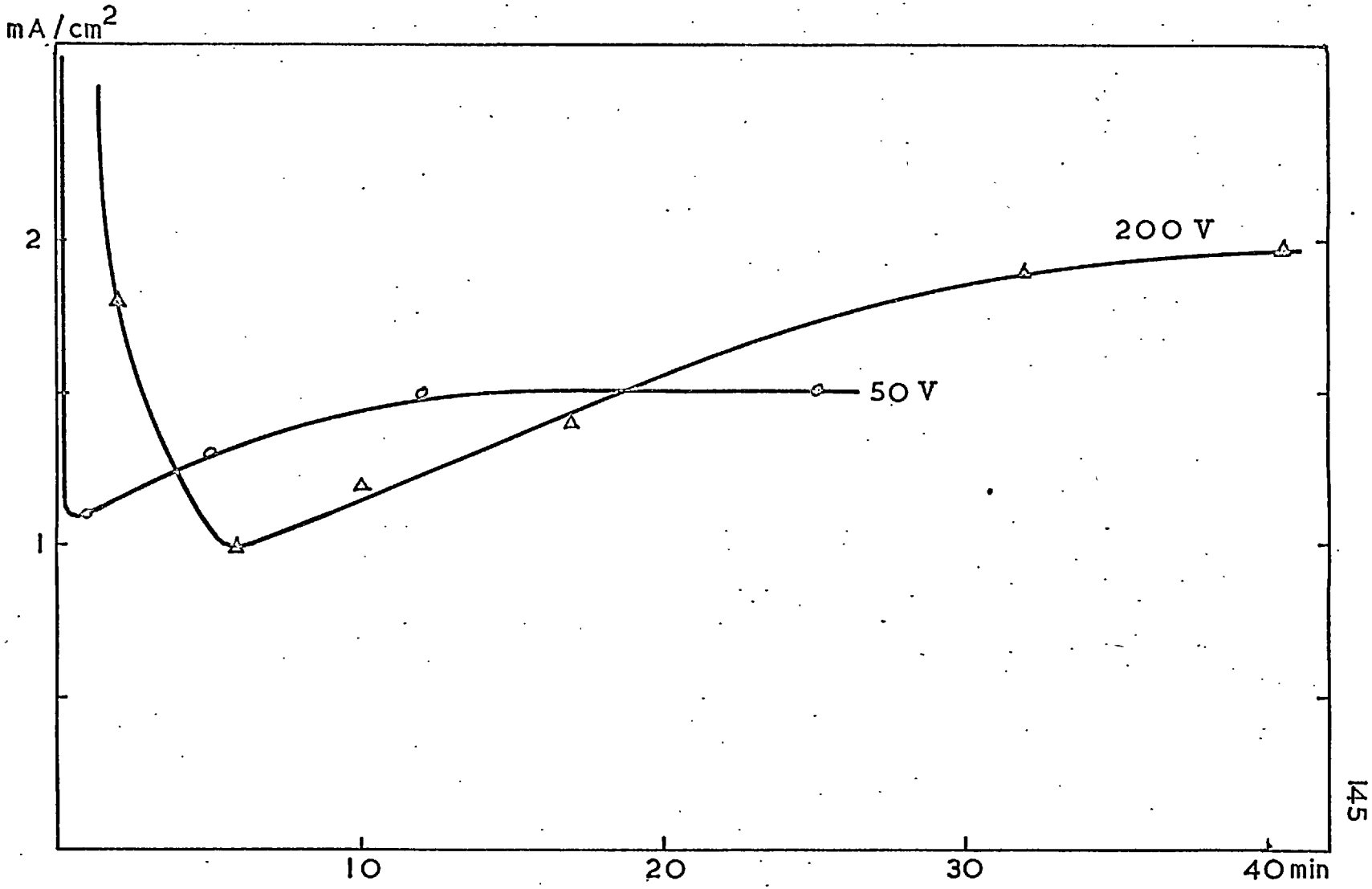


Fig.21 Current – Time curves for anodic film growth on Aluminium in Borate at 50°C

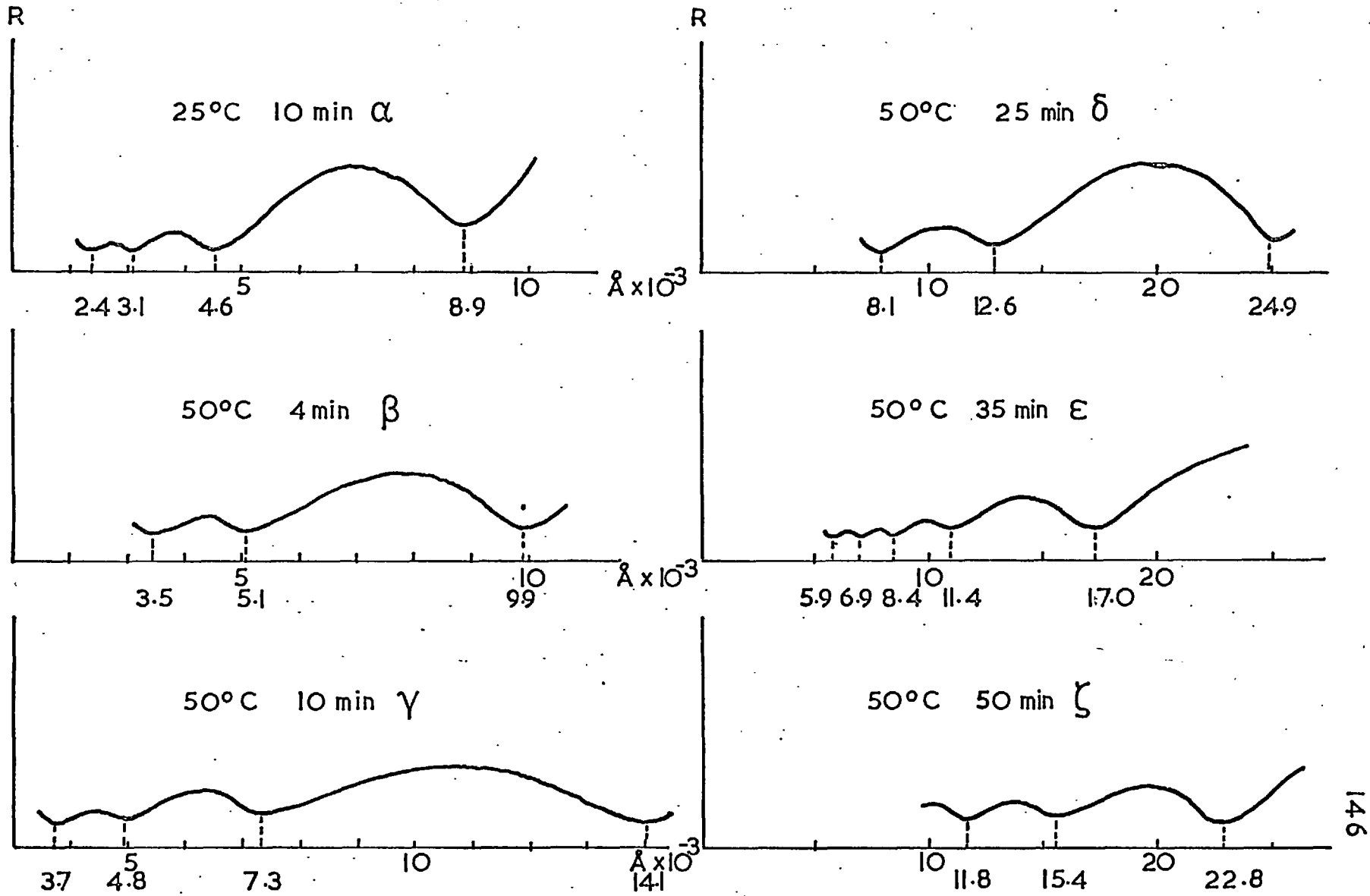


Fig.22 Reflectance—Wavelength curves for stripped anodic films grown on Aluminium in Borate to 200 V at 25°C and at 50°C for varying times

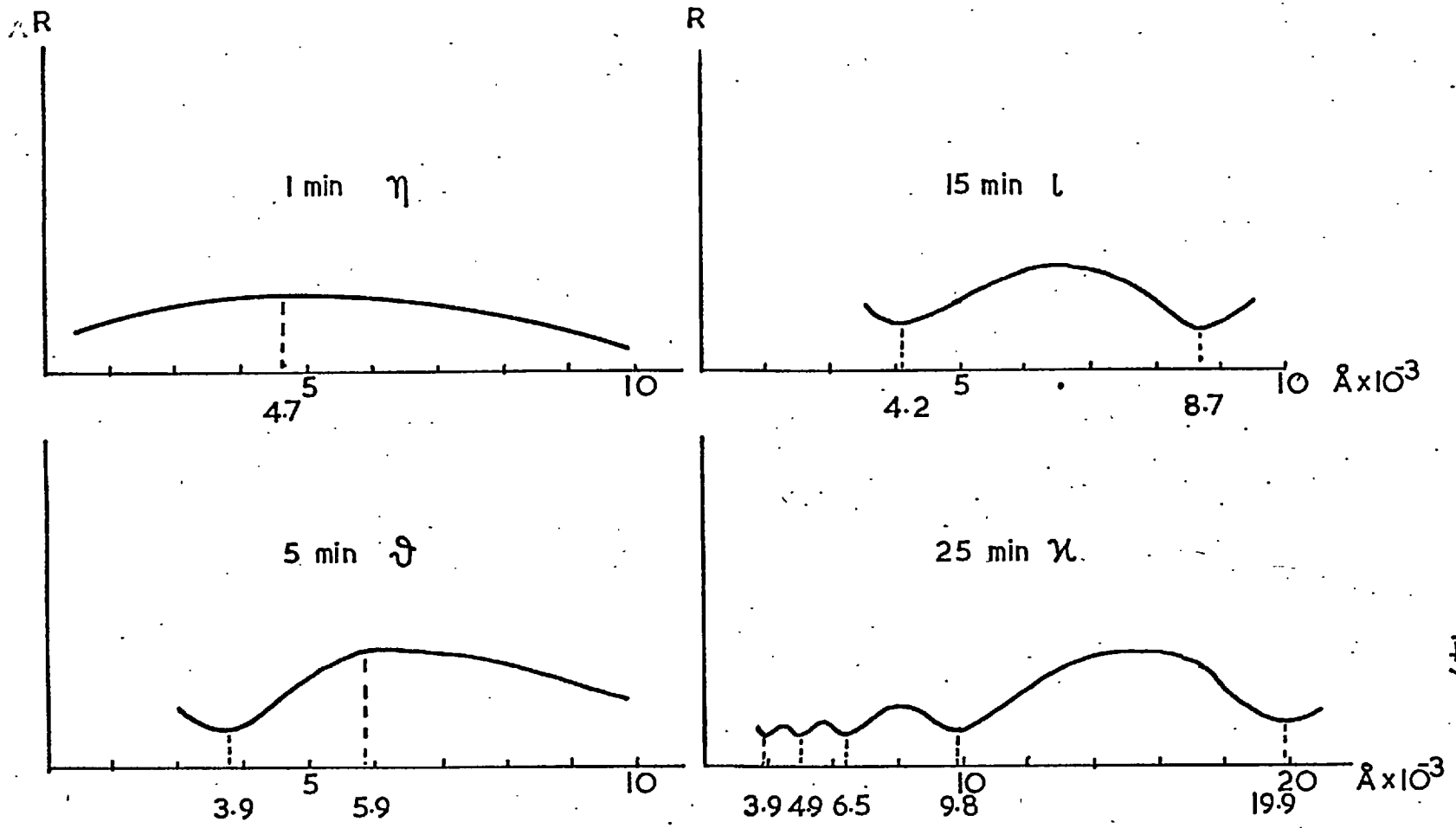


Fig. 23 Reflectance – Wavelength curves for stripped anodic films grown on Aluminium in Borate at 50° C and 50 V

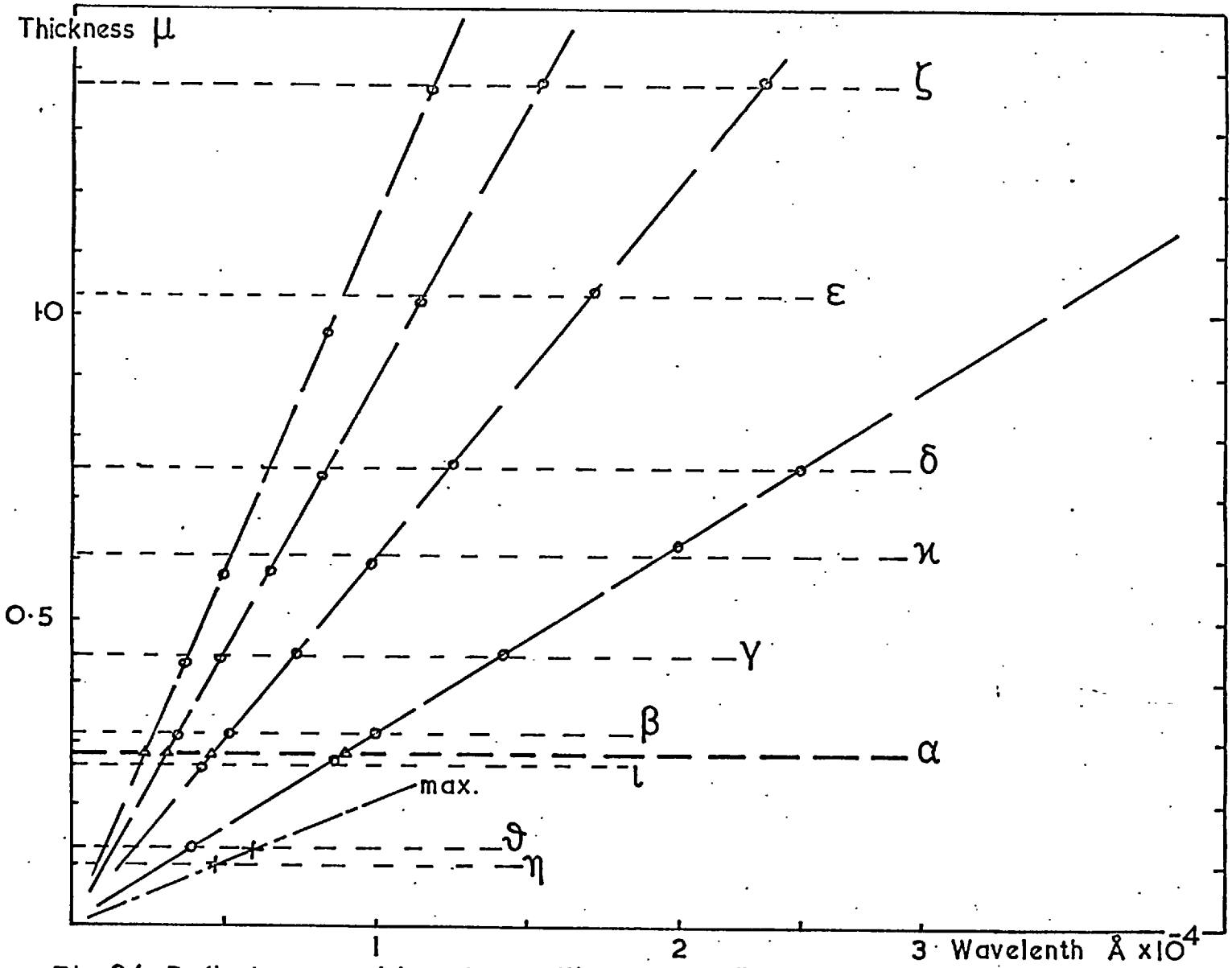


Fig. 24 Reflectance minima from Figs22 &23calibrated assuming film α to be 2800 Å

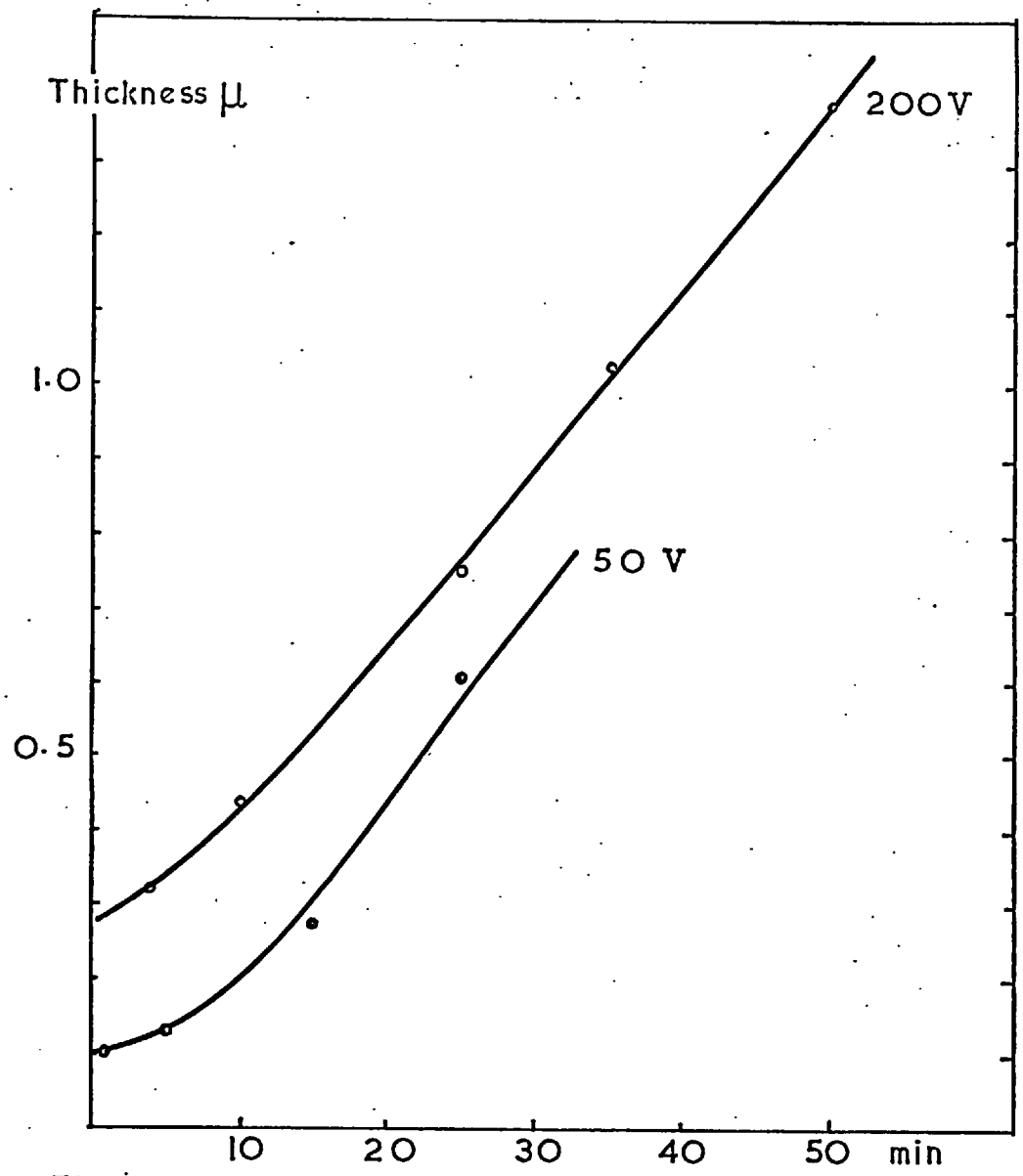


Fig. 25 Growth of oxide film on Aluminium anodised in Borate at 50° C

Fig. 26. Anodic oxide film grown on aluminium to 100 V in borate at 20°C.

Fig. 27. Anodic film grown on aluminium at 100 V for 1 minute after reaching voltage. Borate electrolyte at 50°C.

Fig. 28. Anodic oxide film grown on aluminium at 100 V for 5 minutes after reaching voltage. Borate electrolyte at 50°C.

Fig. 29. Anodic oxide film grown on aluminium at 100 V for 15 minutes after reaching voltage. Borate electrolyte at 50°C.

Fig. 30. Anodic oxide film grown on aluminium at 100 V for 25 minutes after reaching voltage. Borate electrolyte at 50°C.

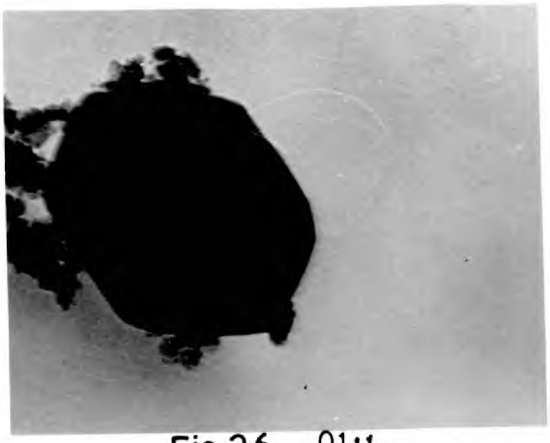


Fig 26 0.1 μ

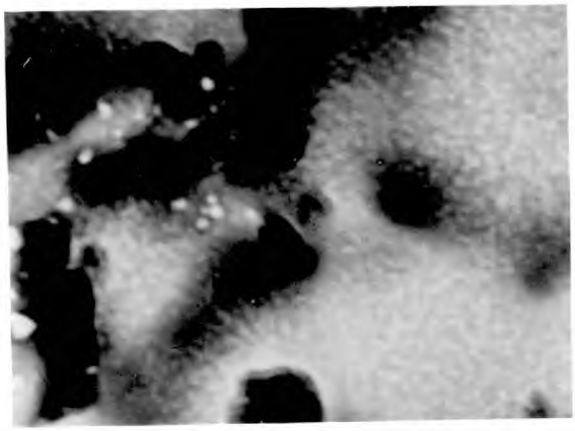


Fig 27 0.1 μ

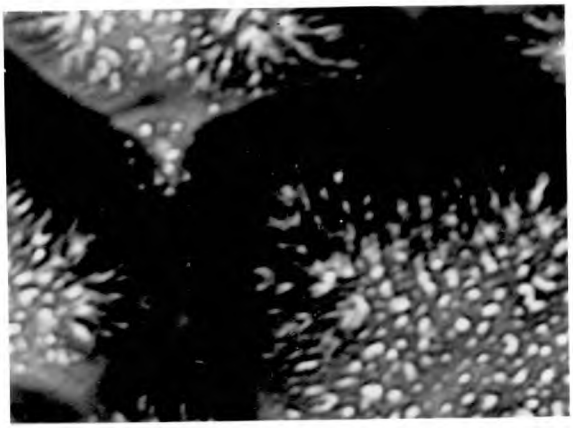


Fig 28 0.1 μ



Fig 29 0.1 μ

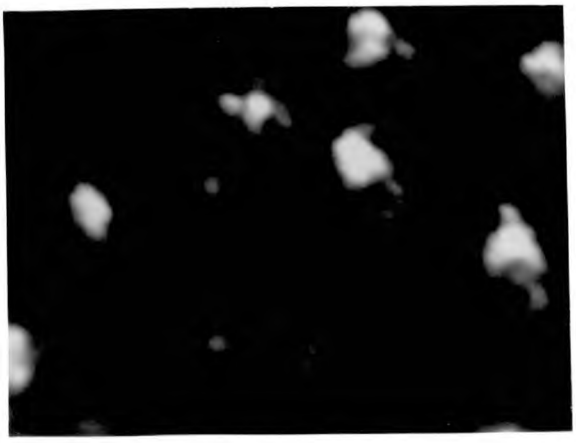


Fig 30 0.1 μ

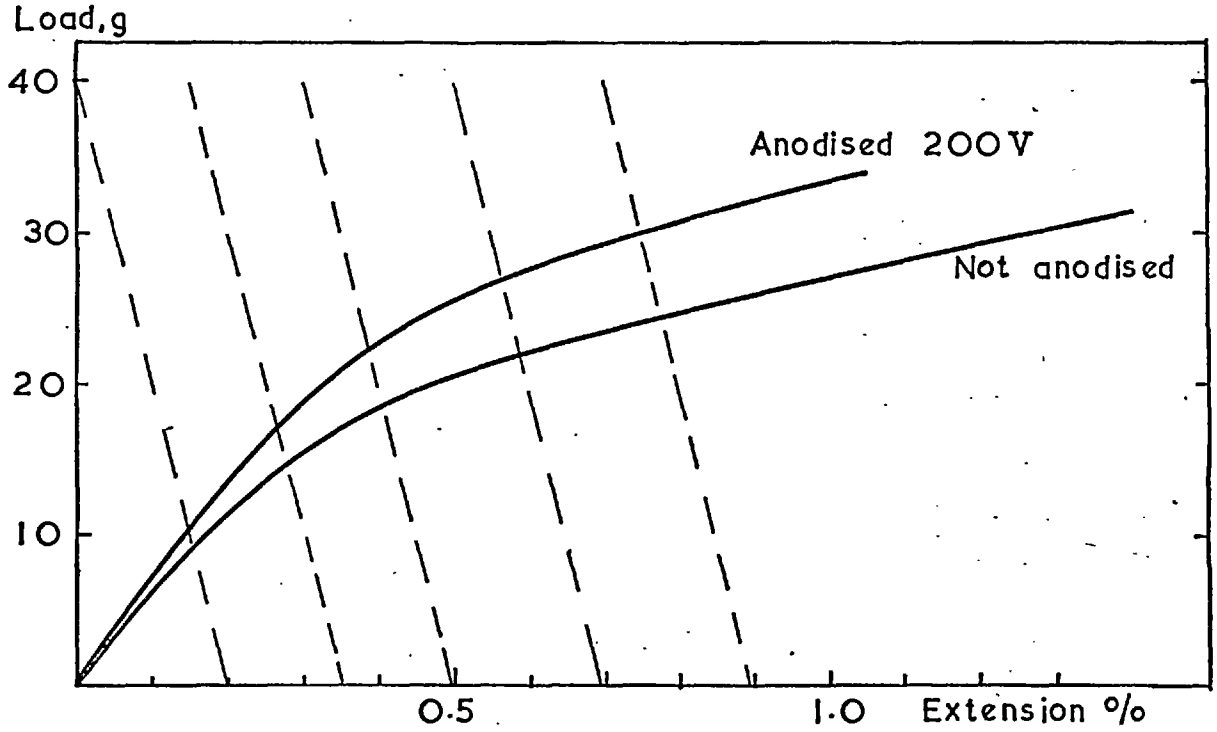


Fig. 31 Stress–strain curves for 0·1 mm dia. aluminium wires. (Broken lines indicate correction for movement of load cell during a 'constant strain' experiment)

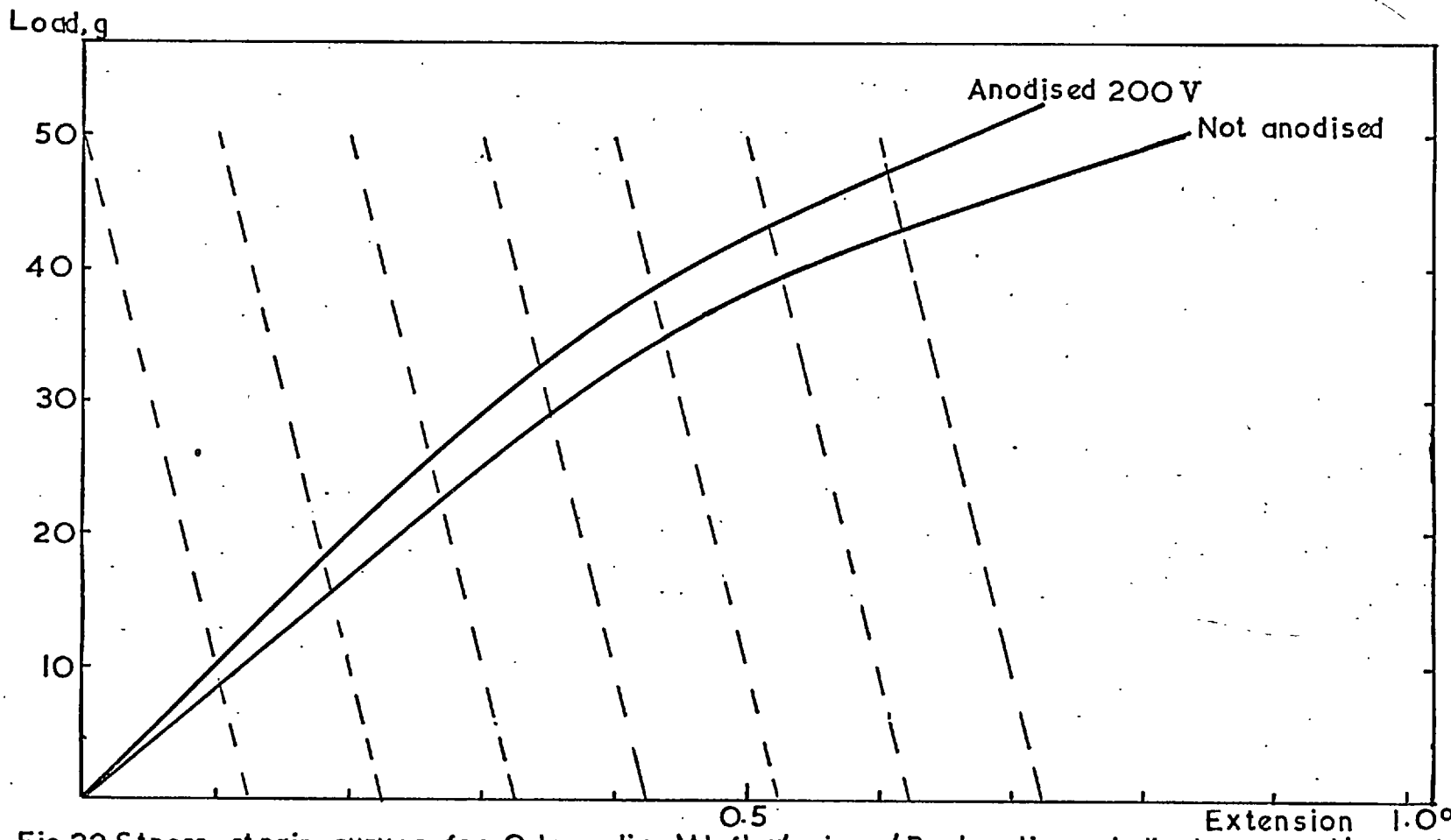


Fig.32 Stress–strain curves for 0.1 mm dia. 'Aluflex' wires. (Broken lines indicate correction for movement of load cell during a 'constant strain' experiment)

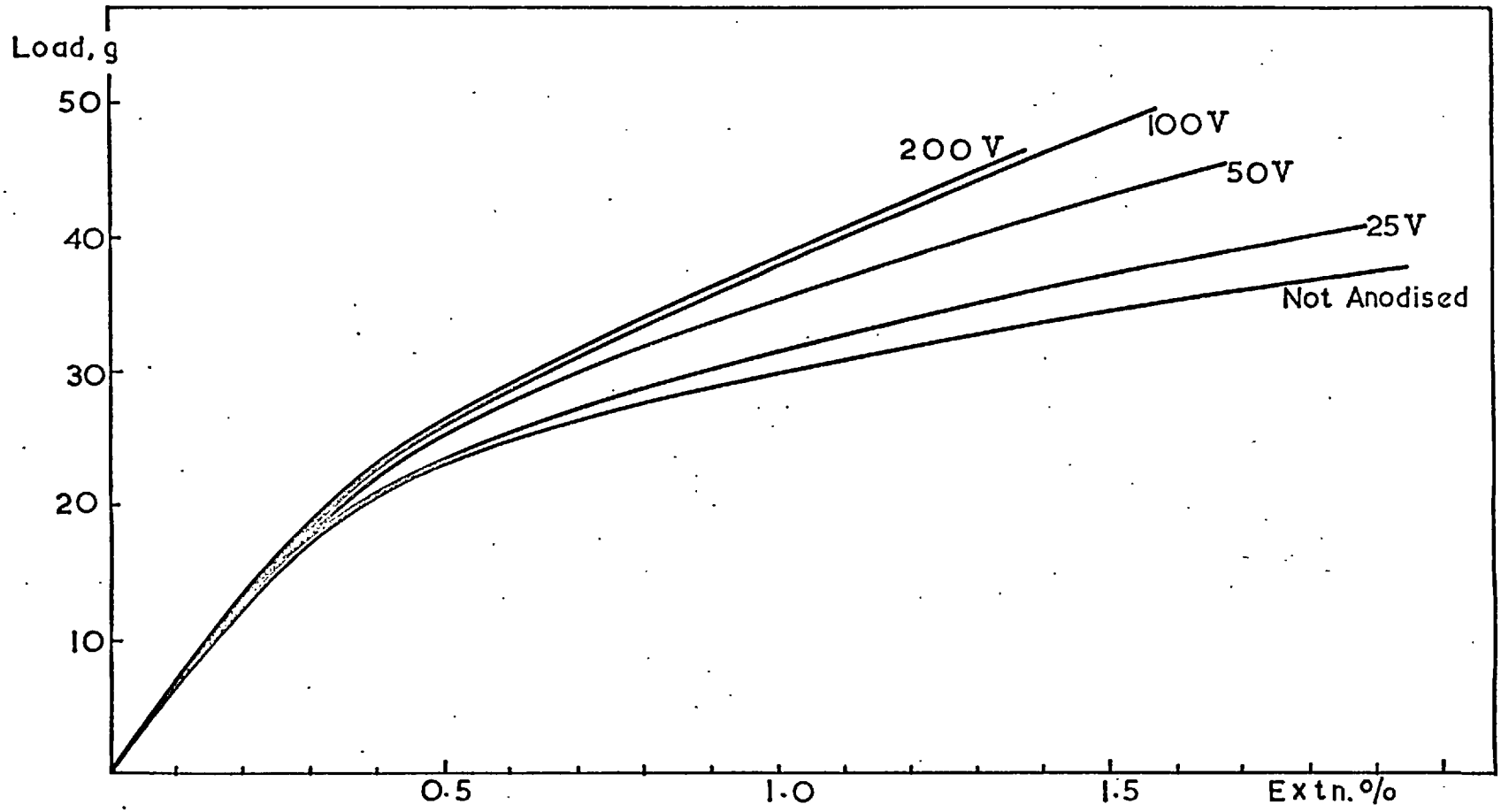


Fig. 33 Strengthening of 0·1 mm Aluminium wires by anodic films grown to varying voltages in Borate

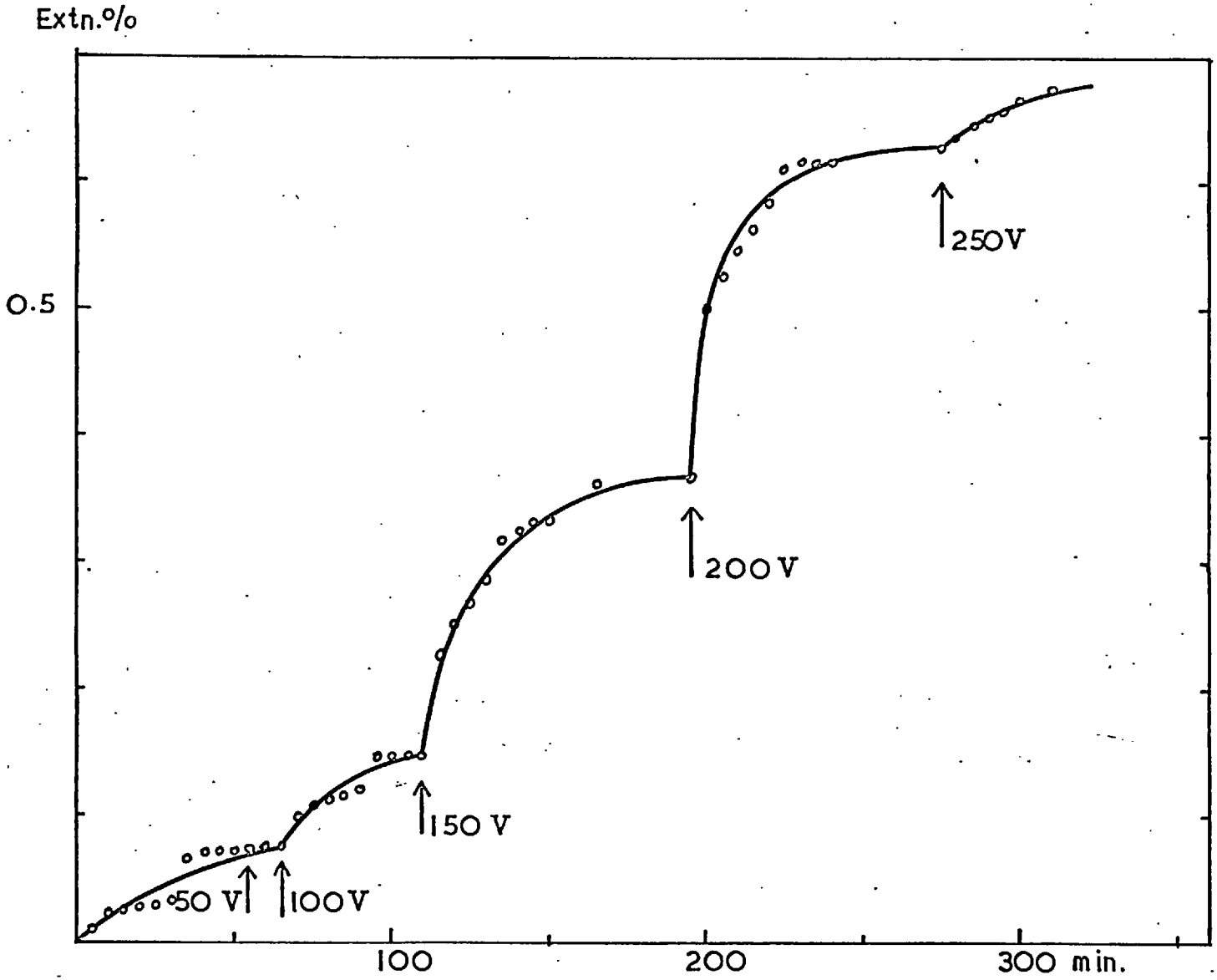


Fig. 34 Extension under 25g load of Aluminium wire anodised to 200V in Borate

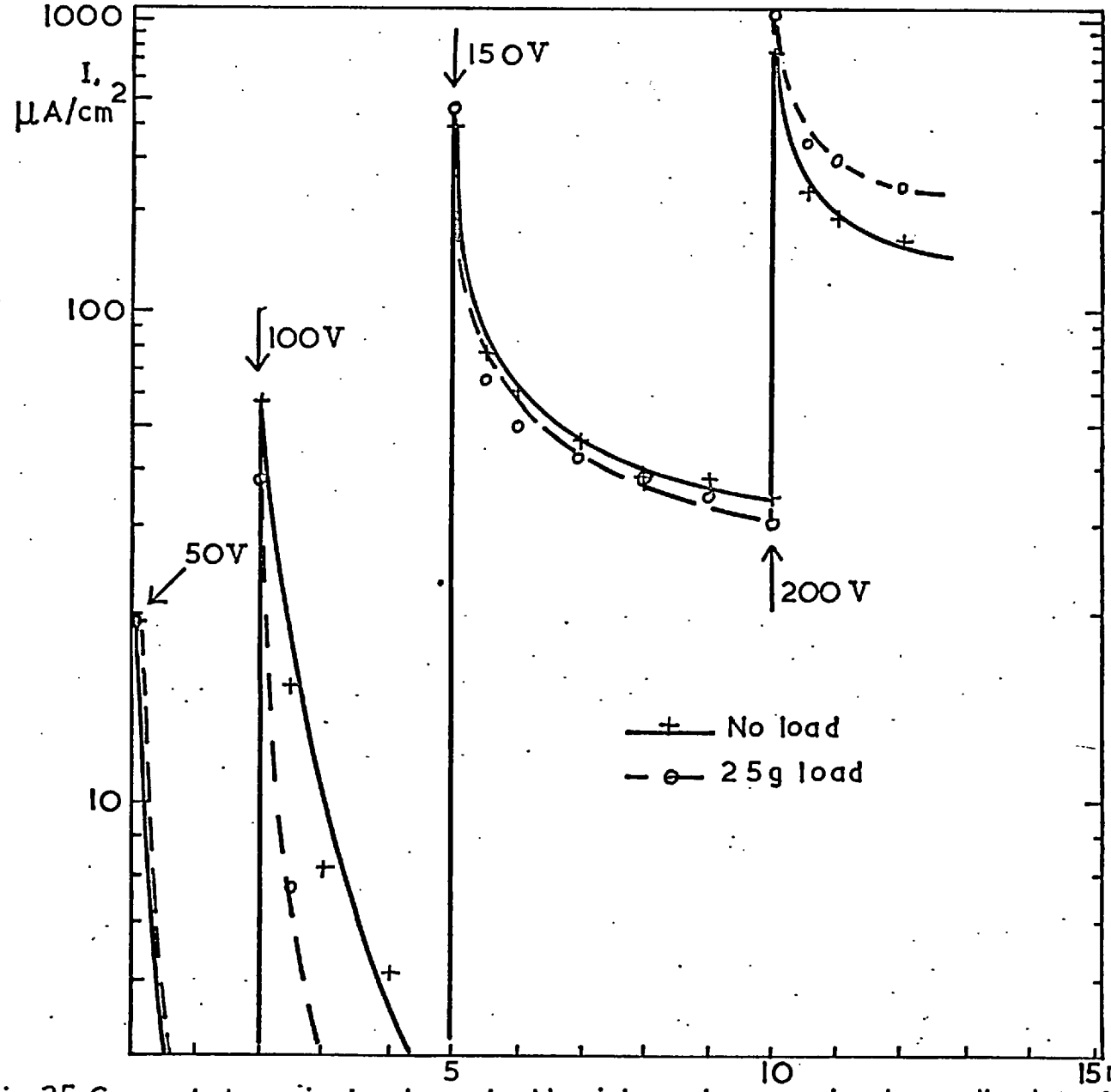


Fig.35 Current transients shown by Aluminium wires previously anodised to 200 V in Borate

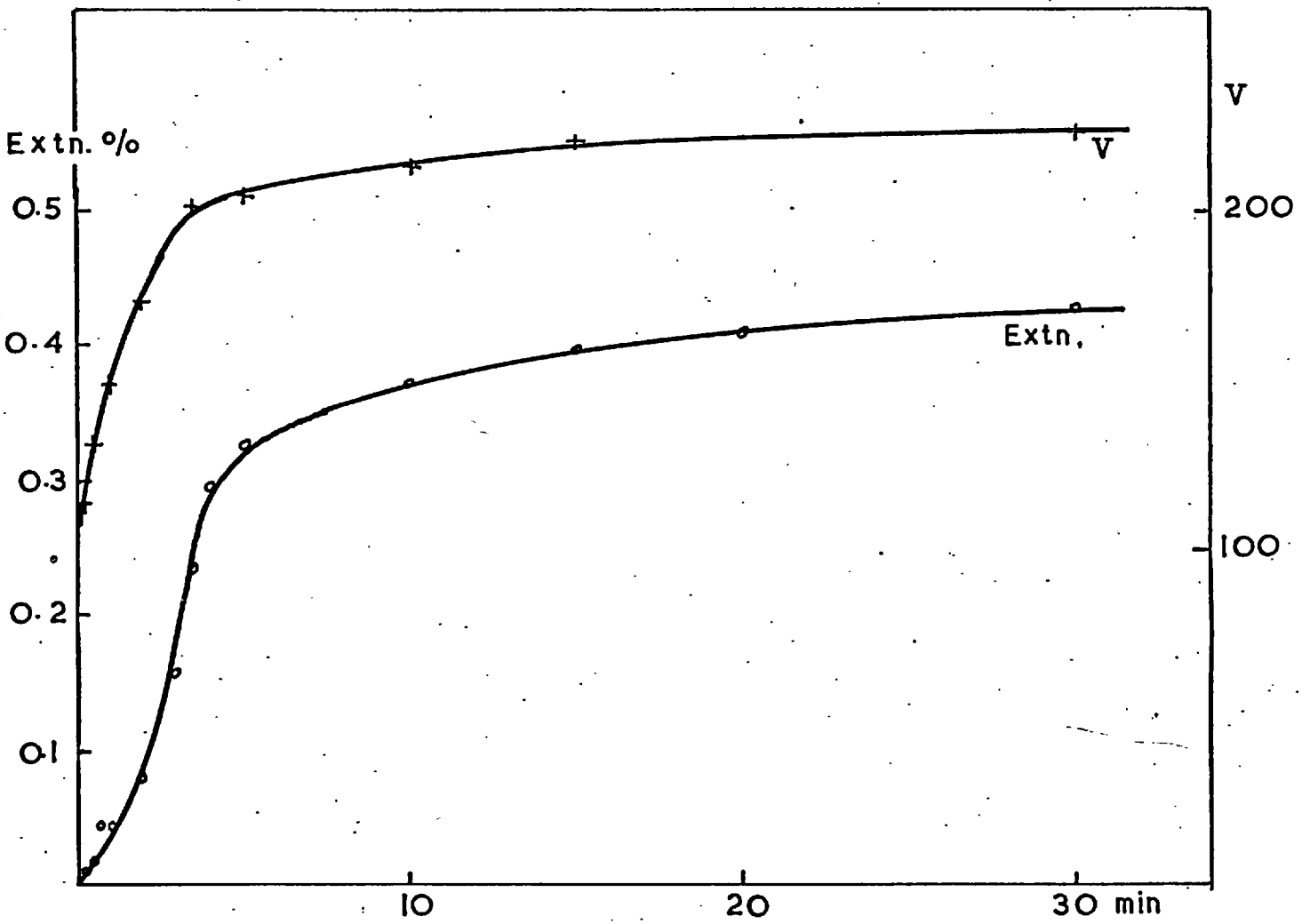


Fig.36 Voltage and Extension at 0.156 mA/cm^2 and under 25g load of Aluminium wires anodised to 200V in Borate

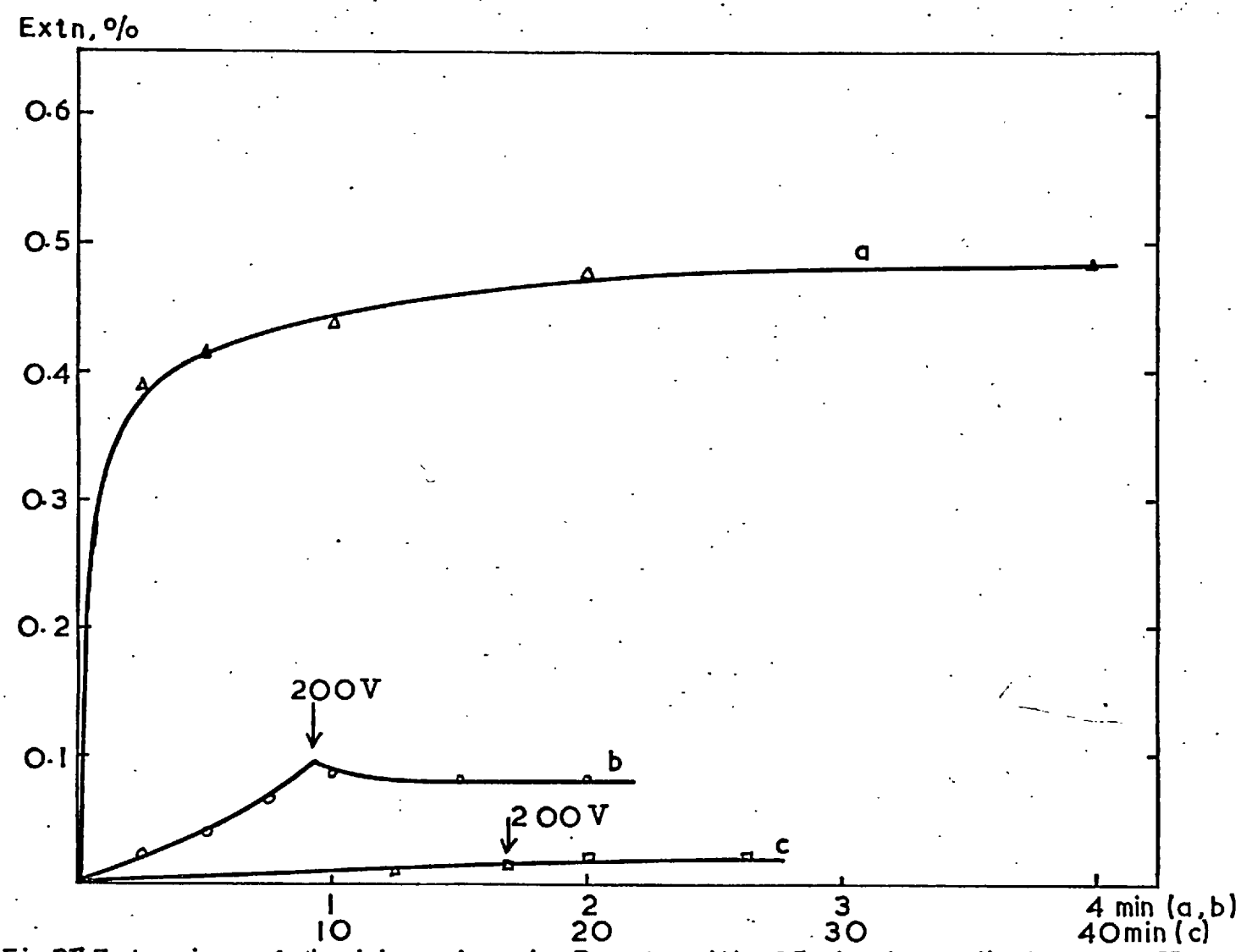


Fig.37 Extension of aluminium wires in Borate with 25g load; anodised to 200V
a) Pre-anodised, field re-applied after loading. b) Anodised at 10mA/cm^2
c) Anodised at 0.64 mA/cm^2

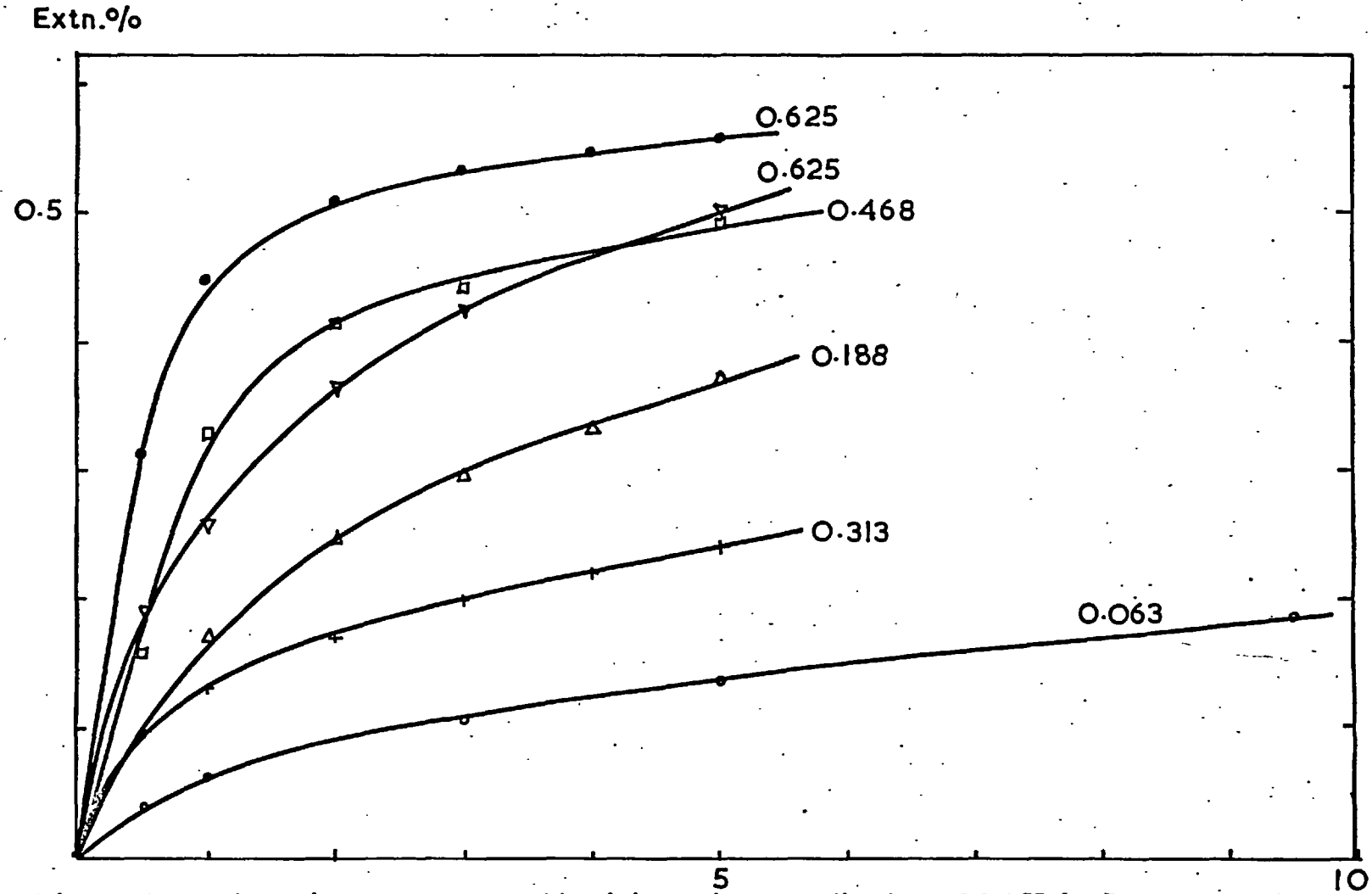


Fig.38 Extension–time curves for Aluminium wires anodised to 200V in Borate and extended at constant current (marked in mA/cm^2) under 25g load.

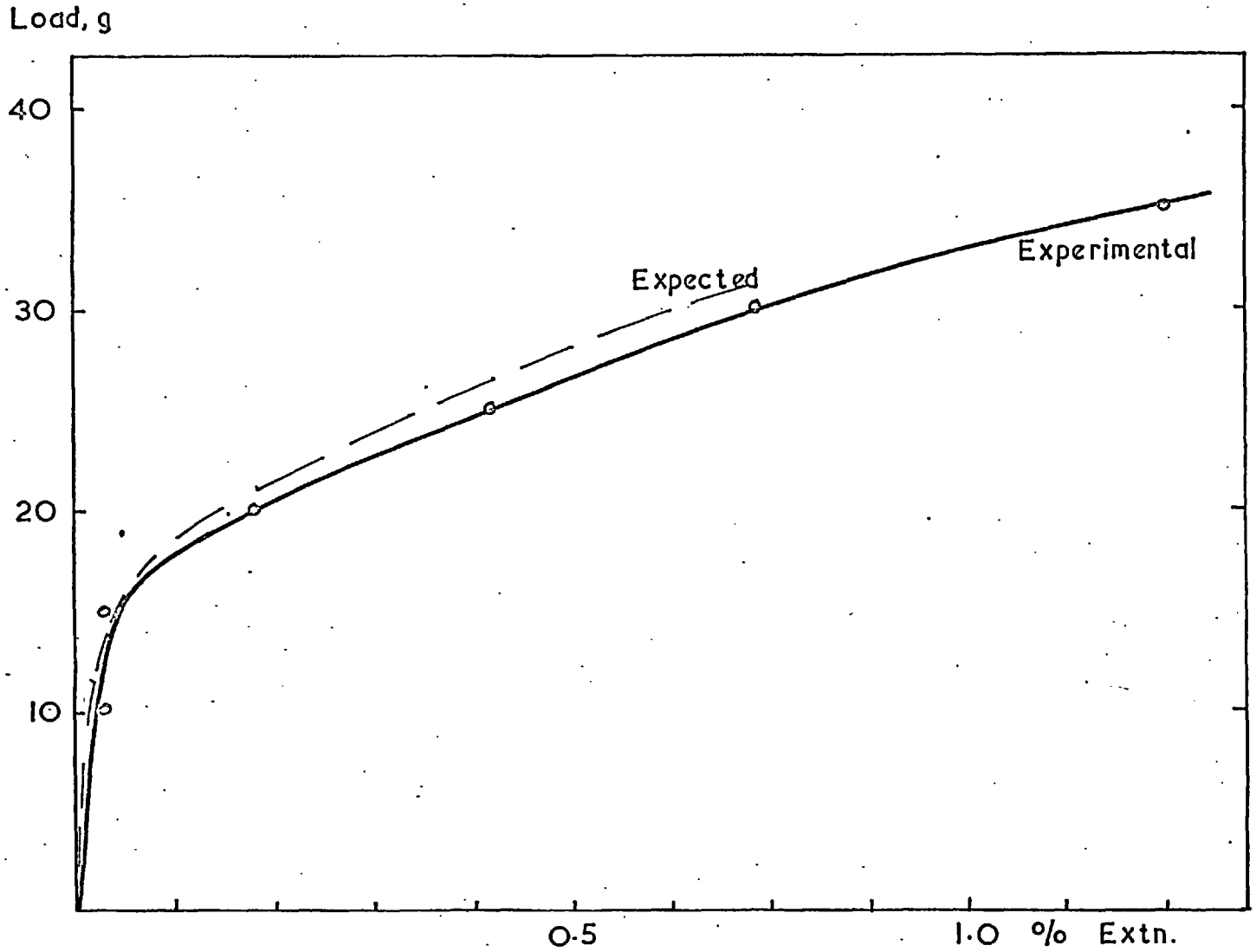


Fig. 39 Total extension of Aluminium wires anodised to 200 V in Borate and extended under load at 210 V

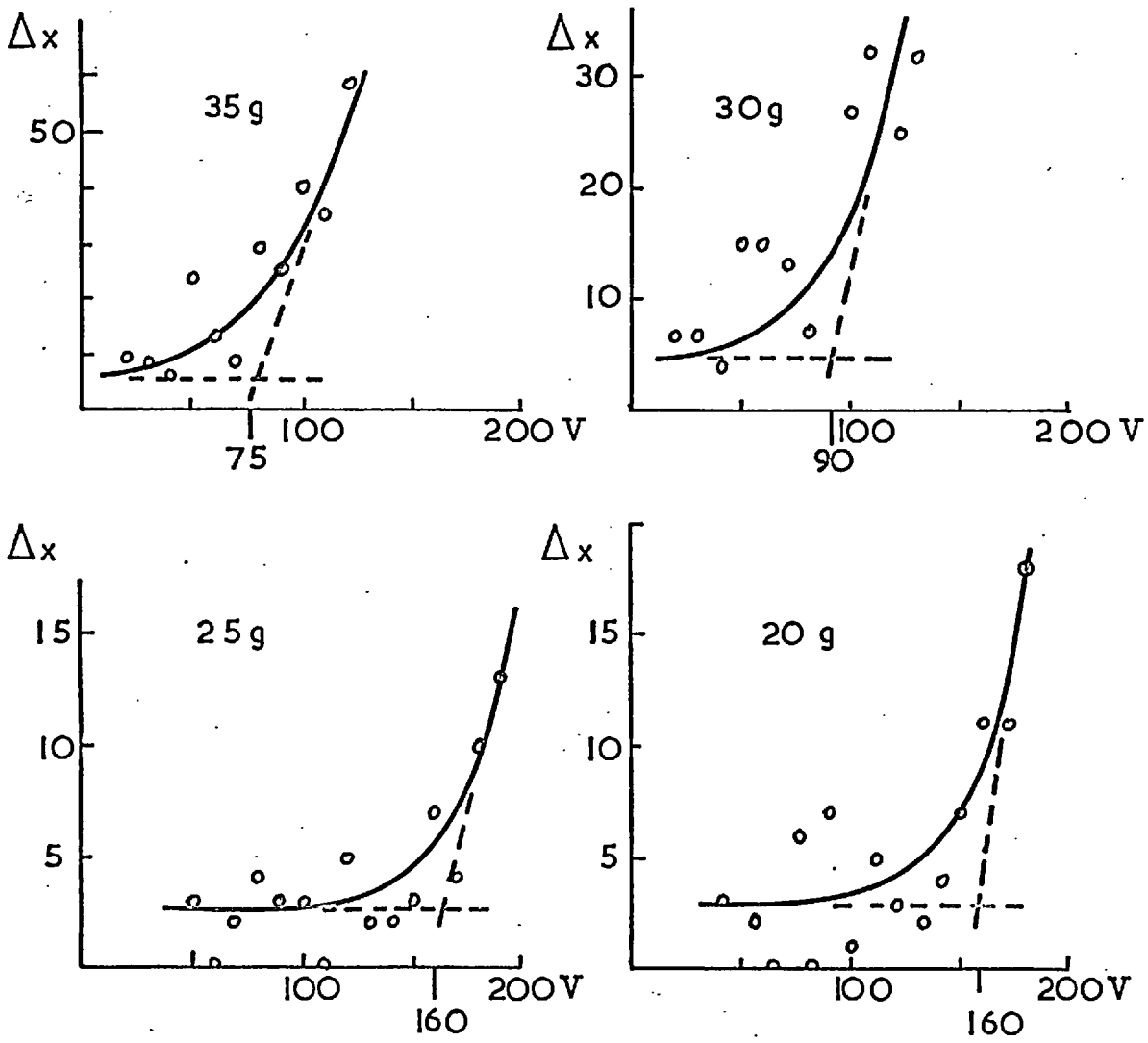


Fig40Extension increments with increasing applied voltage of Aluminium wires anodised to 200V in Borate.

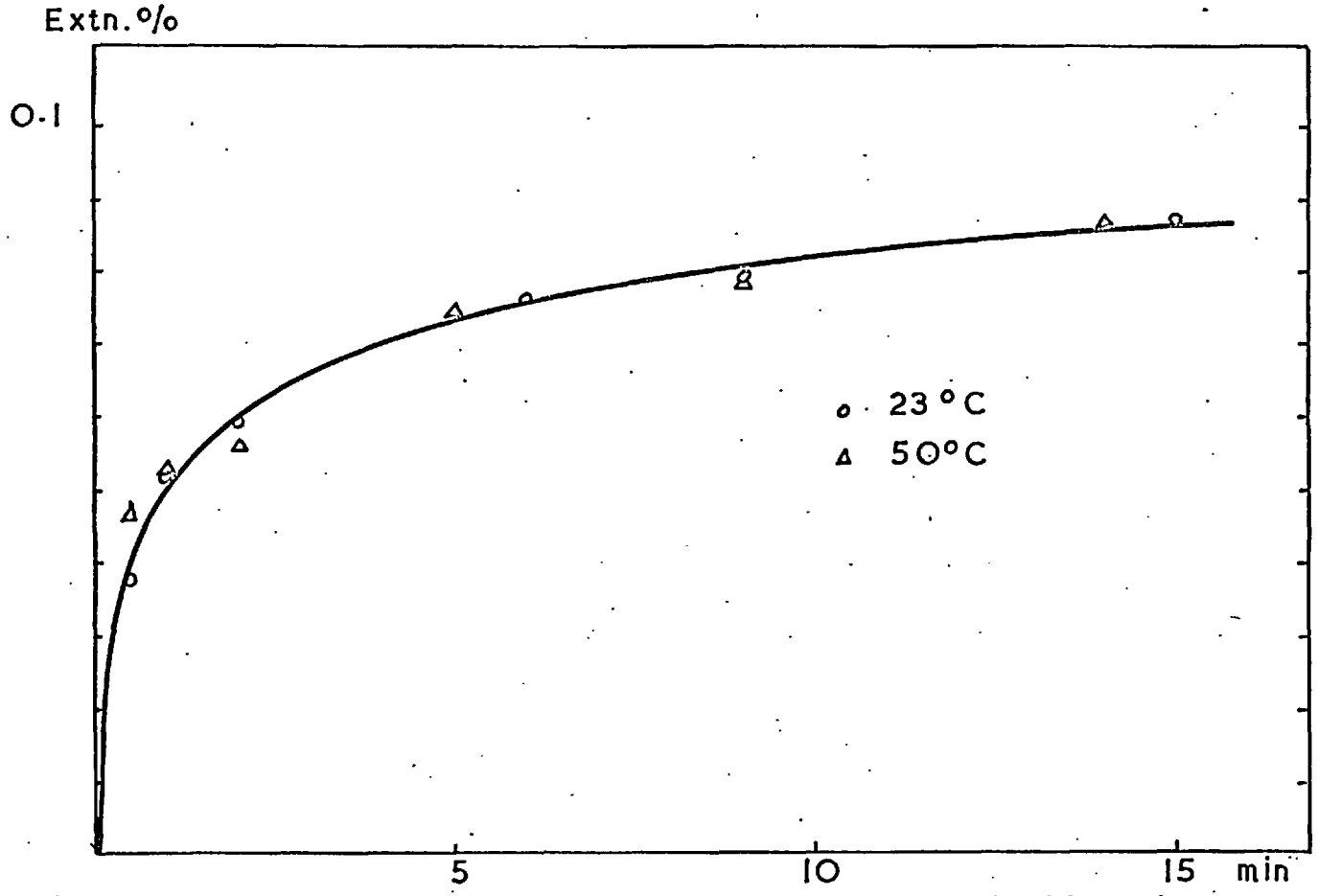


Fig.41 Effect of temperature on extension of anodised Aluminium wires at 200V and 20g load in Borate

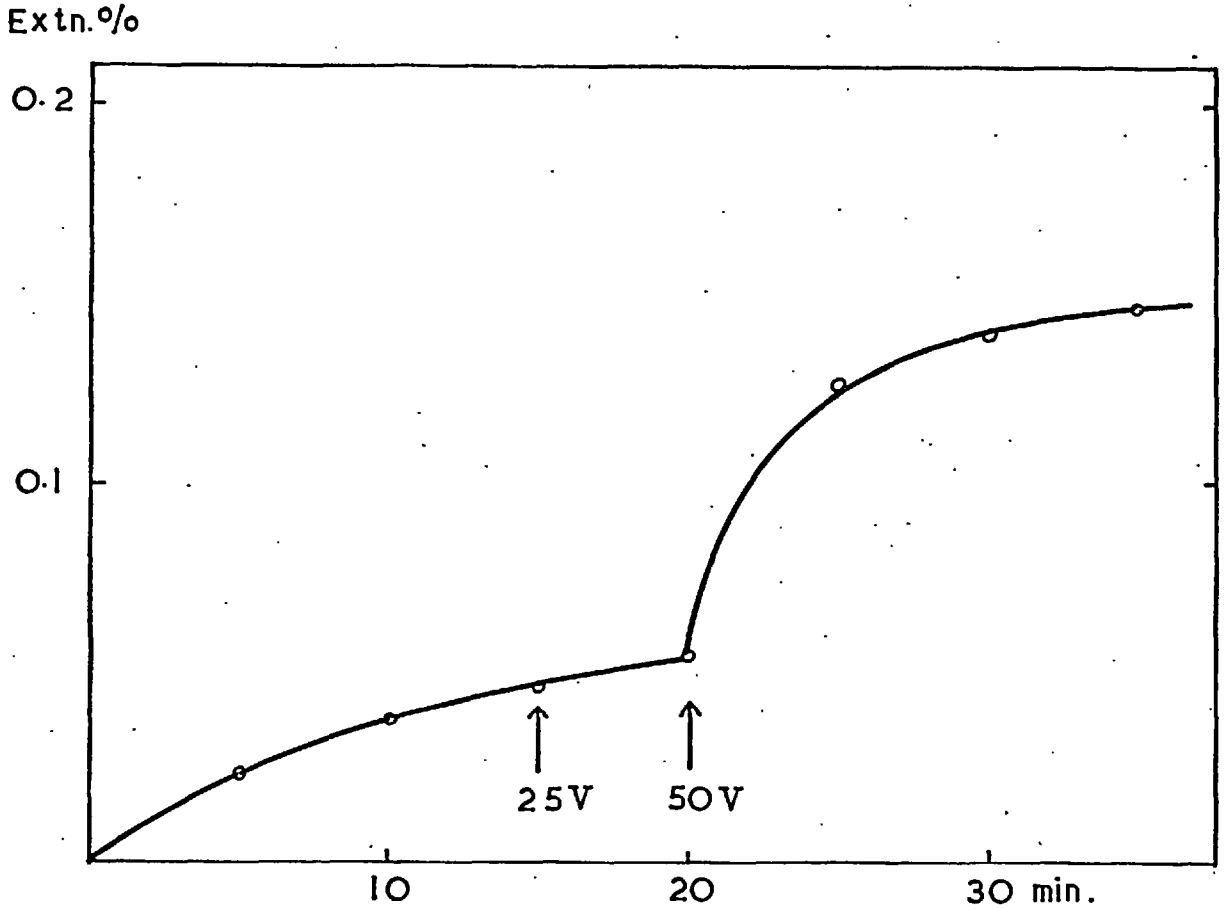


Fig.42 Extension under 20g load of Aluminium wire anodised to 50V in 5% solution of hydrated Ammonium Borate in Ethanediol

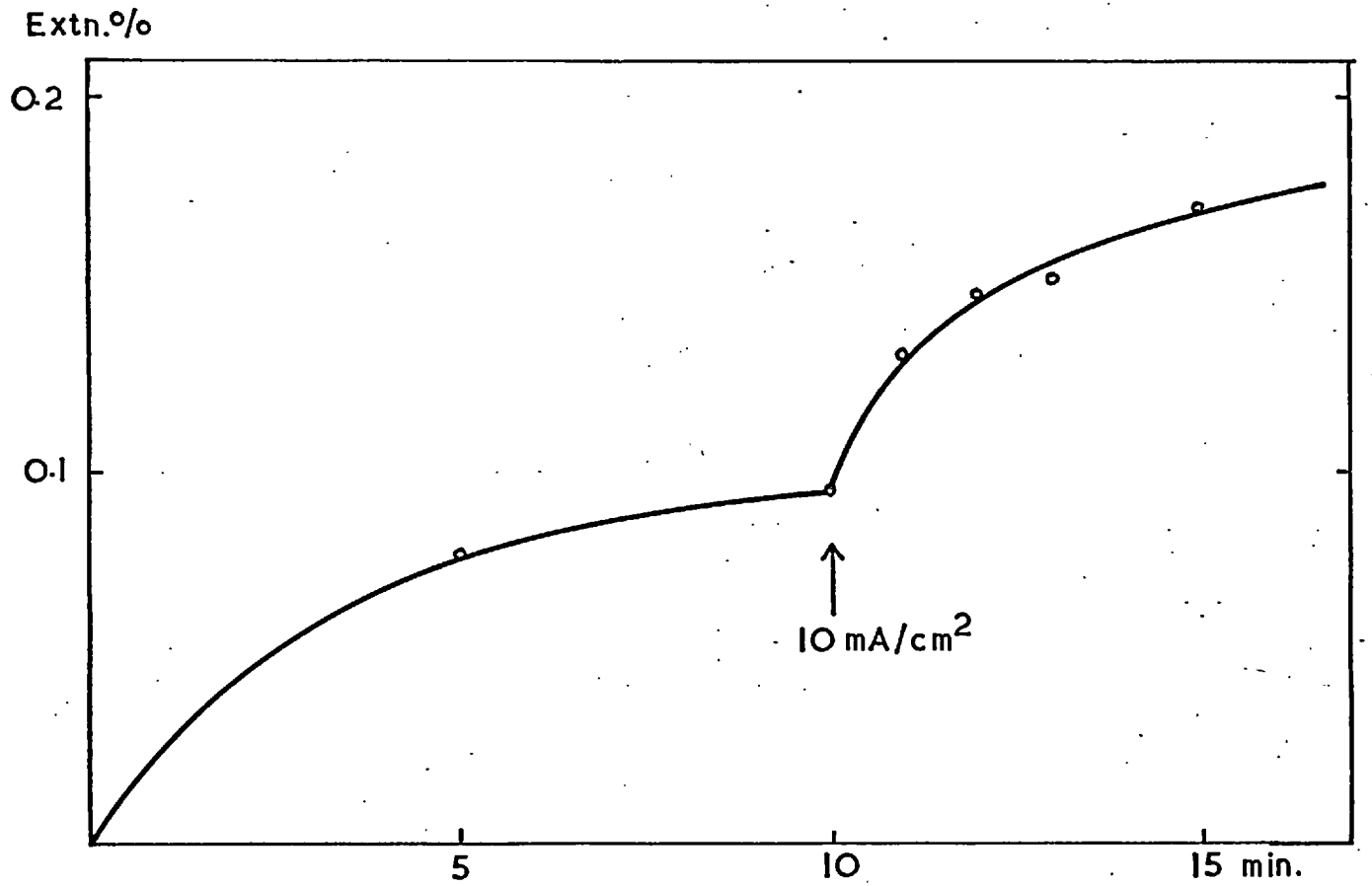


Fig.43 Extension under 20g load of Aluminium wire anodised for 5 min. at 10 mA/cm^2 in 15% H_2SO_4

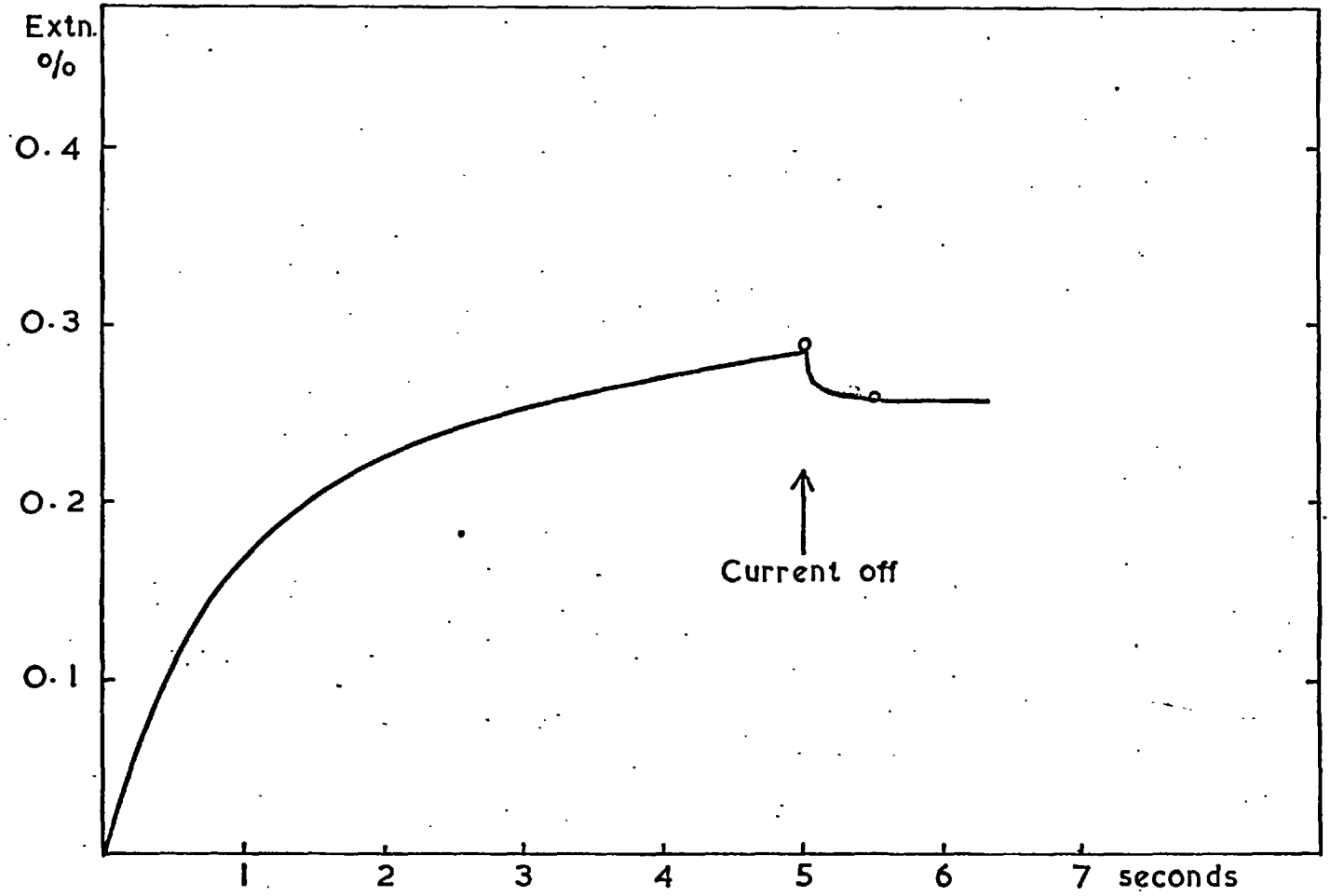


Fig.44 Extension of 0.1mm. dia. aluminium wire under 30g load during electropolishing at 625 mA/cm^2

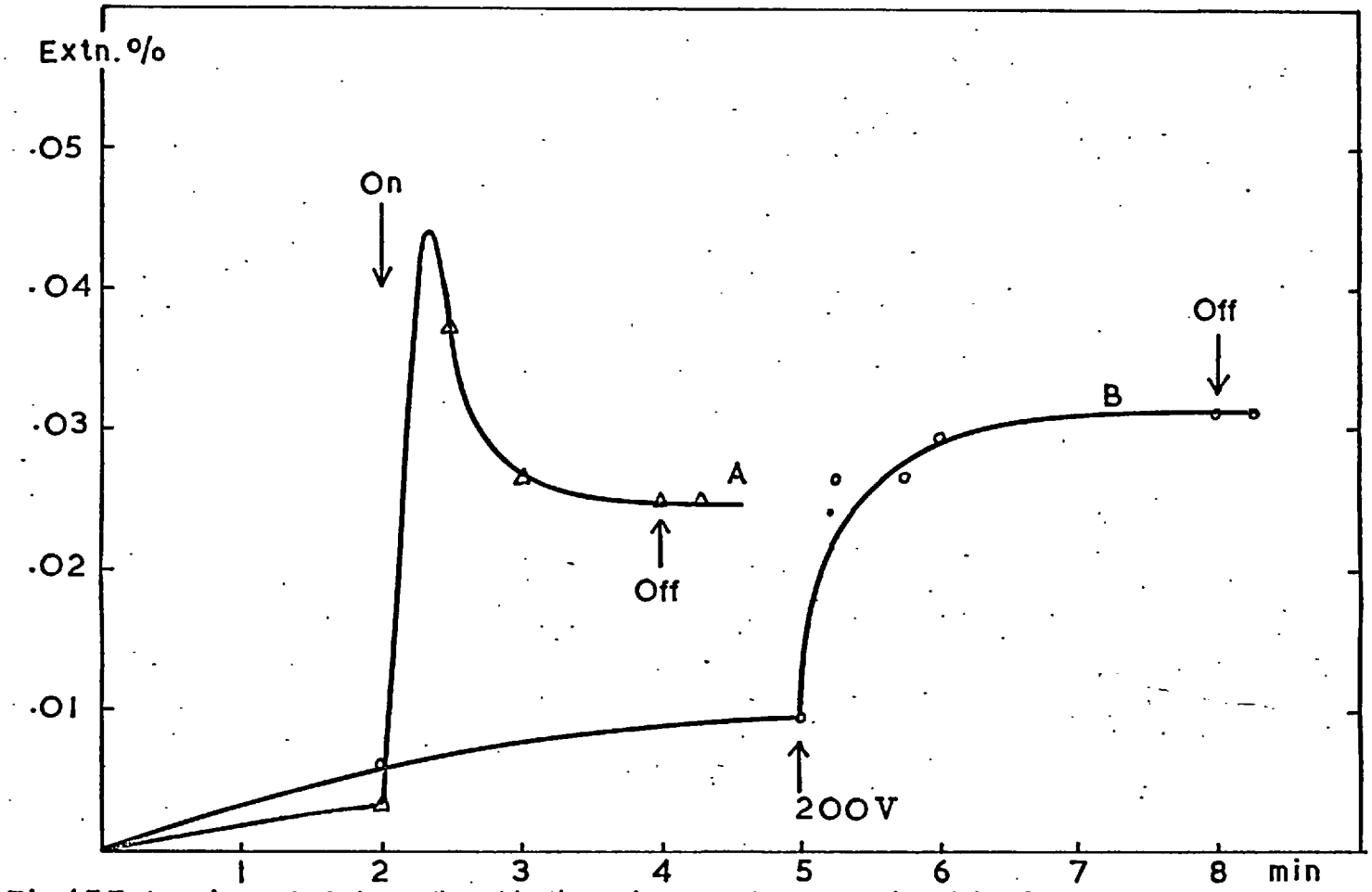


Fig.45 Extension of 0.1mm dia. Aluflex wires under 40g load in Borate.

A) Wire loaded and anodised to 200V at 20 mA/cm^2

B) Wire pre-anodised to 200V : field re-applied after loading

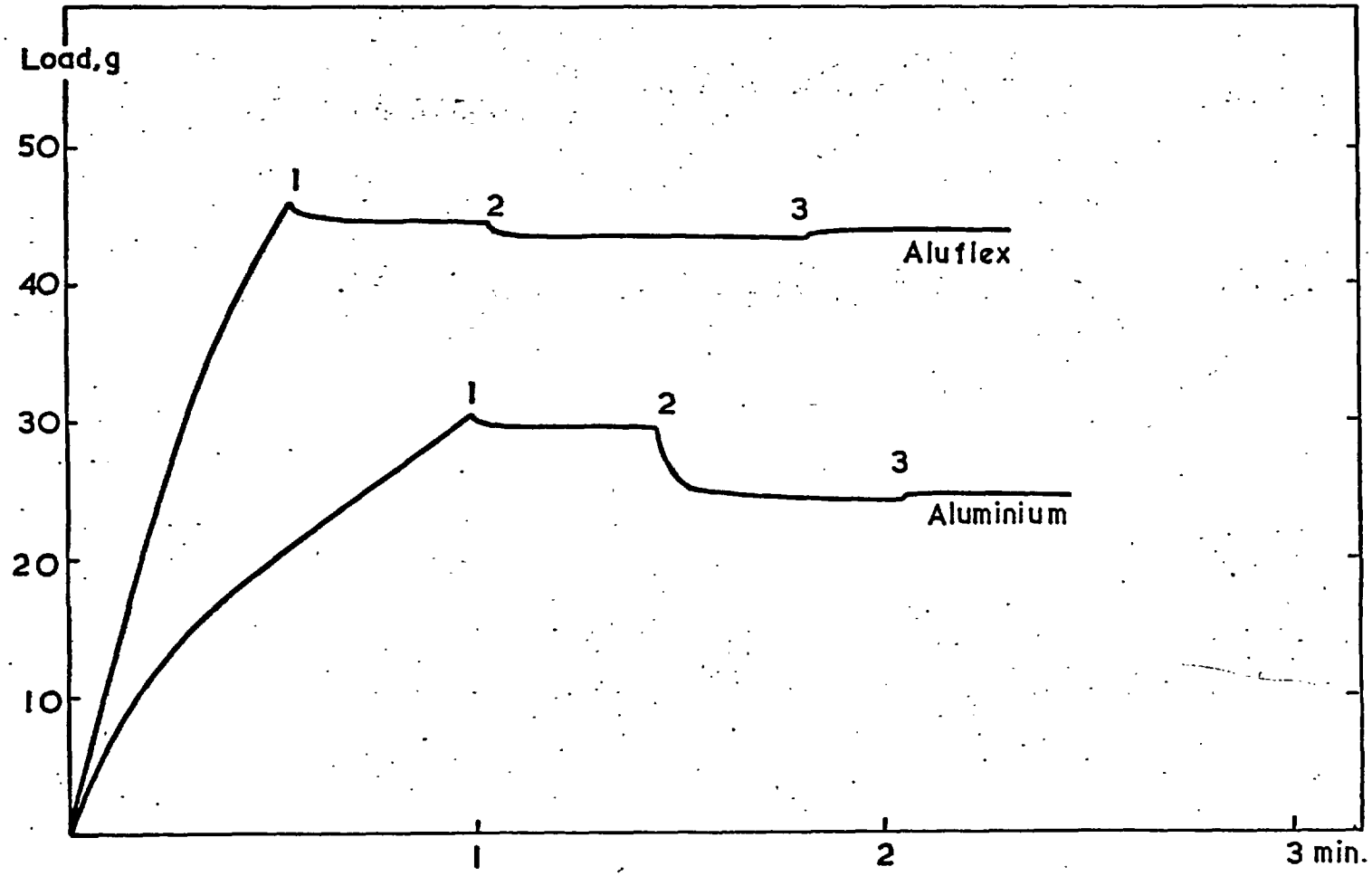


Fig. 46 Stress changes on 0·1mm dia. wires anodised to 200V and subjected to a fixed strain.
1) Straining stopped. 2) 200 V re-applied. 3) Field removed.

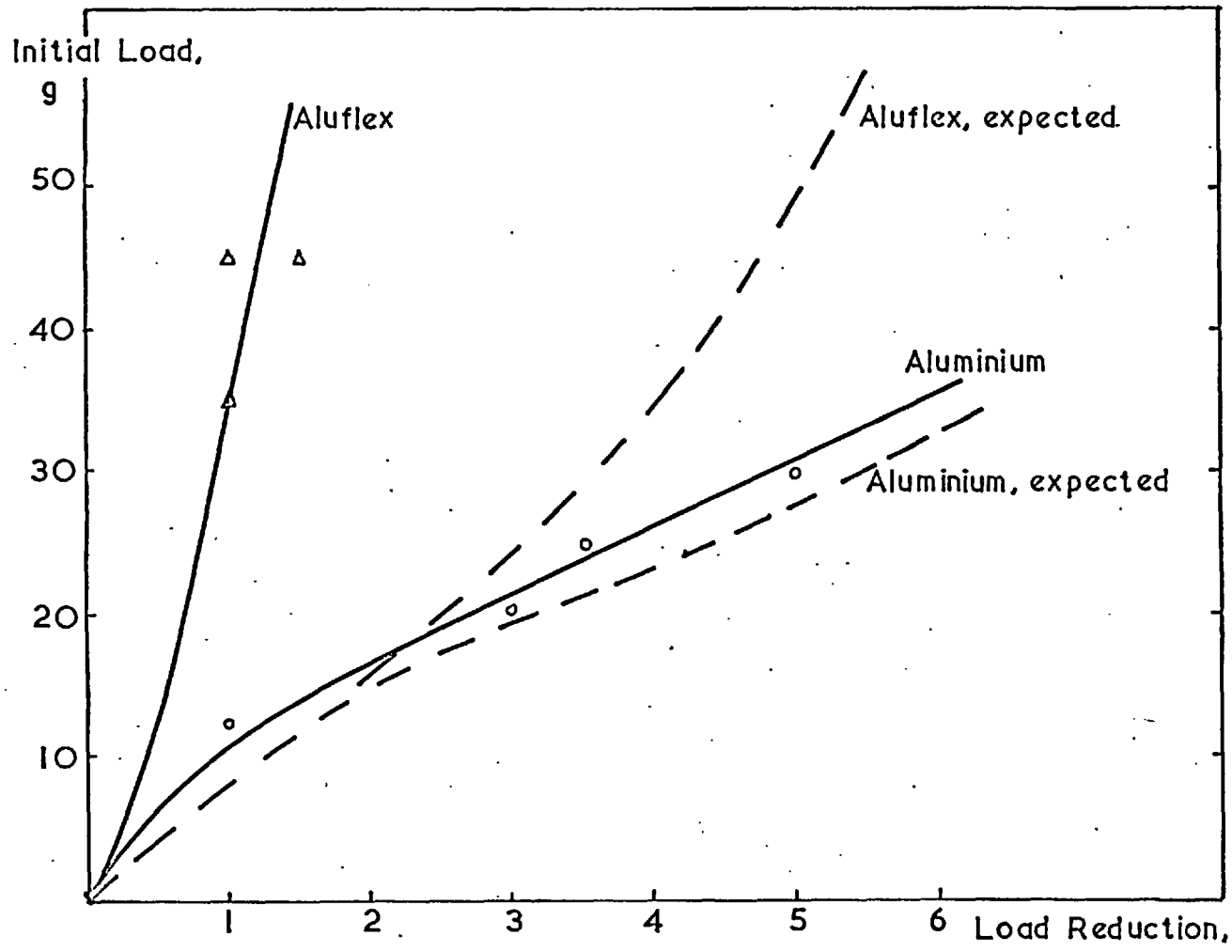


Fig. 47 Reduction in load on 0·1mm dia. wires anodised to 200V in Borate and under a fixed strain when 200V is re-applied.

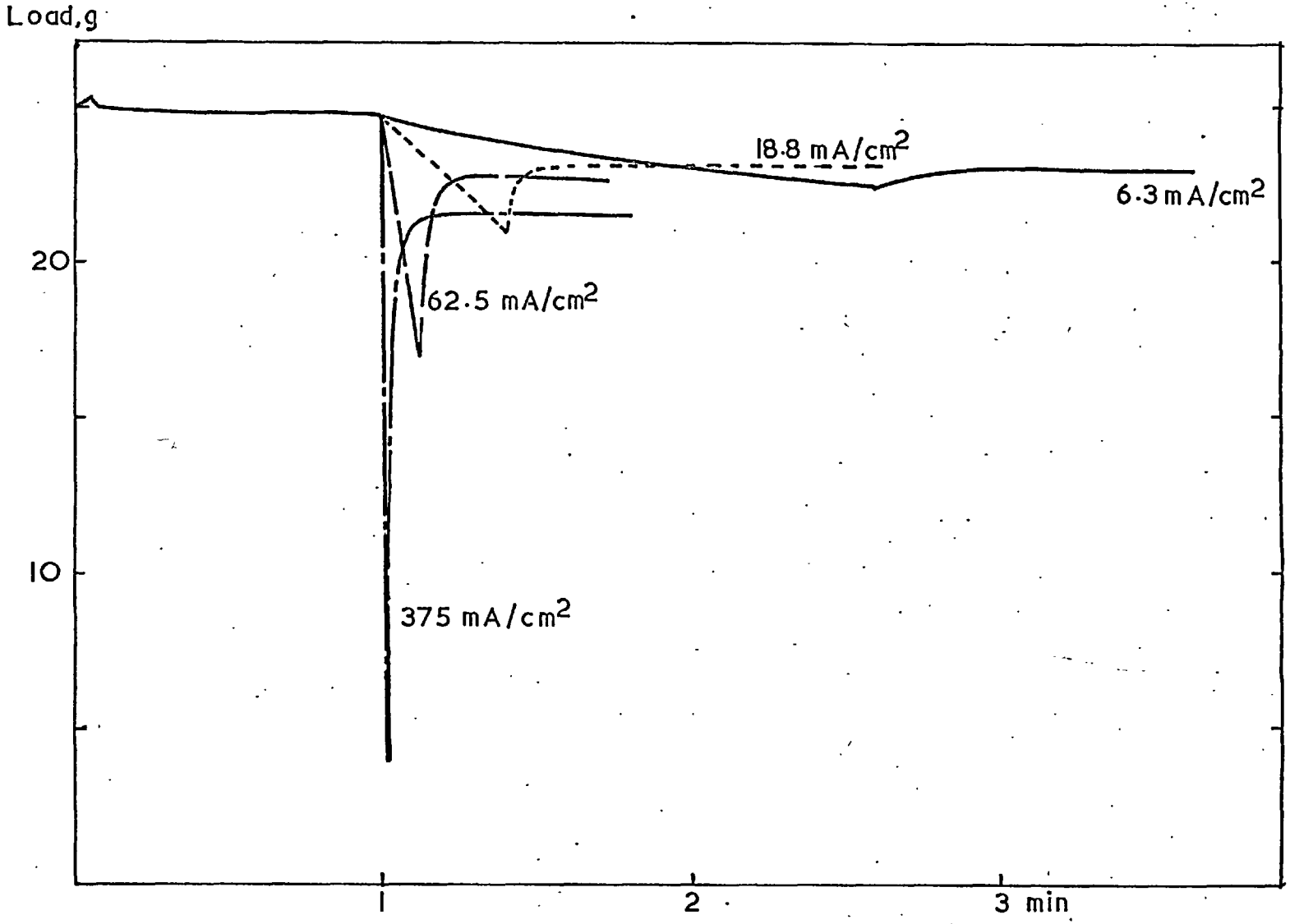


Fig 48 Stress changes during anodising of 0.1 mm aluminium wires to 200V at varying current densities in Borate with a fixed pre-strain.

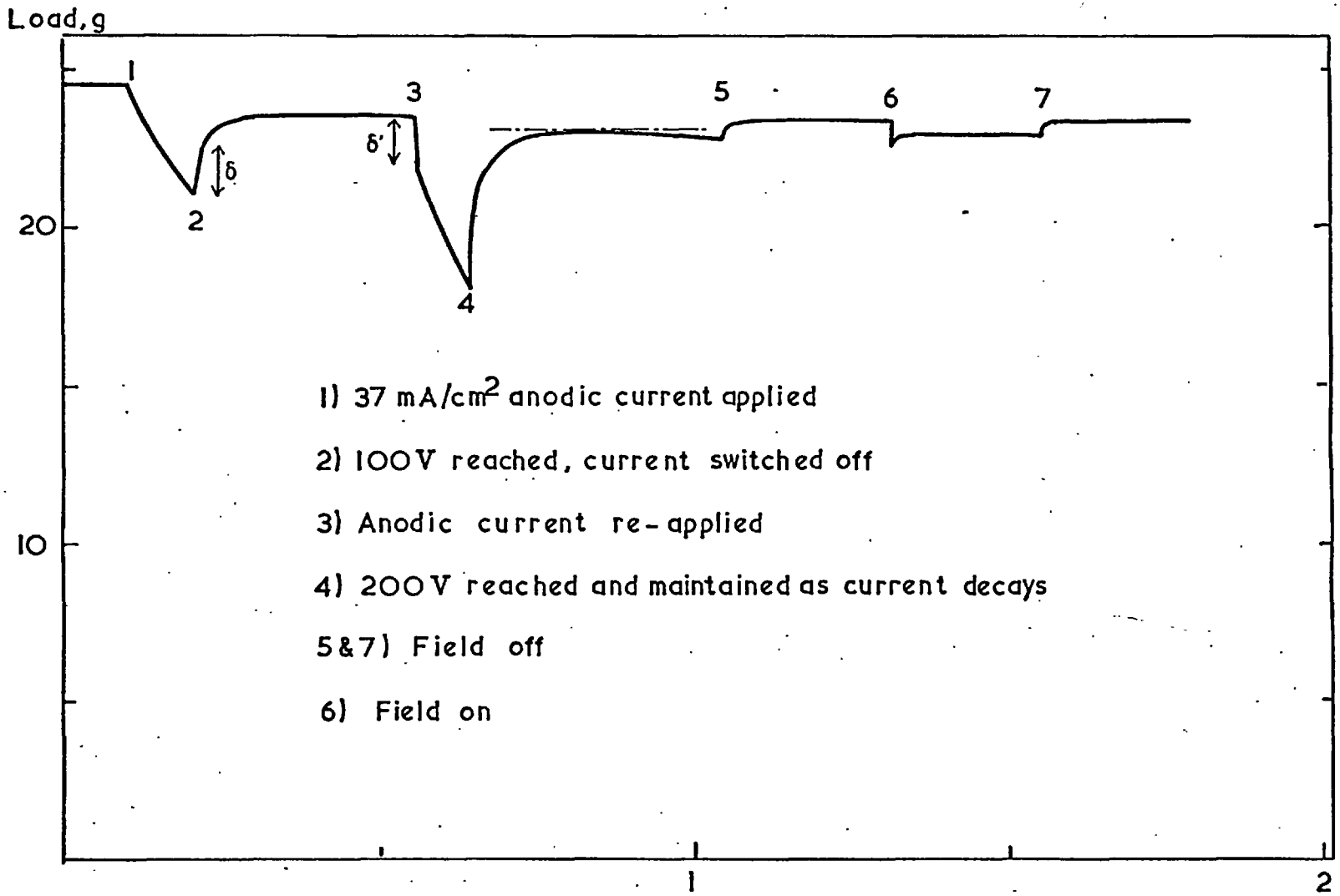


Fig.49 Stress changes during anodising in Borate of a pre-strained 0.1 mm dia. aluminium wire.

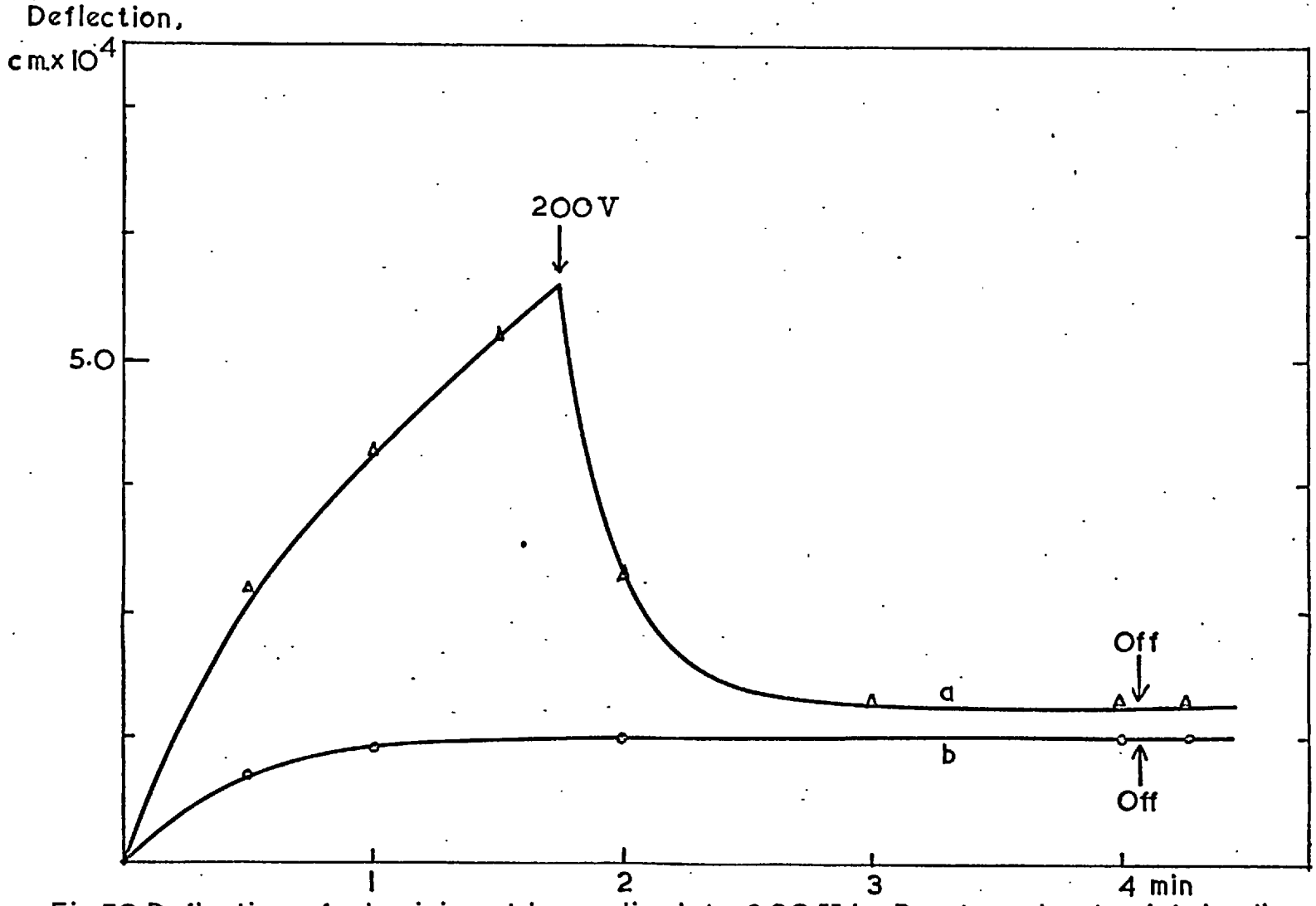


Fig. 50 Deflection of aluminium strip anodised to 200 V in Borate under 4-point bending
a) Anodised at 5 mA/cm^2. b) Pre-anodised, field re-applied after loading.

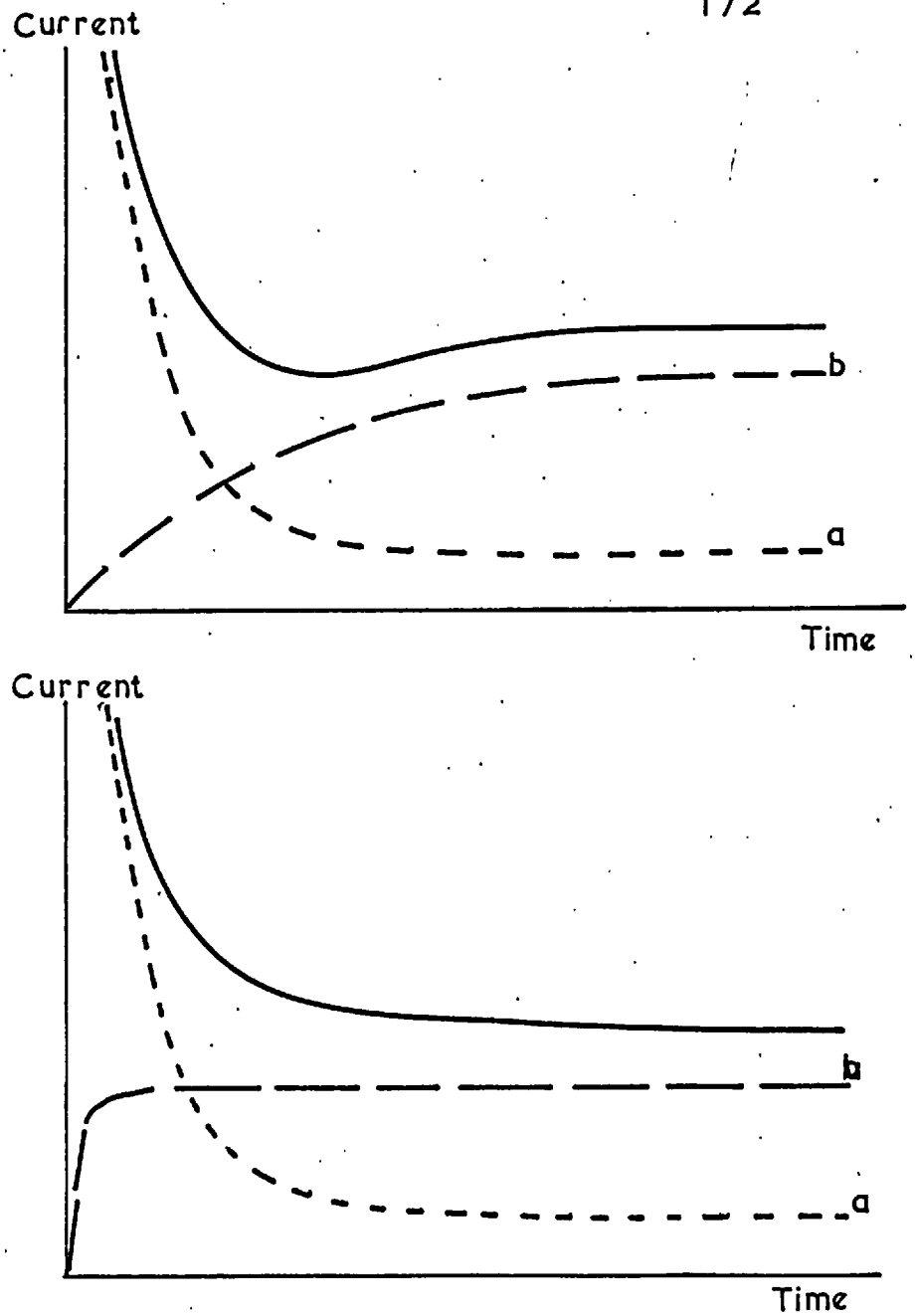


Fig. 51 Current decay during the formation of porous anodic films

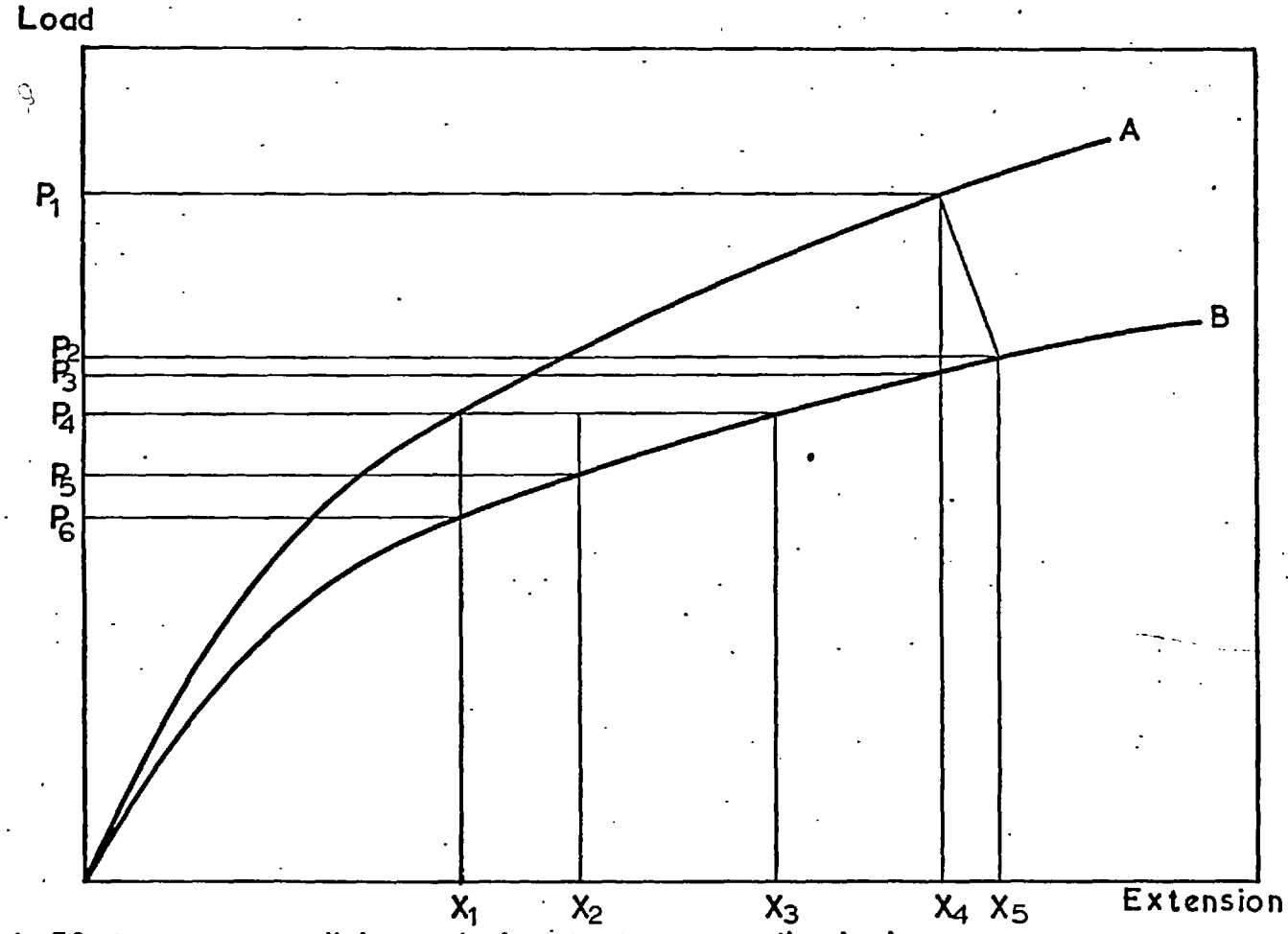


Fig.52 Stress conditions during tests on anodised wires

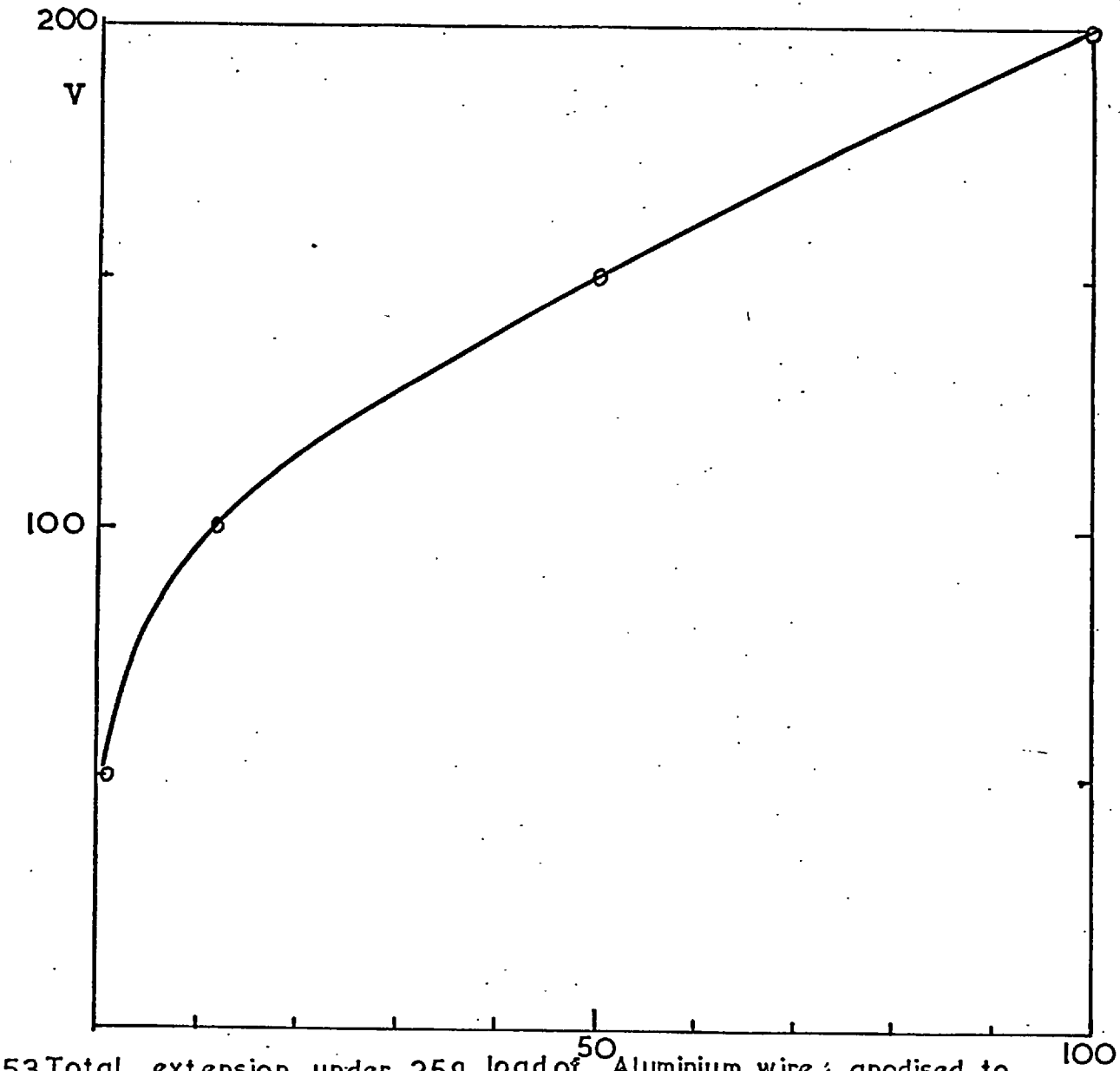


Fig.53 Total extension under 25g load of Aluminium wire anodised to 200 V in Borate. Extension at 200 V is taken as 100 %

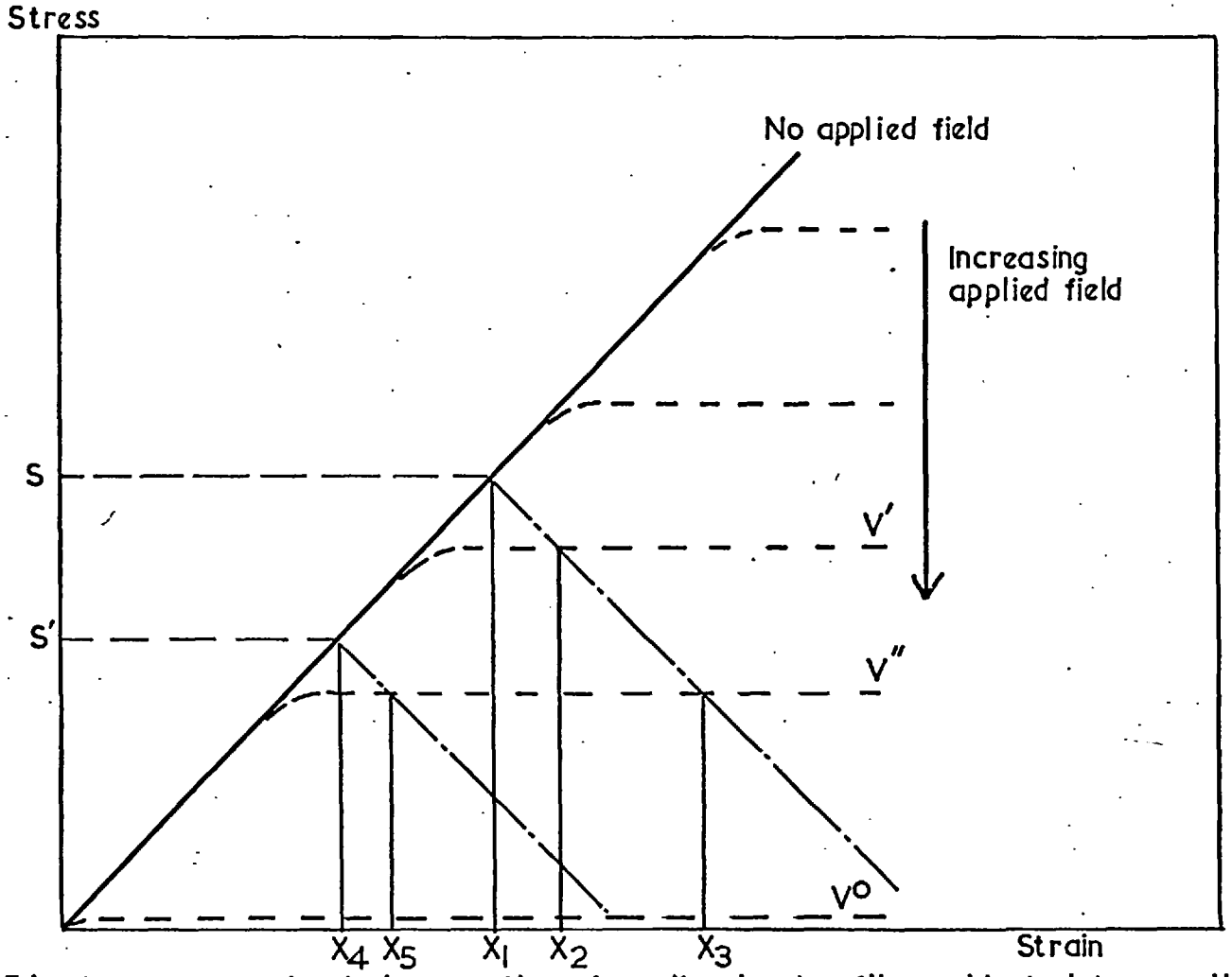


Fig.54 Apparent mechanical properties of anodic alumina film subjected to anodic field. Original growth field is V^{o}

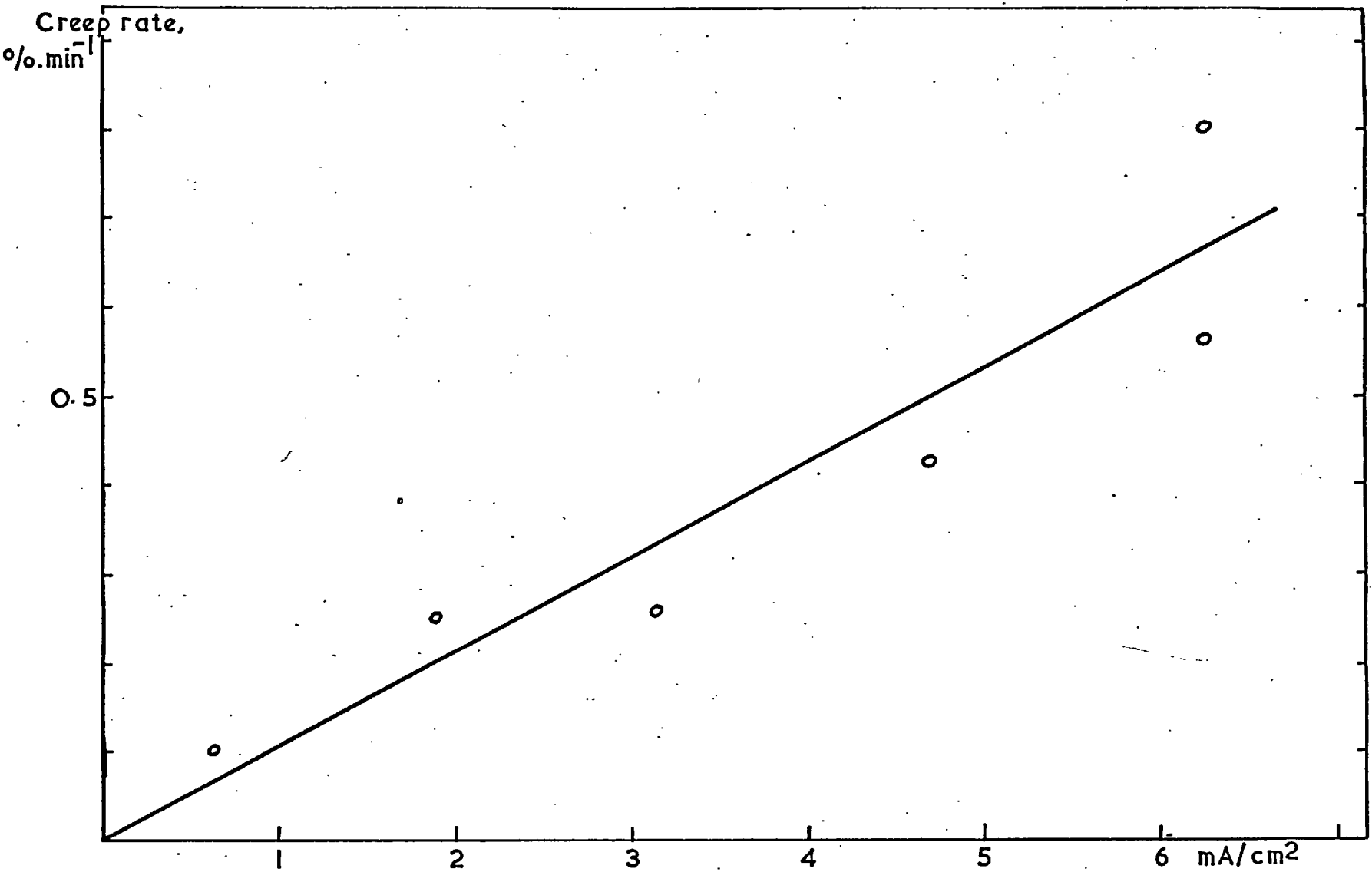


Fig. 55 Initial creep rate of Aluminium wires anodised to 200 V in Borate and extended at 25g load at varying current densities

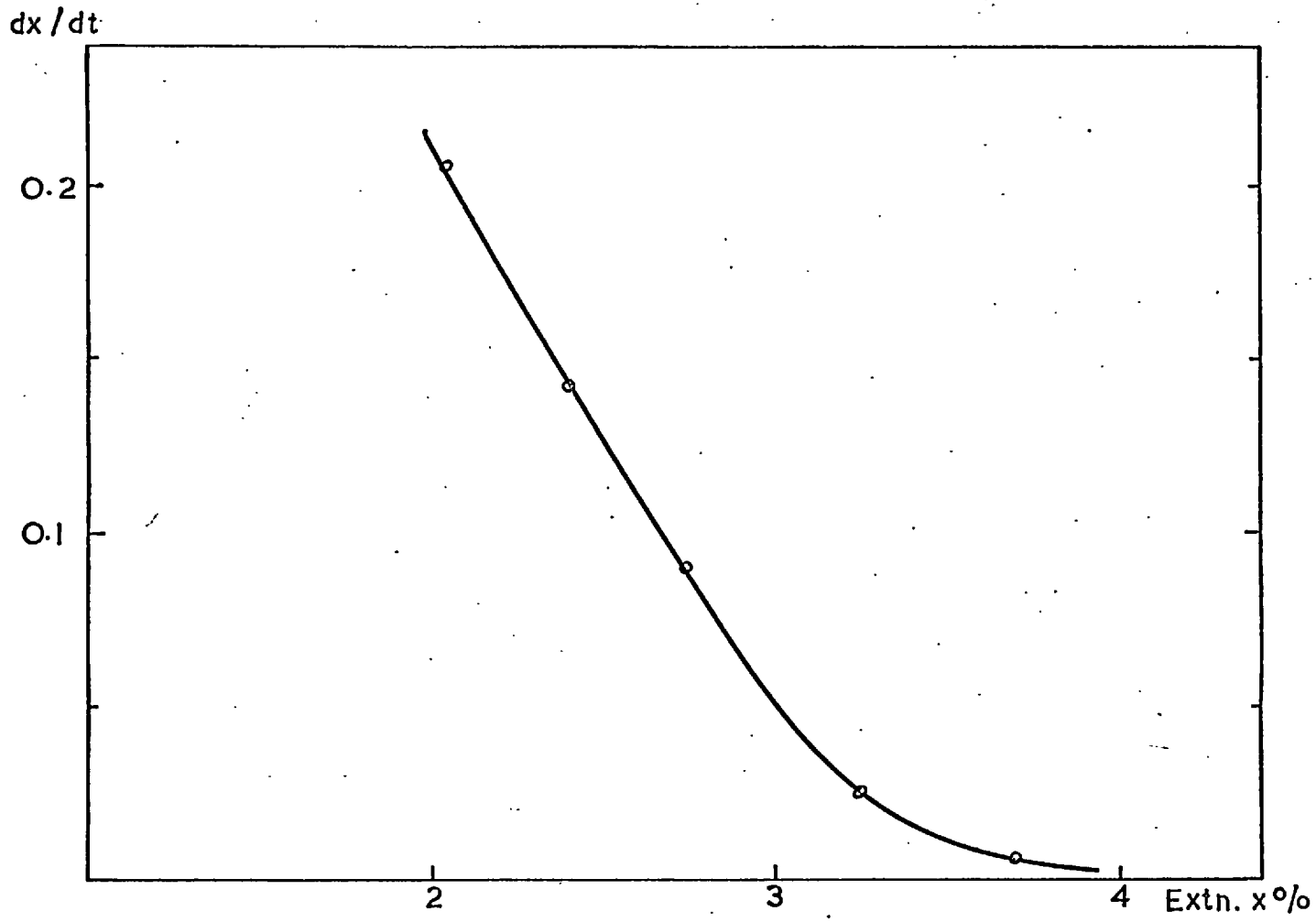


Fig. 56 Creep rate vs. extension plotted from Fig. 36